EVOLUTION OF XENOPUS VOCAL PATTERNS: RETUNING A HINDBRAIN CIRCUIT DURING SPECIES DIVERGENCE

Charlotte L. L. Barkan

Submitted in partial fulfillment of the
Requirements for the degree
of Doctor of Philosophy under the Executive Committee
in the Graduate School of Arts and Sciences

COLUMBIA UNIVERSITY

2017

ABSTRACT

Evolution of vocal patterns of *Xenopus*: retuning a hindbrain circuit during species divergence

Charlotte L. L. Barkan

Circuits underlying motor patterns of closely related species provide an ideal framework in which to study how evolution shapes behavioral variation. Male African clawed frogs (*Xenopus* and *Silurana*) advertisement call to attract female mates and silence male rivals. Males of each species produce a unique vocal pattern that serves as a species-identifier. *Xenopus laevis* is the most well-studied species in terms of its vocal behavior and underlying anatomy and physiology. The clade that includes *X. laevis*, or *X. laevis senso lato*, also includes 3 other species that diverged ~8.5 million years ago. All 4 of these species produce advertisement calls that include fast trills – trains of fast rate (~60 Hz) sound pulses. However, their calls differ substantially between species in measures of trill duration and period. I examined the premotor circuit underlying vocal patterning in three of these species: *X. laevis*, *X. petersii*, and *X. victorianus*. I used extracellular recordings to find that a premotor nucleus, DTAM, which is part of the vocal central pattern generator, is the likely source of species-variation of vocal patterns. Species-specific trill duration and period are intrinsic to the region of the hindbrain that includes DTAM. Next, I used blind whole-cell patch recordings in DTAM of *X. laevis* and *X. petersii* to examine the cells that encode trill duration and period. I identified homologous populations of premotor vocal cells in both species that code for trill duration and period in a species-specific manner. Together, these results support an autonomous role of the DTAM circuit for generation of species variation in call duration and period.

TABLE OF CONTENTS

List of Figures ii

Chapter I: Introduction 1
Abstract 1
Introduction 2
Overview 21

Chapter II Evolution of vocal patterns: retuning hindbrain circuits during species divergence 29
Abstract 30
Introduction 31
Materials and Methods 33
Results 39
Discussion 46

Chapter III Evolution of vocal circuits: tuning pre-motor neurons to generate divergent rhythms 68
Abstract 68
Introduction 69
Methods 72
Results 77

Chapter IV Conclusion and future directions 103
Abstract 103
Ion channels could impart FTNs with intrinsic species-specific conductances 103
The periphery can shape behavior differences across species 107
Using genetic tools to focus functional studies 110
Concluding Remarks 113

REFERENCES 120

LIST OF FIGURES

Chapter I

Figure 1. *Xenopus laevis* calls 23

Figure 2. Phylogeny of extant species of *Xenopus* and *Silurana* 24

Figure 3. *X. laevis sensu lato* clade and advertisement calls 25

Figure 4. Schematic of *Xenopus* larynx 27

Figure 5. Schematic of *Xenopus* vocal hindbrain circuitry 28

Chapter II

Figure 1. Species-specific advertisement call patterns in the *Xenopus laevis* clade 56

Figure 2. 5-HT application to the *in vitro* brain induces patterned vocal nerve activity across species 58

Figure 3. Comparison of the temporal features of *in vivo* calling to *in vitro* nerve activity 60

Figure 4. A local field potential wave in DTAM corresponds to fast trill in all species. 62

Figure 5. The DTAM LFP wave is NMDA-dependent 64

Figure 6. Species-specific LFP wave duration and period are independent of connection to caudal hindbrain 65

Chapter III

Figure 1. Evolution of the *Xenopus* vocal circuit 90

Figure 2. FTN spikes coincide with fictive fast trill CAPs 92

Figure 3. Consistent spike-triggered CAP delay between species 94

Figure 4. FTN spike rate is associated with CAP rate 96

Figure 5. FTNs do not differ across species in intrinsic cellular measures 98

Figure 6. FTN LLD duration and period is strongly correlated with fast trill duration and period 99

Figure 7. FTNs differ across species in their sensitivity to NMDA 101

Chapter IV

Figure 1. Blocking calcium-dependent potassium channels does not seem to lengthen FTN NMDA-oscillations 114

Figure 2. Blocking L-type calcium channels or calcium-activated non-specific cation channels with high doses may alter FTN NMDA-oscillations 115

Figure 3. Evolution of the peripheral nervous system also influences behavior 116

Figure 4. *X. laevis-X. petersii* hybrid advertisement calls 117

Figure 5. *X. laevis–X. petersii* hybrid advertisement calls are intermediate between parent species in measures of duration and period 118

Acknowledgements

I thank past and present lab mates of the Kelley lab. In particular, thank you to Irene Ballagh for immediately welcoming me into the lab and providing me with guidance, entertaining conversation, and intellectual challenge. Also, thank you to Ursula Kwong-Brown for her constant support, friendship and supply of rainbow cookies, whether from across room or across the country. I also thank Liz Leininger, Ian Hall, and Taffeta Elliott for their great help and company over the years. Thank you to Ben Evans for always answering all my phylogeny questions and eventually figuring out that all my frogs were really a species, not populations! I especially thank Martha Tobias, whose guidance, friendship, and support enriched my every day experiences in the lab.

In particular I thank Erik Zornik for welcoming me into his lab at Reed College and guiding me through the last year of my Ph.D. I've had a fantastically fun and intellectually rewarding year in Portland working with you.

And of course, a great many thanks to Darcy for providing me with the encouragement and freedom to pursue my scientific curiosity. I am sincerely grateful for your endless support and guidance over my years in the lab.

I am also thankful to my committee members, Sarah Woolley and Dustin Rubenstein, and outside examiner, Eric Fortune, for their time, input, and advice that have led me through the development of my project over the years.

Thank you to my classmates, many of whom became wonderful friends and provided entertainment, inspiration, and support. In particular I thank Alexandro Ramirez for his amazing generosity, cocktail drinking company and unrelenting encouragement. Also thank you to Brian Depasquale (and Akemi Martin) for providing a great deal of fun, silliness, and support along the way.

Thank you to my friends and family. Thank you to my sister Phoebe, for arriving in the nick of time, and thank you to my parents, Libby and Chris Barkan for their always unfailing support, generosity and love.

Chapter I

Introduction

ABSTRACT

Motor behaviors require highly tuned circuits that control muscles and execute behaviors. Whether the behavior being performed is walking, swimming, breathing, or singing, neural circuits function – either independently or in concert with one another – to produce the appropriate pattern. Perhaps one of most fascinating challenges in the study of behavior is deciphering what circuit characteristics underlie changes in behavior, whether in an individual animal or across different species. A behavior change can occur in a matter of seconds as a result of neuronal activation –for instance, an environmental stimulus, such as the appearance of a conspecific intruder, can lead to specific neurons turning on and a circuit switch that causes a display of aggression. Alternately, a behavior change can occur over the course of several hours, days or months as a result of neuronal modulation– for instance, hormones such as testosterone can masculinize and completely alter the behavior of a juvenile as it matures. Finally, as is the focus of this thesis, a change in behavior across a much longer timescale can be the result of the gradual forces of evolution acting on genes that regulate neuronal function, ultimately leading to speciation and a behavior difference across species.

Circuits underlying divergent behaviors provide a natural framework for the study of evolution of motor patterns. Small changes to gene expression and its regulation can result in substantial behavioral variation (e.g. Ding et al. 2016, Andersson et al., 2012). Indeed, it is likely that small-scale circuit change leading to large-scale behavior differences during speciation is a common phenomenon repeated throughout evolution (reviewed in Katz and Harris-Warrick, 1999). However, the specific network and neuron level effects of these gene expression changes remain largely unexplored.

Courtship behaviors are particularly compelling motor behaviors to consider in the context of evolution. These displays are essential for species recognition (e.g. Ryan 1998; Ryan and Rand, 1993; Gerhardt, 1994; Picker, 1983). Thus, any inability on the part of the male to attract female mates of the appropriate species, or of a female to recognize the correct species, will have significant consequences for that animal's reproductive success. Therefore, vocalizations produced by males to attract female mates can serve as prezygotic barriers (Hoskin and Higgie, 2010). In the case of species-specific vocalizations, distinct vocal patterns of closely related species can be driven by relatively few physiological changes. The *Xenopus* genus consists of ~25 closely related frogs, each producing a unique vocal pattern, and thus provides an ideal system in which to investigate these physiological changes.

INTRODUCTION

Evolution of Xenopus

Xenopus is a genus of anurans whose origins precede the separation of Gondwanaland into the South American and African continents. The genus belongs to the Pipid family that originated from the migration of terrestrial paleobatrachian ancestors from Europe into what would become Africa. All African clawed frogs belong to the aquatic family Pipidae that diverged from terrestrial ancestors ~150 million years ago (Evans et al., 2004). The genus *Xenopus* includes two subgenera, *Xenopus* and *Silurana*; all species are aquatic throughout their entire life cycle. The entire genus except for *X. tropicalis* (Silurana) is polyploid with levels ranging from tetraploid to dodecaploid (Evans et al., 2015). Ploidy levels are believed to reflect ancient hybridization events with allopolyploidization arising from genomic introgression via an intermediate triploid female's backcrossing to a male from a parental species (Evans, 2008).

The phylogenetic relationship between *Xenopus* species has been estimated using nuclear and mitochondrial DNA (Evans et al., 206). Each species produces a unique advertisement call that serves as a species-identifier (Tobias et al., 2011). Phylogenetic analyses (Evans, 2015) separate extant species into 4 groups: S, A, L and M (**Fig. 1**). The S group includes the only diploid species: *X. tropicalis.* The A group includes species that range from tetraploid to dodecaploid. The L group includes *X. laevis sensu lato* and *X. gilli*. The M group comprises 4 described species: *X. borealis, X, muelleri, X. fishbergi* and *X. clivii.* Within *X. laevis sensu lato* are 4 species: *X. laevis, X. petersii, X. victorianus* and *X. poweri.* Three of these species are the focus of this thesis.

In every species of *Xenopus*, males produce a characteristic vocalization – the advertisement call- during the breeding season (**Fig. 1**, Tobias et al., 2011). Several classes of vocal pattern (call types) can be identified: click, burst, trill and biphasic. The simplest calls (*X. boumbaensis, X. borealis* and *X. fishbergi)* consist of single pulses at long intervals (1Hz) that occur in bouts of calling. In more complex calls, pulses are produced in repetitive trains or trills. The sound pulses in trills can be repeated at rapid (60Hz) or slower (30Hz) rates. The most complex include trills at two different rates. A parsimony analyses (Tobias et al., 201) suggests that the simplest vocal pattern, single pulses, and the most complex vocal pattern, those consisting of two trill rates, are derived from an ancestral call that was a train of 2-14 pulses.

X. laevis and its 3 most closely related species (group L) belong to the clade *X. laevis sensu lato* (**Fig. 2**). These species diverged from a common ancestor ~8.5 million years ago (Furman et al., 2015). This clade consists of 4 described and geographically separated species: *X. laevis* in Southern Africa, *X. petersii* in West Central Africa, *X. victorianus* in East Africa, and *X. poweri* in Central Africa. Each of these species produces a call consisting of a fast rate trill. *X. laevis* and *X. petersii* calls also include a slow rate trill that alternates with the fast trill. These closely related species present an opportunity to study the mechanisms underlying the divergence of innate vocal patterns during speciation.

The best-characterized species in the genus is *X. laevis*, in part because these frogs can be induced to call by injection of gonadotropin throughout the year and are readily raised in the laboratory (Russell, 1954). While readily observed in the laboratory,

their preferred habitat is murky ponds, a feature that has contributed to the paucity of behavioral field observations.

Behavioral ecology of X. laevis

African clawed frogs live in dark, murky ponds in sub-Saharan Africa; near Cape Town they breed in the winter months (June through December; Tinsley and Kobel, 1996; Tobias et al. 2004) and use their complex vocal repertoire of seven innate calls (**Fig. 3**) to communicate. In the laboratory, frogs use these same seven calls to interact with conspecifics (Tobias et al., 1998, 2004). Calls are made up of sound patterns that create the smallest repeating vocal unit (Tobias et al., 2011). Vocal responses depend on social context (Fig. X; reviewed in Zornik and Kelley, 2011, 2016). Male frogs advertise to attract sexually receptive female mates (Tobias et al., 1998) and silence male rivals (Tobias et al., 2004; 2010). Sexually receptive females swim toward calling males (Picker, 1993) and produce the female fertility call, rapping (Tobias et al., 1998). Males respond to conspecific calls – especially rapping – with a change in call pattern to the answer call (Tobias et al., 1998). Clasping by a male evokes the release call, ticking in females and growling in males. Broadcasts of ticking produces transient vocal suppression of males (Elliot and Kelley, 2007). Sexually active male pairs alternate growling and chirping during encounters. Broadcasts of the advertisement call produce an intensity-dependent, long-lasting vocal suppression in males (Tobias et al., 2004; 2010).

Xenopus vocalize underwater using a specialized larynx

As in other anurans (and in mammals) the *Xenopus* larynx is interposed between the buccal cavity and the lungs. While it shares key components (hyaline, arytenoid and elastic cartilages, for example) with terrestrial anurans, the *Xenopus* larynx has been modified for underwater sound production. Sound pulses are generated by the separation of the ayrtenoid disks in response to contraction of paired laryngeal dilator muscles. Sound pulse production does not require air flow (Yager, 1992) and is thus independent of respiration (Tobias and Kelley, 1987) (**Fig. 4**). Laryngeal muscles are controlled by motor neurons in the hindbrain vocal circuit whose axons project via the laryngeal nerve to the larynx (Tobias and Kelley 1987).

The larynx itself can easily be studied in isolation from the animal. When dissected from the animal and placed in saline, the axons that innervate the muscles can be electrically stimulated resulting in audible pulses of sound produced by the larynx (Tobias and Kelley, 1987). The pattern of pulses produced by the isolated larynx depends on the pattern of stimulation of the laryngeal motor nerves and on the muscle fiber composition (Tobias and Kelley, 1987; Sassoon and Kelley, 1986). Laryngeal muscles are controlled by motor neurons in the hindbrain vocal circuit whose axons project via the laryngeal nerve to the larynx (Tobias and Kelley, 1987).

Xenopus vocalizations are innate and sensitive to hormones

As for most vocal vertebrates, courtship calls in *X. laevis* do not reflect vocal learning but are instead heritable, as evinced by their stereotypy and species-specificity (**Fig. 1**). The vocal patterns of males and females differ (**Fig. 3)**. Females produce 2 call types, ticking and rapping, while males produce 6 (males also tick). Sex-specific vocal patterns are governed by exposure to gonadal steroids in development and adulthood. Females can produce male-like vocal patterns even as adults when treated with androgens (reviewed in Zornik and Kelley 2011). Endocrine-directed plasticity in vocal patterns thus plays an important role in differences between the sexes.

Neural circuitry that generates vocal patterns in Xenopus

The neural circuits responsible for advertisement call patterns are contained within the hindbrain (Rhodes et al. 2007, Yu and Yamaguchi 2010). Vocal motor neurons are located in n. IX-X of the caudal the medulla that also includes glottal motor neurons and the dorsal motor nucleus of the vagus (Kelley, 1980; Simpson et al. 1986; Zornik and Kelley 2007) and is homologous to mammalian nucleus ambiguus (Albersheim-Cater et al., 2015). Left and right n. IX-X are coupled via commissural interneurons (Wetzel et al, 1998, Brahic and Kelley 2003, Zornik and Kelley 2007). n. IX-X also receives input from the premotor nucleus, DTAM (used as a proper noun), located in the pons (Wetzel et al, 1998, Brahic and Kelley 2003); connections are monosynaptic and glutamatergic (Zornik

and Kelley, 2008). n. IX-X and DTAM are reciprocally connected via interneurons in anterior n. IX-X (Brahic and Kelley, 2003; Zornik and Kelley, 2007) (**Fig. 5**).

Vocal motor neurons fire synchronously during vocalization, producing compound action potentials (CAPs; Yamaguchi and Kelley, 2000). In *X. laevis* each CAP results in a corresponding pulse of sound produced by the larynx (Yamaguchi and Kelley, 2000). This correspondence between motor output of the laryngeal nerve and actual behavior supported the development of an isolated *in vitro* brain preparation (Rhodes et al., 2007) in *X. laevis,* that produces "fictive calling": CAP patterns recorded from the laryngeal nerve of the isolated brain bathed in serotonin that closely resemble *in vivo* call patterns. DTAM is required for generating fictive advertising calling: when n. IX-X is isolated from DTAM by transection, fictive calling ceases (Rhodes et al. 2007).

Activity patterns in DTAM generate fictive vocalization patterns. A slow depolarizing wave in *X. laevis* DTAM coincides with fictive fast trill (Zornik et al. 2010). A population of 'fast trill neurons' in DTAM produces these waves (Zornik and Yamaguchi, 2012). Fast trill neurons spike with each CAP and are thus candidates for controlling the rate, duration, and period of fast trill.

Mechanisms underlying evolution of Xenopus vocal divergence

The majority of what we know to date about the *Xenopus* vocal system is based on *X. laevis*. However, the ~25 species in the *Xenopus* phylogeny with distinctive vocal

patterns and spectral features provide an opportunity to examine how proximate mechanisms contribute to motor pattern variation.

The divergence in vocal patterns that occurs across the phylogeny (**Fig. 1**) could reflect heritable changes in the vocal organ, the hindbrain vocal circuit or both. Specifically, Leininger and Kelley (2013) studied two *Xenopus* species from different clades – *X. borealis* and *X. boumbaensis* – that both produce calls consisting of single pulses. In *X. borealis*, the output of the vocal nerve of the isolated brain is single CAPs. Thus, the fictive vocal pattern produced by the brain and the actual *in vivo* call match 1:1 and a single CAP produces a muscle contraction sufficient for generating a sound pulse. In contrast, in *X. boumbaensis*, the fictive call consists of 2-3 CAPs while the actual call is a single sound pulse. As in *X. laevis*, facilitation at the neuromuscular synapse is required for a muscle contraction large enough to produce a sound pulse. This allows it to act as a filter to shorten the call, while in *X. borealis*, the single pulse call results from a single CAP and thus must be the result of the neural mechanisms diverging. These two species converge on a similar call type using distinct neural and muscular mechanisms. This shows that in *Xenopus,* behavioral divergence can result from both central and peripheral modifications. My work looks more closely at central mechanisms underlying divergence of vocal patterns of *Xenopus*.

Xenopus vocalizations are innate and sensitive to hormones

In contrast to the well-studied song system of passerine birds, courtship vocalizations of *Xenopus* are entirely innate. Frogs raised entirely in isolation produce normal vocalizations as adults. These vocal patterns depend strongly on hormones; males and females produce distinct vocal patterns and these patterns can be altered even in adults through hormone manipulation (reviewed in Zornik and Kelley 2011).

Xenopus vocal circuitry

The neural circuits that generate advertisement calling are contained within the hindbrain (Rhodes et al. 2007, Yu and Yamaguchi 2010). Vocal motor neurons are located in the vocal motor nucleus (n. IX-X) in the medulla (Kelley, 1980; Simpson et al. 1986; Zornik and Kelley 2007). Both n. IX-X are coupled bilaterally via commissural interneurons (Wetzel et al, 1998, Brahic and Kelley 2003, Zornik and Kelley 2007). n. IX-X also receives excitatory monosynaptic input from the premotor nucleus, DTAM (used as a proper noun), located in the pons (Zornik and Kelley, 2008). n. IX-X also projects reciprocally back to DTAM (Brahic and Kelley, 2003; Zornik and Kelley, 2007) (**Fig. 5**).

The larynx itself can easily be studied in isolation from the animal. When dissected from the animal and placed in saline, the axons that innervate the muscles can be electrically stimulated resulting in audible pulses of sound produced by the larynx (Tobias and Kelley, 1987). Furthermore, because vocalization in *Xenopus* depends only

on a single set of muscles, this makes the brain's vocal output particularly accessible.

Vocal motor neurons fire synchronously during vocalization, producing compound action potentials (CAPs). Previous work showed that in *X. laevis* each CAP results in a corresponding pulse of sound produced by the larynx (Yamaguchi and Kelley, 2000). This approximate match between motor output of the laryngeal nerve and actual behavior supported the development of an isolated *in vitro* brain preparation. In *X. laevis,* isolated brains produce "fictive behavior" – CAP patterns that resemble *in vivo* call patterns – when serotonin is applied (Rhodes et al., 2007). Furthermore, DTAM is required for vocal patterning – when n. IX-X is disconnected from DTAM, fictive behavior ceases (Rhodes et al. 2007). Activity patterns in DTAM underlie fictive vocalization patterns. A slow depolarizing wave can be recorded extracellularly in *X. laevis* DTAM that coincides with fictive fast trill (Zornik et al. 2010). A population of 'fast trill neurons' was identified in DTAM that underlie these slow waves (Zornik and Yamaguchi, 2012). These neurons spike phasically with each CAP and seem to dictate the rate, duration, and period of fast trill in *Xenopus laevis.*

Proximate mechanisms underlying evolution of Xenopus vocal divergence

Previous work on the mechanisms underlying *Xenopus* vocal evolution has examined the role of the brain and the larynx as evolutionary substrates for transforming motor output into behavior. Specifically, Leininger and Kelley (2013) studied two different pulse-type callers. In *X. borealis*, the output of the brain, as measured via the

laryngeal nerve, consisted of a single CAP. Thus, there was a match between the fictive vocal pattern produced by the brain and the actual *in vivo* call. In contrast, in *X. boumbaensis*, the fictive call was 2-3 CAPs, consistent with the putative ancestral call type. However, the *in vivo* advertisement call of *X. boumbaensis* consists of a single pulse of sound. This suggests that in *X. boumbaensis*, behavioral divergence results from changes in the periphery by the larynx that allow it to act as a filter, while in the case of *X. borealis*, behavioral divergence is caused by neural mechanisms diverging. This shows that in *Xenopus*, modifications can occur both centrally and peripherally to result in distinct patterns. My work looks more closely at central mechanisms underlying divergence of vocal patterns of *Xenopus*.

Evolution of motor behaviors

An ideal framework in which to study behavioral variation is the circuitry underlying the distinct behaviors of closely related species. The underlying circuitry is likely homologous and relatively unchanged, except a few physiological features driving the behavioral divergence. Furthermore, studying the small changes to circuits of closely related species is likely to provide insight into common evolutionary strategies (Katz 2011). Here I focus on the neural mechanisms responsible for differences in courtship call patterns in recently diverged species of the *Xenopus laevis* clade because of the expectation that key neurons may be homologous and that their divergent features may yield insights into the function of specific circuit elements.

Pattern Generation

How do central pattern generators produce distinct behavior? Pattern generation in its most simple form consists of a single bistable pacemaker neuron that is intrisically capable of producing a rhythm. Multi-neuronal networks can follow the rhythm of a pacemaker neuron or generate a rhythm without a pacemaker due to their connectivity (Marder and Bucher, 2001). Changes that lead to circuit output variation and thus behavior variation can occur in network connectivity, neuron number, synaptic properties, and intrinsic cellular properties, as well by neuromodulation, which can modify all these aspects of the network (e.g. Bumbarger et al., 2013; Baltzley and Lohmann, 2008; Espinoza et al., 2006; Newcomb and Katz, 2009; Fenelon et al., 2004; Chiang et al. 2006; Leininger and Kelley, 2013; Baltzley et al., 2010; Goaillard et al., 2009; Meyrand and Moulins, 1988a; 1988b). Understanding in detail how circuit changes produce behavioral variation across species is facilitated by studying homologous neurons. For this reason, most studies across species have focused on identified neurons in invertebrates that are homologs.

Synaptic connectivity

The emergence of connectomics has facilitated high-resolution examination of synaptic connectivity differences in related species that produce distinct behaviors. Homologous neurons whose activity generates one behavior can change their connectivity within the

network to produce another behavior in a related species. The complete connectivity wiring diagram for the nematode *Caenorhabditis elegans* makes it an ideal system in which to study how synaptic connectivity changes can result in behavior variation. The pharyngeal system of *C. elegans* was the first circuit mapped and includes 20 identified neurons of 14 cell types. *C. elegans* uses its pharynx to feed on bacteria, while another nematode, *Pristionchus pacificus*, is cannibalistic and eats using teeth-like structures in the mouth. *P. pacificus* predatory behavior is also mediated by the pharnygeal nervous system. Bumbarger et al. (2013) used thin section transmission electron microscopy to compare the synaptic connectivity of *P. pacificus* to *C. elegans*. They found that a massive rewiring of homologous neurons in the pharyngeal system was responsible for the distinct behaviors. Therefore, homologous neurons can underlie different behaviors when their connectivity is altered, causing the network's output to change.

Synaptic valence

Another mechanism for behavioral change is altering the valence of the connections between excitatory and inhibitory (Baltzley et al., 2010). Two species of leeches, *Hirudo verbana* and *Erpobdella obscura*, differ in behavior response to mechanical skin stimulation. *Hirudo* displays a local one-sided contraction ipsilateral to the site of the stimulus, while *Erpobdella* contracts both the contralateral and ipsilateral side of the stimulated body segment. Each ganglion involved in body contraction has four pressure mechanosensory cells and these each innervate a body wall quadrant. In *Hirudo*,

activation of one of these sensory cells leads to polysynaptic inhibition of the other three sensory cells, which control the contralateral side of the body. However, in *Erpobdella*, activating one of these sensory cells leads to polysynaptic excitation of the other sensory cells, resulting in a full body bend. The change from inhibitory to excitatory synapses leads to a clear behavior difference between these two species. Thus, behavior variation does not necessarily require connectivity changes, but can result from modification to the synapses properties, such as their valence.

Synaptic strength and conductance

Another mechanism underlying emergence of distinct behaviors in related species is modification of synaptic strength and conductance. Chiang et al. (2006) found that differences in synaptic strength seem to underlie differences in feeding strategies. As described earlier, *C. elegans* feeding behavior is well-described and the muscle activity responsible for feeding is controlled by the defined-pharyngeal nervous system. The authors characterized the feeding behavior and evolution of other free-living soil dwelling nematodes and developed a model of how differences in nematode feeding behaviors evolved. The family that includes *C. elegans* – *Rhabditidae* – switched from the ancestral pharyngeal behavior of peristalsis to pharyngeal pumping. If a calcium-activated potassium channel gene SLO-1 is inactivated, the synaptic strength of an excitatory neuron controlling the terminal bulb of the pharynx increases because SLO-1 negatively modulates neurotransmission. By creating a slo-1 mutant, the authors

confirmed that behavioral differences between the species could be explained by increased synaptic strength caused by slo-1 mutation. Thus, these authors found that modifying a neuron's synaptic strength can influence the behavior being produced by the circuit. A similar mechanism may be operating in the example of *X. borealis* described above, in which the laryngeal neuromuscular synapse – weak and facilitating in *X. laevis* – is instead strong (Leininger and Kelley, 2013).

Neuromodulation

Neuromodulation can alter behavioral output by reconfiguring the underlying networks through modulation of synaptic strength and intrinsic cellular properties, and even allow neurons from the CPG of one behavior to influence the CPG underlying a different behavior (Katz and Harris-Warrick, 1999). For example, extant species of the sea slug clade *Nudipleura* exhibit different escape swimming strategies. Some species, such as *Tritonia diomedea,* use dorsal-ventral flexion to swim, while others, such as *Melibe leonina,* use left-right flexion. The swimming CPG neurons have been identified in both species, but the neurons are not homologous for the two CPGs. The interneurons in the dorsal-ventral CPG are serotonergic and required for the *Tritonia* swimming pattern. Homologues of these interneurons are present in *Melibe*, but they are not part of the left-right swimming CPG and are not required for production of this pattern. However, activation of these serotonergic homologues or application of serotonin is sufficient to activate the left-right swimming pattern in *Melibe*. Therefore, these cells can have a

modulatory effect on the *Melibe* swimming CPG. Homologous neurons can have distinct functions in different behaviors (Newcomb and Katz, 2009) and neuromodulation intrinsic to one CPG can influence another behavior's CPG.

Cellular properties

Perhaps the best studied CPG is the stomatogastric nervous system of crustaceans. These networks produce two rhythms: the pyloric and the gastric mill. Large decapods produce a triphasic pyloric rhythm resulting from the sequential bistable activity of the DP, LP, and PY neurons. However, the shrimp *Palaemon* produces only a monophasic or biphasic rhythm. Despite this behavioral difference, studies have shown that the connectivity in the network of *Palaemon* is very similar to that of large decapods (Meyrand and Moulins, 1988a). It was shown that this behavioral difference is due to intrinsic properties of a single set of homologous neurons, the pyloric dilator neurons (AB-PD). These neurons are distinct in *Palaemon* because they do not possess intrinsic bistable properties. Only LP neurons are intrinsically oscillatory in *Palaemon* shrimp (Meyrand and Moulins, 1988b).

Other studies in the STG CPG have found that natural variation in intrinsic properties, such as ion channel expression and current amplitude, and synaptic properties, such as synaptic strength, correlate with natural variation in behavior. For instance, mRNA expression for outward rectifier channels is positively correlated with pyloric

rhythm period (Goaillard et al., 2009). This supports the idea that individual variation in behavior can be caused by variation in rhythmic neuron and network properties.

Distinct cellular and synaptic properties can still support homologous behaviors

Physiological and computational studies have also shown that networks can differ substantially in terms of their intrinsic cellular properties and synaptic strengths without significant change to the behavior pattern produced. (e.g. Saideman et al., 2007; Marder and Goallard, 2006). For instance, in a model of a simplified STG circuit, similar network behavior can still result with very different underlying cellular conductances and synaptic strengths (Prinz et al., 2004). Therefore, while changing cellular and synaptic properties can sometimes lead to behavior changes, they often do not.

Divergent CPGs with distinct connectivity can continue to produce homologous behaviors

Not only can differences in cellular and synaptic properties not necessarily lead to significant behavior differences, it is also the case that divergent CPGs can underlie homologous behaviors. For instance, in the nudibranch escape behavior system, two species with homologous behaviors have divergent CPGs. *Dendronotus iris* and *Melibe leonina* both use a left-right flexion strategy for swimming that likely evolved from a common ancestor that used this same strategy, thus their behaviors are homologous and

likely evolved only a single time. However, the *Dendronotus* CPG is a simple mutually inhibitory half-center oscillator made up of four neurons, while the *Melibe* CPG is more complicated and includes 8 cells with complex patterns of connectivity. Therefore, while both animals display a homologous swimming behavior (Sakurai et al., 2011; Sakurai et al., 2014), the CPGs underlying their behaviors have diverged through modifications to network connectivity and neuron number. Here we see that it is possible for behaviors to remain the same, but for their underlying circuitry to diverge and produce the behavior pattern in a novel way.

Genetic regulation

Recent work has taken a genetic approach to identifying potential causes of behavioral variation in both invertebrates and vertebrates. In prairie voles, for example, vasopressin receptor expression patterns differ in a pair-bonding species, *Microtus ochrogaster*, from expression patterns in a solitary species, *Microtus montanus*. A mutation in the 5' flanking region of the vasopressin receptor gene occurs in monogamous voles. When this mutant gene was expressed transgenically in mice, the expression pattern of vasopressin resembled that of *M. ochrogaster* and the mice also displayed increased affiliative behavior toward females (Young et al., 1997, Young et al., 1999). While these studies identified a genetic component to the social behavior differences in these two species, they did not pinpoint how resulting differences in vasopressin receptor expression affect the motor circuits underlying these behaviors.

Work by Andersson et al. (2012) examined the genetic basis of distinct gait patterns in horses. Some Icelandic horses display 4 gaits: walk, tolt, trot, and gallop, while others display 5 gaits: walk, tolt, trot, gallop, and pace. Pacing is unusual because the same-side leg movements are synchronized, while other gaits are considered ambling, where the front leg moves synchronously with the diagonal back leg. Researchers identified a single mutation – a premature stop codon in the DMRT3 gene (which codes the transcription factors dsx and mab-3) – that appears responsible for the presence of the pace gait in 5 gaited horses. When the mutated DMRT3 gene is expressed in mice normal locomotor patterning is disrupted. DMRT-3 is expressed in spinal interneurons, but the exact effect of the mutation on locomotor circuitry remains unknown. Because DMRT-3 encodes transcription factors, its impact on the circuit is likely to be complex and multifunctional.

Ding et al. (2016) are perhaps the first to identify the genetic cause of natural behavior variation in two different species. Using QTL mapping they determined that a locus in the *slowpoke (slo)* gene encodes a calcium-activated potassium channel that is responsible for the carrier frequency difference in the courtship song of *Drosophila simulans* and *Drosophila mauritiana*. These two species diverged ~240 thousand years ago and their courtship songs differ in sine song carrier frequency by 9.7 Hz. Researchers found that deletion of a retroelement insertion in the *slo* intron in *D. simulans* eliminates song differences between *D. simulans* and *D. mauritiana,* while eliminating the gene completely leads to a severe disruption in song. The authors hypothesize that tissue-specific expression and alternative splicing diverge during evolution resulting in distinct

behavioral phenotypes. While this work identifies a probable genetic basis for the species' difference, the specific circuits and neurons affected by this genetic change are not known.

Calcium-activated potassium channels are known to regulate intrinsic properties, such as plateau potentials, of CPG neurons (El Manira et al., 1994). Ding et al. may thus have identified a channel that affects the rhythm-generating properties of the motor circuits underlying *Drosophila* courtship song. Their next step would be to identify the neurons that express this specific isoform of slo and characterize their intrinsic properties and activity during song. In *Xenopus*, we have already identified premotor neurons that encode the temporal characteristics of courtship calls in *X. laevis*. Here, I will use closely related species to characterize how cellular differences between species result in behavioral differences.

OVERVIEW

An ideal way to understand the natural progression of the evolution of the neural circuits underlying divergent behavior is to look at closely related species (Katz and Harris-Warrick, 1999). Here I examine the vocal circuitry underlying the distinct advertisement calls of three species of African clawed frogs that diverged ~8.5 million years ago. Males of each species produce vocalizations to attract mates of their own species. While their calls are similar in terms of sound pulse rate, they differ greatly in call duration and period. I examine the central pattern generator underlying vocal patterns in all three species: *X. laevis, X. petersii* and *X. victorianus*. In Chapter 2 I discuss experiments in

which I pinpoint the rostral hindbrain nucleus, DTAM, as the control locus for species-specific call durations and periods. In Chapter 3, I examine a population of premotor cells in DTAM using whole-cell patch recordings and determine that these fast trill neurons (FTNs) likely underlie species' differences in call patterns. It is likely that a combination of intrinsic cellular properties, as well as network properties such as synaptic connectivity within DTAM and to other areas of the CPG, contribute to the distinct vocal patterns of each species. In Chapter 4, I discuss future directions of for this work. Specifically, with a focus on determining which intrinsic differences in ion channels are involved in imparting these premotor cells with intrinsic differences. More broadly, we I consider how genetic approaches to our question have contributed to understanding behavioral variation in other systems and how they might be applied here. Finally, I look outward from the central nervous system to the periphery and consider how variation in the vocal organ and influences the divergence of courtship song patterns.

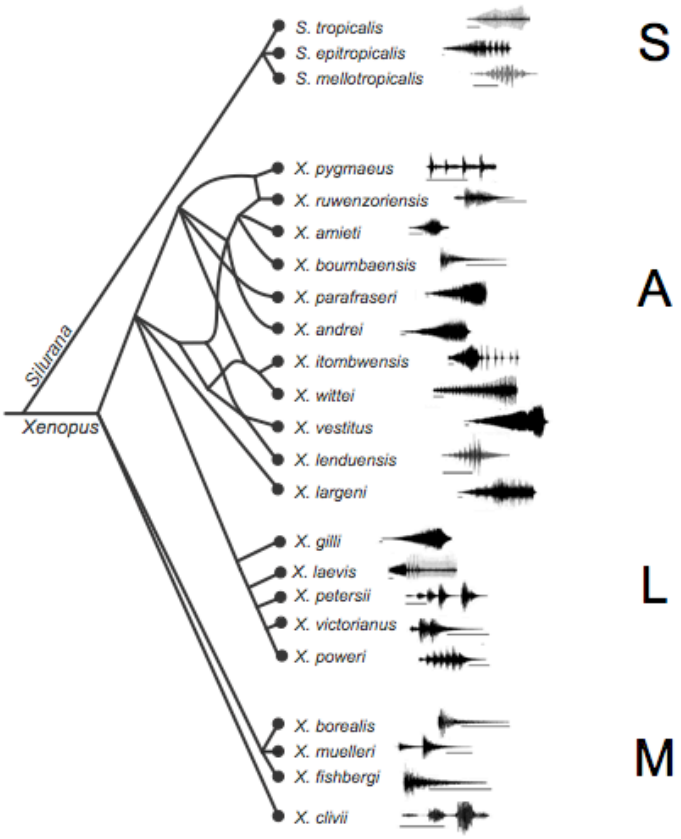

Figure 1: Phylogeny of extant species of *Xenopus* and *Silurana* and their advertisement calls

A molecular phylogeny of *Xenopodiae* created using nuclear and mitochondrial DNA. Mapping of advertisement calls onto phylogeny shows that calls are homoplasious. Parsimony analysis suggests that the ancestral call type was a train of 2-14 sound pulses. Calls are illustrated as oscillograms (intensity vs. time). Scale bars are 50 ms. Phylogeny modified from Tobias et al., 2011; Furman et al. 2015 and Evans et al. 2015).

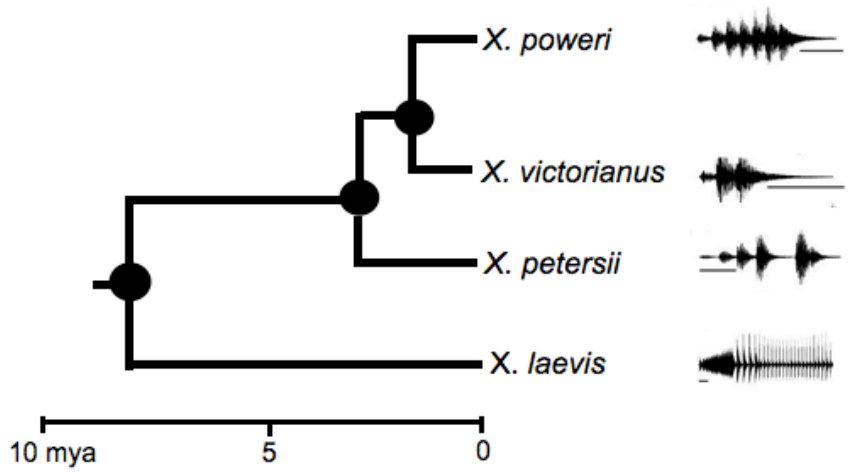

Figure 2: *X. laevis sensu lato* clade and advertisement calls

Advertisement calls produced by each species of the *X. laevis* clade. The species in this clade diverged from *X. laevis* ~ 8.5 million years ago. All species produce a call that includes a fast trill, a train of fast rate sound pulses (~60 Hz). Two species, X. laevis and X. petersii produce a call that also includes a slow rate trill (~30 Hz). The call of *X. laevis* is substantially longer than the calls of the other 3 species. Scale bars are 50 ms. Modified from Furman et al., 2015 and Tobias et al., 2011.

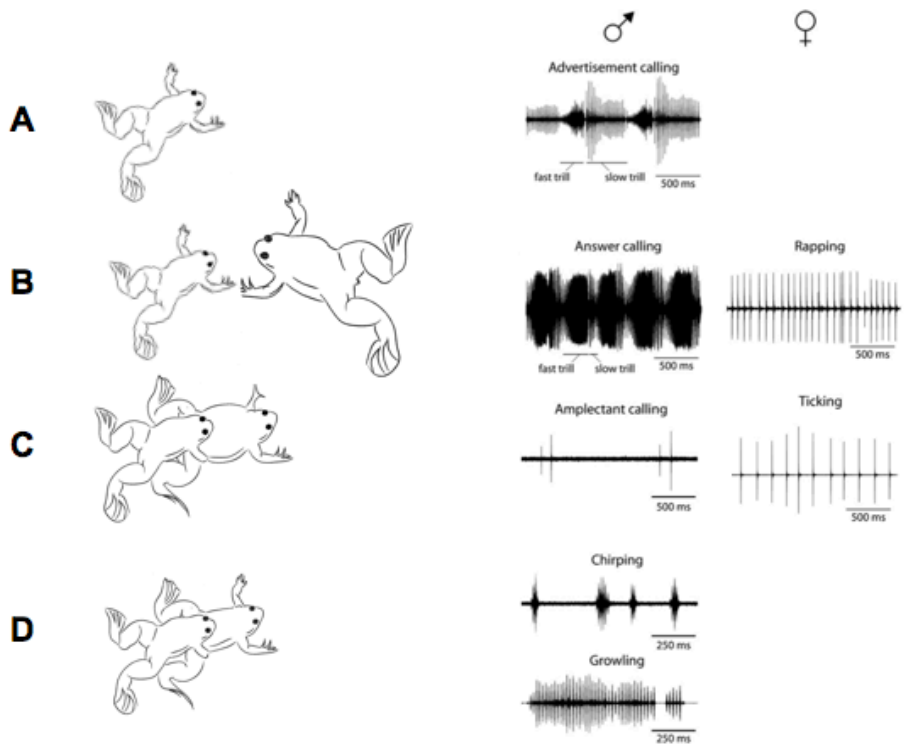

Figure 3: *Xenopus laevis* calls

(A) Male *X. laevis* frogs produce an advertisement call: alternation of amplitude modulated trills of slow (30 Hz) and fast (60 Hz) sound pulses when they are alone or in the presence of other frogs.

(B) Sexually receptive female frogs that are ready to oviposit produce trains of 12 Hz sound pulses (rapping) in response to males. Males modify their advertisement call to be an answer call, which consists of longer fast trill, shorter slow trill, and increased amplitude modulation.

(C) Males clasp female frogs. Male frogs sometimes produce brief amplectant calls (~4 - 10 Hz) when clasping females. If the female is unreceptive, she will tick (4 Hz sound pulses) as a release call.

(D) Two calls are produced only in the context of another male. Chirps are brief fast

trains (~60-80 Hz) and can be produced without contact or when clasping a male. Clasped males produce a long (500 ms-1s) low frequency growl (~50-80 Hz) or tick (4-8 Hz) as a release call.

Modified from Zornik and Kelley, 2011

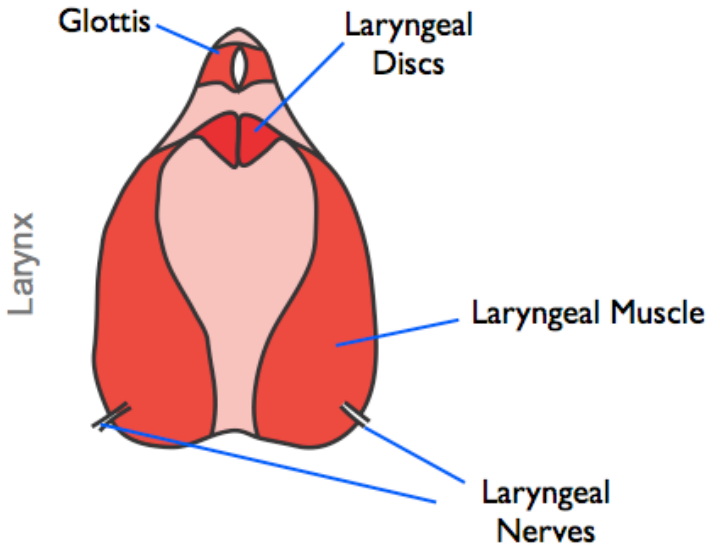

Figure 4: Schematic of *Xenopus* larynx

Dorsal view of larynx with glottis located at the rostral end of the organ. Glottal muscles contract during breathing and are closed during vocalization. When a compound action potential is produced by the synchronous activity of vocal motor neurons, the signal travels bilaterally from both motor nuclei, down the laryngeal nerves, and innervates the laryngeal dilator muscles. Muscle contraction causes the laryngeal discs to snap apart, producing an audible pulse of sound. Schematic modified from Irene Ballagh.

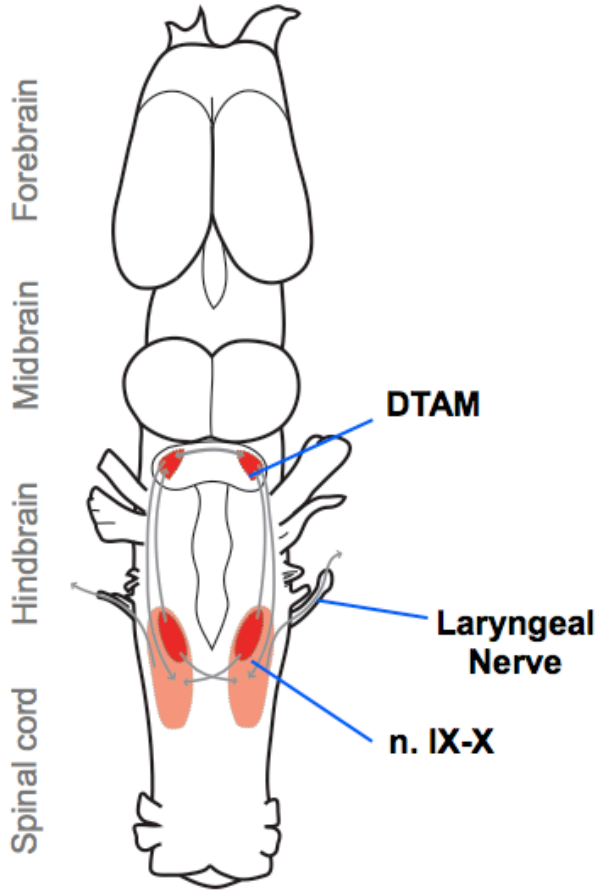

Figure 5: Schematic of *Xenopus* vocal hindbrain circuitry

The vocal motor nucleus (n. IX-X) contains vocal motor neurons as well as respiratory motor neurons. These neurons project their axons to the larynx via the posterior rootlet of the laryngeal nerve. n. IX-X is reciprocally connected with premotor nucleus DTAM. DTAM has monosynaptic glutamatergic projections to n. IX-X. DTAM and n. IX-X are both reciprocally connected to themselves. Dark red indicates the location of interneurons, while light red indicates the location of motor neurons. Grey lines indicate direction of connectivity between nuclei. Schematic modified from Irene Ballagh.

Chapter II

Evolution of vocal patterns: retuning hindbrain circuits during species divergence

Charlotte L. Barkan[1], Erik Zornik[2] and Darcy B. Kelley[1,3]

[1]Doctoral Program in Neurobiology and Behavior, Columbia University, New York, NY 10032 USA; [2]Biology Department, Reed College, Portland, OR 97202, [3]Department of Biological Sciences, Columbia University, New York, NY 10025 USA

Corresponding author's email address: dbk3@columbia.edu

Keywords: central pattern generator, vocalization, communication, *Xenopus*, evolution, motor

SUMMARY STATEMENT: Courtship song dynamics arise from finely tuned motor circuits. Alterations in the activity of a key nucleus of the hindbrain vocal circuit accompany call pattern divergence during speciation in African clawed frogs.

ABSTRACT

The neural circuits underlying divergent courtship behaviors of closely related species provide a framework for insight into the evolution of motor patterns. In frogs, male advertisement calls serve as unique species identifiers and females prefer conspecific to heterospecific calls. Advertisement calls of three relatively recently (~8.5mya) diverged species - *Xenopus laevis*, *X. petersii* and *X. victorianus* - include rapid trains of sound pulses (fast trills). We show that while fast trills are similar in pulse rate (~60 pulses/second) across the 3 species, they differ in call duration and period (time from onset of call to the onset of the following call). Previous studies of call production in *X. laevis* used an isolated brain preparation that produces compound action potentials in the vocal motor nerve that correspond to the advertisement call pattern (termed fictive calling). Here, we show that serotonin evokes fictive calling in *X. petersii* and *X victorianus* as it does in *X. laevis*. As in *X. laevis*, fictive fast trill in *X. petersii* and *X victorianus* is accompanied by an N-methyl-D-aspartate receptor-dependent local field potential wave in a rostral hindbrain nucleus, DTAM. Across the three species, wave duration and period are strongly correlated with fast trill duration and period, respectively. When DTAM is isolated from the more rostral forebrain and midbrain and/or more caudal vocal motor nucleus, the wave persists at species-typical durations

and periods. Thus, intrinsic differences within DTAM could be responsible for the evolutionary divergence of call patterns across these related species.

INTRODUCTION

The complex temporal dynamics of motor patterns arise from finely tuned circuits in the central nervous system. Differences in courtship behaviors between populations can contribute to pre-mating isolation and thus to speciation (Hoskin and Higgie, 2010). Within extant species of African clawed frogs (*Xenopus* and *Silurana)*, males produce a species-specific advertisement call that coordinates courtship (Tobias et al., 2011). Differences in temporal features of advertisement calls can serve as species-identifiers (Tobias et al., 2011). Female anurans, including *Xenopus laevis*, prefer conspecific to heterospecific advertisement calls (e.g. Ryan and Rand, 1993; Gerhardt, 1994; Picker, 1983). Thus, call divergence during speciation could contribute to prezygotic reproductive isolation, reinforcing the genetic divergence of populations and driving speciation. While the ultimate results of divergence in courtship signaling have been extensively examined (e.g. West-Eberhardt, 1983; Kirkpatrick and Ryan, 1991; Gerhardt, 1994), specific changes in the neural circuits responsible for the evolution of signaling have only recently been identified (e.g. Chakraborty and Jarvis, 2015; Leininger and Kelley, 2015; Katz, 2016). Neural circuits controlling stereotyped courtship behaviors produced by closely-related species can reveal these proximate mechanisms (Katz and Harris-Warrick, 1999).

Each species of *Xenopus* produces a distinctive advertisement call believed to

reflect simplification or elaboration of an ancestral call consisting of a train of several sound pulses (Tobias et al., 2011; Leininger and Kelley, 2015). The laevis clade - *X. laevis sensu lato* - consists of four geographically separated species that diverged ~8.5 million years ago (Furman et al. 2015, Evans et al., 2004; **Fig. 1A**), each with a distinctive advertisement call (Tobias et al. 2011, e.g. **Fig. 1 B-D**). Because these species diverged relatively recently, the neural circuits producing these temporally distinct patterns are likely to be similar, allowing us to identify mechanisms for tuning specific temporal call features.

Xenopus vocal behavior and its underlying neural circuitry have been studied most extensively in *X. laevis* (reviewed in Zornik and Kelley, 2016). The male *X. laevis* advertisement call consists of highly stereotyped, alternating, trains of fast and slow rate sound pulses (trills: see **Fig. 1B**). Compound action potentials (CAPs), produced by groups of hindbrain vocal motor neurons, travel via cranial nerve IX-X to the vocal organ, the larynx, generating muscle contractions and sounds (Tobias and Kelley 1987; Yager 1992). The pattern of CAPs recorded from the laryngeal nerve of calling *X. laevis* males corresponds to the *in vivo* call trill pattern (Yamaguchi and Kelley, 2000). Fictive advertisement calling – CAP patterns that parallel *in vivo* call patterns – can be evoked by application of serotonin (5-HT) to the *in vitro* male brain (**Fig. 2A**, Rhodes et al., 2007), providing a powerful preparation for understanding the underlying neural circuits.

Using this preparation, a central pattern generator (CPG) located in the hindbrain was identified as responsible for fictive call patterns in *X. laevis* (Rhodes et al. 2007; Zornik et al., 2010). The CPG includes a rostral premotor nucleus, DTAM (used as a

proper name), as well as neurons in a caudal hindbrain nucleus, n. IX-X (Wetzel et al., 1985; Zornik and Kelley, 2007), homologous to nucleus ambiguus of mammals (Albersheim-Carter et al., 2015) (**Fig. 2A**). Neurons in DTAM monosynaptically excite n. IX-X motor neurons that produce vocal patterns (Zornik and Kelley, 2008; Yamaguchi et al., 2008; Zornik et al., 2010, Zornik and Yamaguchi, 2012). A local field potential (LFP) wave recorded from DTAM coincides with fast trill and is NMDA receptor dependent (Zornik et al., 2010). Activity of DTAM neurons underlying the LFP wave is tightly correlated with fictive call timing and disrupting their activity eliminates fictive fast trill. Taken together, available evidence suggests that in *X. laevis* DTAM neurons drive the LFP wave and control call duration and period (Zornik and Yamaguchi, 2012).

What mechanisms underlie vocal divergence in the laevis clade? While all species in the clade produce fast trills, the duration and period (time from onset of call to the onset of the following call) of their calls differ substantially (Tobias et al., 2011). We used the *in vitro* brain preparation originally developed in *X. laevis* (Rhodes et al., 2007) to compare motor and premotor activity during fictive calling in *X. laevis*, *X. petersii* and *X. victorianus*. In this study, we test the hypothesis that retuning of the DTAM circuitry underlies call divergence in the laevis clade.

MATERIALS AND METHODS

Procedures

Animals: All animal care and experimental procedures conformed to guidelines set forth by the National Institutes of Health and were approved by Columbia University's

Institutional Animal Care and Use guidelines (protocol no. AC-AAM1051). Sexually mature male *X. laevis*, *X. petersii*, and *X. victorianus* were used in experiments. Animals were raised in the laboratory colony or purchased from Xenopus Express (Brooksville, FL), group housed in polycarbonate tanks, each with 10 liters of filtered water changed twice weekly following feeding with frog brittle (Xenopus Express) and kept on a 12L: 12D schedule at 20ºC (*X. laevis*) or 23ºC (*X. petersii* and *X. victorianus*).

Vocalization recordings: Male frogs (n=5 each for *X. laevis*, *X. petersii*, and *X. victorianus*) were injected via the dorsal lymph sac with 200 µM human chorionic gonadotropin 48 and 24 hours before calls were recorded. Each frog was placed in a glass aquarium (60 x 15 x 30 cm; water depth = 25 cm; temperature = 20-22º) in a room illuminated dimly with red light. After 10 minutes of habituation, a conspecific female was placed in the tank for 30-45 minutes or overnight during a sound-activated recording (Audacity(R)). Vocalizations were recorded with a hydrophone (CA30 or H2a, Aquarian Audio Products, Shoreline, WA); the signal was digitized (Omega SV, Lexicon Pro), and saved to a personal computer in .WAV format (Amadeus Pro, HairerSoft, Kenilworth, United Kingdom or Audacity (R)).

In vitro brain preparation: Male frogs (*X. laevis* n=12, *X. petersii* n = 14, *X. victorianus* n=5) were deeply anesthetized by injection of 1.3% tricaine methanesulfonate (MS-222; Sigma; *X. laevis*: 500 - 700 µl, *X. petersii* and *X. victorianus*: 200 µl) into the dorsal lymph sac and brains removed from the cranium in ice-cold saline (in mM: 96 NaCl, 20 $NaHCO_3$, 2 $CaCl_2$, 2 KCl, 0.5 $MgCl_2$, 10 HEPES, and 11 glucose, pH 7.8, oxygenated with 99% O_2). Following recovery for one hour in saline at room temperature, the brains

were pinned in a silicone elastomer-lined recording dish (Sylgard; Dow Corning, Midland, MI) and constantly superfused with fresh-oxygenated saline at ~22°C. Compound action potentials (CAPs) were recorded with an extracellular suction electrode placed on the posterior rootlet of cranial nerve IX-X that contains the axons of the laryngeal motor neurons (Simpson et al., 1986). To elicit a fictive motor pattern on the laryngeal nerve, 5-HT (Sigma) was bath-applied to the recording dish to a final concentration of 30 or 60 μM (Zornik and Yamaguchi, 2012). The signal from the nerve was amplified x1000 (Model 1700; A-M Systems, Carlsborg, WA) and band-pass filtered (10 Hz to 5 kHz), digitized at 10 kHz or 20 kHz (Digi-data 1400A; Molecular Devices, Sunnyvale, CA), and recorded on a personal computer. After 5 minutes of application, 5-HT washout was begun by reinstating saline superfusion. 5-HT was then re-applied every 60 min for the next 4-8 hours.

Local field potentials (LFPs) in DTAM were recorded using a low impedance carbon fiber extracellular electrode (300-500 kΩ, Kation Scientific, Minneapolis, MN) while simultaneously recording activity in the laryngeal nerve. The signal was amplified x100, digitized at 10kHz or 20kHz and bandpass filtered at 0.1 Hz to 10 kHz. Either the pia covering the cerebellum was removed to allow the DTAM electrode to penetrate or the cerebellum and tectum were transected sagittally at the midline, reflected laterally to expose DTAM, and pinned. The DTAM electrode was placed ~100 μm posterior to the tectum–cerebellum border, ~200 μm from the lateral edge of the fourth ventricle and ~650 μm below the pial surface. In 5 *X. laevis* brains, 5 *X. petersii* brains, and 2 *X. victorianus* brains, the brain was transected in the transverse plane, caudal to nerve VIII,

to isolate DTAM from the vocal motor nucleus IX-X (n. IX-X). Two *X. laevis* brains and 3 *X. petersii* brains were transected in the transverse plane just rostral to DTAM, in addition to the caudal transection, to also remove any descending inputs from the midbrain and forebrain.

Pharmacology: In 1 *X. laevis* brain (to confirm previous finding: Zornik et al., 2010), 3 *X. petersii* brains, and 2 *X. victorianus* brains, DL-2-Amino-5-phosphonopentanoic acid **(**APV, Sigma) was bath-applied to the recording dish at concentrations of 100-500 μM. Changes in the LFP wave in response to drug application were recorded in DTAM and fictive calling was monitored via the nerve suction electrode. After 5 minutes of APV application, 30 or 60 μM 5-HT was added to the bath for 10 minutes. After reinitiating saline superfusion for an hour, 5-HT was applied alone to determine whether the effect of APV was reversible.

Analyses

Calls: Calls were sampled from 5 males of each species. A single call (**Fig.1, B-D**) is the smallest vocal unit containing a characteristic and repeating pattern of sound pulses (Tobias et al., 2011). For all species, samples were randomly selected continuous bouts of calling that lasted a minimum of 10 seconds and a maximum of 30 seconds. Samples contained a minimum of 15 calls and 100 pulses for each animal. Pulses were detected and analyzed using custom-made MATLAB scripts (MathWorks Natick, MA; all MATLAB scripts are available upon request from C.L.B.). Pulse rates ranging from 0 to 100 Hz were binned (2 Hz bin width) and then analyzed to determine fast trill threshold.

50 Hz was selected as the threshold for fictive fast trill because rate histograms revealed minima with an upper bound of ~50 Hz in all 3 species. In all species, slow trill onset was defined as 2 or more successive pulses with an instantaneous pulse rate <50 Hz and >10 Hz, while fast trills were defined as 2 or more successive pulses with a pulse rate >50 Hz and <100 Hz. Call durations were measured from call onsets to offsets. Periods were measured from the onset of a call to the onset of the following call.

In vitro brain analysis: Fictive vocal CAP patterns produced following 5-HT application were collected and analyzed (*X. laevis*: n = 5, *X. petersii*: n = 6, *X. victorianus*: n = 3) using custom-made MATLAB scripts. Samples comprised a minimum of 20 seconds (7 - 14 fictive calls, made up of numbers of CAPs that varied according to species as described above for *in vivo calls*) and a maximum of 30 seconds of continuous fictive calling from each brain. Samples contained a minimum of 15 calls and 100 pulses for each animal. Instantaneous CAP rate was calculated as the reciprocal of the time interval between two successive CAPs. Rates ranging from 0 to 100 Hz were binned (2 Hz bin width) and then analyzed to determine fictive fast trill threshold. 50 Hz was selected as the threshold for fictive fast trill because rate histograms revealed minima with an upper bound of ~50 Hz in all 3 species. Fictive slow trills were defined as a series of 2 or more pulses with an instantaneous pulse rate <50 Hz and >10 Hz, while fictive fast trills were defined as a series of 2 or more pulses >50 Hz and <100 Hz. Fictive call durations were measured from fictive call onsets to offsets. Periods were measured from the onset of a fictive call to the onset of the following call.

The DTAM local field potential (LFP) was low-pass filtered at 5 Hz for *X. laevis* and 20 Hz for *X. petersii* and *X. victorianus* to reveal a wave corresponding to fictive fast trill. Wave onset was defined as the first peak in the second derivative of the low-pass filtered signal prior to the wave peak. Wave offset was defined as the first peak in the second derivative of the low-pass filtered signal following the wave peak. Onset and offset were visually confirmed and manually adjusted if necessary. Call and wave durations were measured from onset to offset time. Periods were measured from one call onset time to the following onset time.

Evoking fictive calling from the isolated brain requires the preservation of motor nerve connections to n.IX-X during dissection, an intact hindbrain and effective oxygenation to preserve neural function. The success rate for these experiments is variable and can be low. Because the availability of mature male *X. victorianus* was extremely limited, fictive calling data points are reported individually in cases where $n < 5$.

Statistics: Statistical analyses were carried out using MATLAB (MathWorks, Natick, MA) and Prism (GraphPad, San Diego, CA) software. Two-way ANOVAs were used to compare animal means (*in vivo* fast and slow pulse rate vs. *in vitro* fast and slow CAP rate, *in vivo* call duration vs. *in vitro* call duration, and *in vivo* call period vs. *in vitro* call period across species) followed by Tukey's multiple comparisons tests. Linear regression models were used to compare *in vivo* fast trill duration and period to *in vitro* fast trill duration and period, respectively. To compare the relationship between the onset and offset of the DTAM LFP to fast trill, the median for each species was used. A 2-way

ANOVA followed by Tukey's multiple comparisons tests was used to compare animal means for DTAM LFP wave duration and period in intact brains and for transected brains between *X. laevis* and *X. petersii*.

RESULTS

Advertisement calls across species

We recorded advertisement calls from five adult male *X. laevis*, *X. petersii* and *X. victorianus.* All three species produce a distinctive male advertisement call consisting of repeated trains of sound pulses or trills (**Fig 1B-D, Table 1**). *X. laevis* calls alternate between a slow trill (~30 Hz) of ~25 pulses and a fast trill (~60 Hz) of ~12 pulses (**Fig. 1B**). Similarly, *X. petersii* calls (**Fig. 1C**) consist of a slow trill with ~3 pulses followed by a fast trill made up of 2 sound pulses (**Fig 1Ci**); the fast trill events are often shortened to a single pulse (**Fig 1Cii**). The advertisement call of *X. victorianus*, however, consists only of fast trills (**Fig. 1D**); slow trills are absent. The *X. victorianus* fast trill consists of 3 or 2 sound pulses (**Fig 1D,i, ii**). Fast trills thus occur in all three species, but have a shorter duration and period in *X. petersii* and *X. victorianus* than *X. laevis*.

5-HT induces fictive calling by the isolated *in vitro* brain

When the *X. laevis* brain is removed and placed in an oxygenated saline solution (diagrammed in **Fig. 2A**), bath-application of serotonin (5-HT) results in characteristic activity patterns recorded from the laryngeal nerve (**Fig. 2B-D**). In male *X. laevis*, the temporal features of these *in vitro* compound action potentials (CAPs) parallel the pattern

of sound pulses in the *in vivo* advertisement call (compare **Fig. 1B** to **Fig. 2B**) and have thus been termed fictive advertisement calling (Rhodes et al., 2007). If fundamental neural circuit properties for calling are conserved across the *X. laevis* clade, we hypothesized that 5-HT should also elicit fictive advertisement calling in *X. petersii* and *X. victorianus.*

We found that bath-application of 5-HT to isolated brains also elicited patterned vocal nerve CAPs in *X. petersii* (n=6) and *X. victorianus* (n=3, due to limited availability of adult males of this species (**Fig. 2C, D**). As in *X. laevis* (n=5, **Fig. 2B**), these CAP patterns closely resembled the patterns of each species' advertisement call (compare **Fig. 1** to **Fig. 2**). CAPs were produced at fast (~60 Hz; **Fig 2: yellow**) and slow (~30 Hz: **Fig 2: blue**) rates in *X. laevis* and *X. petersii*; *X. victorianus* brains produced only fast CAPs. Four of the six *X. petersii* brains produced slow trill CAPs and all produced fast trill CAPs. We conclude that fictive calling elicited by 5-HT is a fundamental neural circuit property conserved across these three species.

Table 1. Comparison of *in vivo* and *in vitro* call characteristics

Species	**Fast pulse rate mean ± σ (Hz)**	**Fast CAP rate mean ± σ (Hz) [Individual values]**	**Slow pulse rate mean ± σ (Hz)**	**Slow CAP rate mean ± σ (Hz)**	***in vivo* call duration mean ± σ (ms)**	***in vitro* call duration mean (ms) ± σ [Individual values]**	***in vivo* call period mean ± σ (ms)**	***in vitro* call period mean (ms) ± σ [Individual values]**
X. laevis	59.7±2.3	58.5	27.7±	31.1	1142.9	1273.1±303.	1142.9	1260.0±297.7

(in vivo n=5; *in vitro* n=5)		±4.5	0.7	±3.3	±305.1	0	±305.1	
X. petersii *(in vivo* n=5; *in vitro* n=6)	64.4±4.5	61.3 ±6.2	26.8 ±4.7	29.3 ±0.36	178.2 ±30.7	177.2±86.4	538.7 ±99.6	683.4±225.5
X. victorianus *(in vivo* n=5; *in vitro* n=3)	68.2±5.8	63.9±5.4 [58.0, 65.8, 68.3]	N/A	N/A	23.0±5.1	32.6±9.9 [44.1, 27.1, 26.7]	343.0± 105.8	391.5±9.1 [381.1, 396.0, 397.7]

In vitro CAP rates parallel *in vivo* pulse rates within a species

We compared fast and slow *in vitro* CAP rates to fast and slow *in vivo* sound pulse rates during advertisement calls (**Fig. 3, Table 1)**. Slow trill pulse rates and slow trill CAP rates did not differ significantly (2-Way ANOVAs; $F_{1, 14} = 3.979$, $p > 0.05$; **Fig. 3A, Table 1**). Fast trill pulse rates and fast CAP rates also did not differ significantly ($F_{1, 23} = 2.245$, $p > 0.05$; **Fig. 3B Table 1**). Next, we examined differences in pulse and CAP rates across species. Slow trill CAP and sound pulse rates in *X. laevis* and *X. petersii* did not differ significantly ($F_{1, 14} = 0.810$, $p > 0.05$). Fast trill CAP and sound pulse rates did however differ between species ($F_{2, 23} = 4.288$, $p = 0.03$). The interaction of species and preparation (*in vivo* vs. *in vitro*) was not significant for fast or slow trill ($F_{2, 23} = 0.2020$, $p > 0.05$, $F_{1, 14} = 0.078$, $p > 0.05$). We conclude that fictive calling CAP rates elicited by 5-HT *in vitro* correspond to *in vivo* calling sound pulse rates in all 3 species; across species, only slight variation in fast trill rates was found.

***In vitro* call period and duration parallel *in vivo* call period and duration within a species**

We also used a 2-way ANOVA to compare call duration (**Fig. 3C, Table 1**) and call period (**Fig. 3D, Table 1**) between *in vivo* calling and *in vitro* fictive calling within and across species. Within each species, the *in vivo* call did not differ significantly from the *in vitro* fictive call ($F_{2, 21} = 0.382$, $p > 0.05$ for call duration; $F_{2, 23} = 0.894$, $p > 0.05$ for period, compare single *in vivo* to single *in vitro* fictive call, **Fig. 1** and **2**). We conclude that fictive calling patterns elicited by 5-HT *in vitro* correspond to *in vivo* calling patterns in these 3 species within the laevis clade.

***In vitro* and *in vivo* call period and duration differ significantly between species**

Call duration (**Fig. 3C, Table 1**) and period (**Fig. 3D, Table 1**) *in vivo* and *in vitro* differed significantly between species ($F_{2, 21} = 104.1$, $p < 0.0001$ for duration; $F_{2, 23} = 36.12$, $p < 0.0001$ for period). *X. laevis* call durations were longer than *X. petersii* and *X. victorianus* both *in vivo* and *in vitro* (Tukey's multiple comparisons test, $p < 0.05$ for these comparisons). However, *X. victorianus in vivo* and *in vitro* call durations and periods did not differ significantly from *X. petersii* call durations and periods ($p > 0.05$ for these comparisons). The species and preparation interactions were also not significantly different ($F_{2, 21} = 0.341$, $p > 0.05$ for duration; $F_{2, 23} = 0.113$, $p > 0.05$ for period). *X. petersii* and *X. victorianus* call patterns did differ qualitatively in pattern; *X. victorianus* calls lack a slow trill both *in vivo* (**Fig. 1**) and *in vitro* **(Fig. 2**). We conclude

that fictive calling CAP patterns elicited by 5-HT *in vitro* reflect species differences in *in vivo* calling sound pulse patterns in these 3 species within the *X. laevis* clade.

An LFP wave in premotor DTAM during fictive fast trill

We recorded from DTAM during *in vitro* fictive calling in *X. laevis* (n = 5), *X. petersii* (n = 6), and *X. victorianus* (n = 2). A depolarizing LFP wave in DTAM (**Fig. 4A**) was associated with fictive fast trill **(Fig. 4B)** in all 3 species. This wave began before fictive fast trill (median ± σ ms difference: *X. laevis*: -160.0 ± 115.8, *X. petersii*: -59.2 ± 13.6, *X. victorianus*: -47.6 ± 9.99) and terminated after fictive fast trill (median ± σ ms difference: *X. laevis*: 106.7 ± 73.3, *X. petersii*: 49.4 ± 8.3 *X. victorianus*: 28.3 ± 12.2) (**Fig. 4C**).

Because *in vivo* and *in vitro* call durations and periods were significantly longer in *X. laevis* compared to *X. petersii* and *X. victorianus* (above, **Fig. 3D,E**), and the DTAM LFP coincides tightly with fast trill in each species, we examined the relationship between the duration and period of the LFP wave and the duration and period of fictive fast trill using linear regression in pooled individuals of all three species (*X. laevis* n=5, *X. petersii* n=6, *X. victorianus* n=2). Wave duration was linearly (**Fig. 4D**) and strongly ($R^2 = 0.947$, slope = 0.6618 $p < 0.0001$) related to fictive fast trill duration. Wave periods in all three species were also linearly (**Fig. 4E**) and strongly ($R^2 = 0.991$, slope = 1.0028, $p < 0.0001$) related to periods between successive fast trills. We conclude that the temporal relation of the DTAM LFP to fictive fast call duration and period is conserved across the 3 species.

In *X. laevis,* fictive fast trills and the DTAM LFP wave are both NMDA-dependent (Zornik et al. 2010). We hypothesized that if similar mechanisms underlie calling in *X. petersii* and *X. victorianus*, as is suggested by the similarities in the underlying DTAM activity, calling would be NMDA-dependent in all species examined here. We thus applied APV [(2*R*)-amino-5-phosphonopentanoate, a competitive NMDAR antagonist] to fictively singing brains in *X. laevis* (n=1, to confirm previous findings; see Zornik et al. 2010), *X. petersii* (n=3) and *X. victorianus* (n=2) to determine if NMDAR-dependence is conserved. One hour prior to APV application, all preparations produced fictive calling accompanied by an LFP wave in DTAM (**Fig. 5A)** in response to 5-HT application. Pretreatment for 15 minutes with APV blocked both fictive calling and the LFP wave in response to 5-HT (**Fig. 5B)**. An hour after APV washout, 5-HT-induced fictive calling and the DTAM wave returned (**Fig. 5C**). The NMDA-dependence of the DTAM wave is thus conserved within the laevis clade.

LFP wave generation appears autonomous to DTAM

Next we set out to determine if DTAM alone is responsible for generating the LFP wave, rather than other components of the vocal circuit, such as interneurons located in the anterior portion of the vocal motor nucleus (red portion of n. IX-X: **Fig. 2A**). These neurons innervate DTAM (Zornik and Kelley, 2007), raising the possibility that the motor nucleus controls the timing of the LFP wave. To address this question we transected the *in vitro* brain between DTAM and the vocal motor nucleus, just caudal to nerve VIII. After transection, 5-HT application produced a DTAM LFP wave that closely

resembled the DTAM LFP wave produced by intact brains in *X. laevis* (n = 5), *X. petersii* (n = 5), and *X. victorianus* (n = 2, not included in ANOVA) (**Fig. 6A,B)**. Transections did not significantly alter wave durations in *X. laevis* or *X. petersii* (2-way ANOVA: $F_{1, 16} = 0.535$, $p > 0.05$, Mean ± σ in ms: *X. laevis*: 444.2 ± 29.6 (intact), 465.3 ± 28.9 (transected); *X. petersii*: 108.7 ± 7.3 (intact), 118.0 ± 2.3 (transected); Fig. 6C). Although not included in statistical analyses, LFP wave durations in 2 *X. victorianus* also appear to be unaltered by the transection (individual values in ms: 119.8 and 105.4 (intact); 113.2 and 121.1 (transected; **Fig. 6C**). Wave periods in *X. laevis* and *X. petersii* were also unaffected by transection (2-way ANOVA: $F_{1, 16} = 0.676$, $p > 0.05$, Mean ± σ in ms: *X. laevis*: 1,115.6 ± 188.8 (intact), 1,016.2 ± 71.4 (transected); *X. petersii*: 695.7 ± 157.5 (intact), 733.9 ± 194.4 (transected); Fig. 6D). As for wave duration, wave period also did not change dramatically following the transection in *X. victorianus*, only a slight increase was apparent (individual values in ms: 372.9 and 396.6 (intact), 442.5 and 463.3 (transected); **Fig. 6D**). The significant species difference in duration ($F_{1, 16} = 270.2$, $p < 0.0001$) and period ($F_{1, 16} = 23.86$, $p < 0.0002$) between the species remained after the transections, with X. *laevis* having a longer duration and period than *X. petersii* (Tukey's multiple comparisons test, $p < 0.05$ for both comparisons). There was no significant interaction between transection and species for duration ($F_{1, 16} = 0.0813$, $p > 0.05$) or period ($F_{1, 16} = 0.918$, $p > 0.05$). We conclude that the duration and the period of the DTAM LFP wave does not reflect inputs from n. IX-X in these three species.

DTAM also receives input from the central amygdala located in the ventral forebrain (Brahic and Kelley, 2003; Hall et al., 2013). Because previous work has also

shown that removal of the midbrain and forebrain does not disrupt fictive calling in *X. laevis* (Yu & Yamaguchi, 2010), we predicted that species-specific LFP wave patterns are generated autonomously within the hindbrain compartment that includes DTAM. To test this prediction, we combined a transection that eliminated n. IX-X inputs with an additional transection just anterior to the cerebellum that removed inputs from the midbrain and forebrain in 2 *X. laevis* and 3 *X. petersii* brains. We found that following both transections the LFP waves persisted in response to 5-HT application (wave duration in ms: *X. laevis*: 395.5, 334.3, *X. petersii*: 141.5, 166.5, 130.4; wave period in ms: *X. laevis*: 1,212.7, 1,092.6, *X. petersii*: 724.2, 1,024.0, 662.1; compare to values above for intact and transected animals. These more limited observations suggest that DTAM LFP wave parameters also do not reflect inputs from midbrain or forebrain in the *X. laevis* clade, reinforcing the idea that intrinsic features of the DTAM LFP govern species differences in vocal patterns.

DISCUSSION

Divergent temporal features of songs are supported by shared neural circuit elements

Three relatively recently (8.5 mya) diverged species within the laevis clade - *X. laevis, X. petersii* and *X. victorianus* (Furman et al., 2015) - produce male advertisement calls with distinctive temporal properties (Tobias et al., 2011). All of these species produce advertisement calls that include fast trills, but call durations and periods are much longer in *X. laevis* than in *X. petersii* and *X. victorianus*. We show here that key features of the

neural circuitry responsible for vocal patterning are conserved across these species. Species-specific fictive advertisement calls (nerve activity patterns that parallel sound pulse patterns) can be elicited by applying 5-HT to the isolated brain in each species. However, as is the case for actual advertisement calls recorded *in vivo*, fictive call durations and periods recorded *in vitro* vary significantly across species.

Next, we examined premotor activity that might be responsible for species differences in call duration and period. In each species, fictive fast trills coincide with an LFP wave recorded from the rostral hindbrain nucleus DTAM. Wave duration and period are tightly correlated with fictive fast trill duration and period across individuals of each species. Furthermore, the LFP wave is NMDAR-dependent in all species. Collectively, these findings support conserved involvement of NMDA-dependent DTAM activity in regulating the duration of fast trill and call periods across all three species.

Differences in DTAM LFP wave durations and periods across species might be due to autonomous properties of the nucleus or instead might reflect differences in connectivity with caudal or rostral components of vocal neural circuitry. In support of the former hypothesis, we find that in all species the DTAM LFP wave persists after isolation from caudal inputs of n. IX-X. Furthermore, in *X. laevis* and *X. petersii*, the wave persists when rostral inputs from the forebrain and midbrain are also removed (*X. victorianus* was not tested). These observations suggest that species-typical characteristics of the DTAM LFP wave are intrinsic to the hindbrain compartment that includes DTAM, rather than reflecting activity elsewhere in the vocal circuit, and support an autonomous role for DTAM in control of call duration and period. Differences across species in DTAM

activity could be the result of intrinsic cellular properties of DTAM neurons, network differences in synaptic connectivity within the nucleus or adjacent regions of the anterior hindbrain, or a combination of these factors.

Proximate mechanisms: candidate cellular and network contributions to call duration and period

Premotor vocal neurons in DTAM

DTAM was initially identified as a target for androgens (Kelley et al., 1975; Kelley, 1980), essential hormones that support advertisement calling (Wetzel and Kelley, 1983), and as a source of input to vocal motor neurons (Wetzel et al., 1985). More recent studies identified a population of vocal premotor neurons in *X. laevis* DTAM (fast trill neurons, "FTNs") with phase-locked spikes preceding each fast trill CAP (Zornik and Yamaguchi, 2012). FTNs exhibit a long lasting depolarization (LLD) during spiking that coincides with fictive fast trill and with the DTAM LFP wave. The DTAM LFP wave thus likely reflects the activity of a population of FTNs that depolarize synchronously during fast trill. Our data suggest that a homologous population of FTNs in *X. petersii* and *X. victorianus* also generate a DTAM LFP wave by producing synchronous LLDs. However, because the waves in *X. petersii* and *X. victorianus* are shorter than in *X. laevis*, we predict that FTN LLDs terminate more rapidly in *X. petersii* and *X. victorianus,* leading to a brief fictive fast trill and thus a shorter call.

Intrinsic cellular contributions: ion channels and membrane properties

In *X. laevis,* synaptically isolated FTNs produce rhythmic oscillations in response to NMDA that are similar in duration and period to LLDs recorded during fictive calling (Zornik and Yamaguchi, 2012). Intrinsic cellular properties of FTNs could thus allow them to act as network pacemakers and contribute to fast trill duration and period. Intrinsic properties of *X. petersii* and *X. victorianus* FTNs could differ from *X. laevis* FTNs producing shorter oscillation durations and periods.

Inward currents are likely to underlie the depolarizations associated with these oscillations. For example, persistent inward sodium currents ($I_{Na(P)}$) and calcium-activated nonselective cation currents (I_{CAN}) both contribute to respiratory rhythms in another hindbrain region, the pre-Botzinger complex, which drives inspiration in mammals (Del Negro et al. 2005). Other inward current candidates include NMDA currents and the hyperpolarization-activated inward current (I_h), shown to dramatically alter burst periods in a reciprocally inhibitory stomatogastric nervous system circuit (Sharp et al., 1996). Because DTAM neuron oscillations in *X. laevis* persist in the presence of tetrodotoxin (TTX) (Zornik and Yamaguchi, 2012), $I_{Na(P)}$ is not a strong candidate for control of DTAM temporal features. NMDA currents, however, are good candidates because even in the presence of TTX, NMDA induces oscillations (Zornik and Yamaguchi, 2012). In both *X. petersii* and *X. victorianus,* the DTAM LFP can be blocked by antagonizing NMDARs, also supporting a possible role for NMDA currents in controlling call duration and period differences in the laevis clade.

Outward currents could also contribute to call period and duration by terminating depolarization in FTNs. Some candidates are: calcium-dependent potassium currents (El

Manira et al., 1994; Cazalets et al., 1999; Del Negro et al., 1999; Tahvildari et al., 2008), the sodium-potassium ATPase hyperpolarizing current (pre-Botzinger complex: Rubin et al., 2009), A-type transient potassium currents, (lamprey locomotion: Hess and Manira, 2001) and potassium leak currents (respiration: Koizumi and Smith 2008).

Species differences in ion channels (Harris-Warrick, 2010; Del Negro et al., 2010) expressed by FTN neurons could serve as control elements in species divergence of rhythmic oscillations that produce differing LLD durations and thus LFP wave durations. For example, if outward current channels are more highly expressed or are activated more rapidly in *X. petersii* and *X. victorianus* than in *X. laevis,* the duration of the LLD and LFP should decrease because the neurons would be able to repolarize more rapidly. Beyond species differences in channels, differences in intracellular or extracellular regulation of Ca^{2+} levels by intracellular mechanisms or astrocytes (e.g. Morquette et al., 2015) could affect circuit properties.

Whether the intrinsic features of FTNs in *X. petersii* and *X. victorianus* can account entirely for differences in call duration and period remains to be determined. Features of network connectivity and synaptic strength might also play a role in species differences. In the stomatogastric nervous system, for example, altering synaptic strengths in a reciprocally inhibitory two-cell circuit leads to large differences in burst duration and period (Sharp et al., 1996). In nematodes, differences in connectivity of homologous neurons results in distinct behaviors. *Caenorhabditis elegans* feed on bacteria using pharyngeal pumping while a related species, *Pristionchus pacificus,* uses

its jaws to ingest prey. Homologous neurons produce these distinct behaviors but differ extensively in their connectivity (Bumbarger et al., 2013).

Ultimate mechanisms: evolution of hindbrain circuits

What is DTAM? Hindbrain circuits for respiration and vocalization

In many vocal vertebrates, respiration powers sound production, providing a potential link between hindbrain neural circuits for breathing and calling (*e.g.* Martin and Gans, 1972; reviewed in Leininger and Kelley, 2015). In terrestrial frogs such as *Rana*, vocalization is powered by expiration and requires activity in DTAM (*aka* the pretrigeminal nucleus: Schmidt, 1992; Schmidt, 1993). In *Xenopus*, aquatic anurans derived from terrestrial ancestors (Cannatella and De Sa, 1993; Irisarri et al., 2011), vocalization has been decoupled from respiration. Male *X. laevis* call while submerged, without respiration; glottal motor neurons that gate air movements from the lungs to the buccal cavity are inhibited during vocalization (Zornik and Kelley, 2008). A possible evolutionary scenario for DTAM's role in vocal patterning is repurposing of a neural circuit element, which functions during expiration in other vertebrates, to drive vocal patterning in the absence of actual breathing.

In the lamprey, a basal vertebrate, expiration is driven by the rhythm generating paratrigeminal respiratory group (pTRG) (reviewed in Bongianni et al., 2014). The pTRG is intrinsically rhythmically active, glutamatergic, and projects to vagal motor neurons, (Cinelli et al., 2013), features shared with the *Xenopus* DTAM vocal circuit (reviewed in Zornik and Kelley, 2016). Both the pTRG and DTAM are located in the rostral hindbrain compartment derived from embryonic rhombomere 1 (r1; Murakami et al., 2004; Morona

and Gonzalez, 2009). The several shared features described above support homology of DTAM to the pTRG.

In mammals, however, rhythmic respiratory activity (specifically inspiration) is driven by more posterior hindbrain nuclei that include the parafacial respiratory group (pFRG) and the pre-Botzinger complex (preBotC; Thoby-Brisson et al., 2009). In the mouse, the pFRG forms in r4 and the preBotC in r7 (Tomas-Roca et al., 2016). Thus, though the lamprey pTRG has been considered a homolog of the preBotC (Cinelli et al., 2013), its location in r1 does not support this assignment nor does its prominent role in expiration (as opposed to inspiration which is passive in lampreys; Boganini et al., 2014).

Is there a mammalian homolog of pTRG/DTAM that functions in expiration? The strongest candidate (Wetzel et al., 1985) is the Kolliker-Fuse nucleus of the parabrachial complex (PBC) that includes rhythmically active neurons linked to both inspiration or expiration (Dick et al., 1994) and that has been proposed to drive breathing patterns (Forster et al., 2014). Like neurons in DTAM and pTRG, neurons in the PBC originate in r1 (Tomas-Roca et al., 2016), are glutamatergic (Yokota et al., 2007), are rhythmic (Dick et al., 1994; Forster et al., 2014), and project to vagal and laryngeal motor neurons (nucleus ambiguus: Broadwalh et al., 2015). Thus, DTAM, pTRG and PBC are candidate vertebrate homologs. Neurons in the PBC are also active during vocalization in mammals (Farley *et al.,* 1992; Jurgens, 2002), suggesting a highly conserved role for this hindbrain complex in both respiration and vocalization.

Evolutionary insights from comparative approaches to neural circuits

Conservation of motor patterns As we show here for the laevis clade, control of duration and period of the DTAM LFP wave could provide a conserved tuning mechanism across the *Xenopus* phylogeny. For example, the ability of male *X. boumbaensis* to produce a single sound pulse driven by a short train of CAPs could reflect shortening of the ancestral DTAM LFP duration to produce the very short CAP burst pattern observed *in vitro* (Leininger et al., 2015). This shortening would have limits because at least two nerve CAPs are required in males to release enough neurotransmitter from the motor nerve terminal to evoke one vocal muscle action potential and contraction (reviewed in Leininger and Kelley, 2015).

The major anuran suborders include the Archaeobatrachia (*e.g. Xenopus)* and the Neobatrachia (*e.g. Rana*) (Igawa et al., 2008; Roelants and Bossyut, 2005). A DTAM LFP has also been observed during fictive calling in *Rana pipiens* (Schmidt, 1992), suggesting an ancient (Permian/Tertiary) role for DTAM in vocal patterning within the Anura.

Divergence of vocal pattern and auditory sensitivity; speciation For closely related species, small changes in vocal circuitry can lead call patterns to diverge so that even highly genetically similar species (Furman et al., 2015) exhibit distinct temporal patterns (this study, also see Tobias et al., 2011). Reinforcement of differences between male courtship calls has been proposed as a driver for speciation in recently diverged frog lineages (Hoskin et al*.,* 2005). Species differences in courtship patterns enable individuals to preferentially mate with members of their own lineage and avoid the reproductive costs of hybridization (Hoskin and Higgie, 2010). Behavioral studies have shown that

advertisement calls in frogs serve as a strong premating isolation mechanism; in two-choice phonotaxis experiments, females strongly prefer a conspecific advertisement call over that of another species (Gerhardt and Doherty, 1988).

Related species can exhibit behavioral and neural preferences for different call features. For instance, female *Hyla chrysoscelis* use pulse rate to recognize mates while *Hyla versicolor* females use pulse duration. These species preferences are reflected in differences in selectivity of interval-counting neurons and long-interval selective neurons in the inferior colliculus (Schul and Bush, 2002; Rose et al., 2015; Hanson et al., 2016). The *X. laevis* inferior colliculus is also populated by auditory neurons that respond preferentially to sound pulse rate (Elliot et al., 2011) and auditory sensitivity to temporal features of sound pulses could differ in *X. petersii* and *X. victorianus*.

Thus, tuning of the duration and period of premotor activity in the rhythmically-active premotor hindbrain nucleus, DTAM, is a strong candidate for the divergence of vocal patterns in the closely-related species, *X. laevis, X. petersii* and *X. victorianus*. This mechanism is also a candidate for control of vocal patterns in some more distant species within the phylogeny and within other Anuran species. Changes in DTAM activity of related populations resulting in vocalization differences might have served as pre-zygotic barriers that prevented gene flow and thus facilitated speciation.

Acknowledgements

We thank, Sarah Woolley and Dustin Rubenstein for helpful input on the project, Ben Evans for clarification of phylogenetic terminology, the National Xenopus Resource Center at the Marine Biological Laboratory for hosting scientific consultations, Irene Ballagh for the brain schematic in Figure 2, and Alexandro Ramirez for input on data analyses.

Competing interests

The authors declare no competing or financial interests.

Author contributions

All authors contributed to the design of experiments and the analysis of the data. C.L.B. carried out the experiments and wrote the manuscript with input from D.B.K. and E.Z.

Funding We acknowledge the support of an NSF GRFP (C.L.B.), start-up funds from Reed College (E.Z.) and NS23684 (D.B.K.).

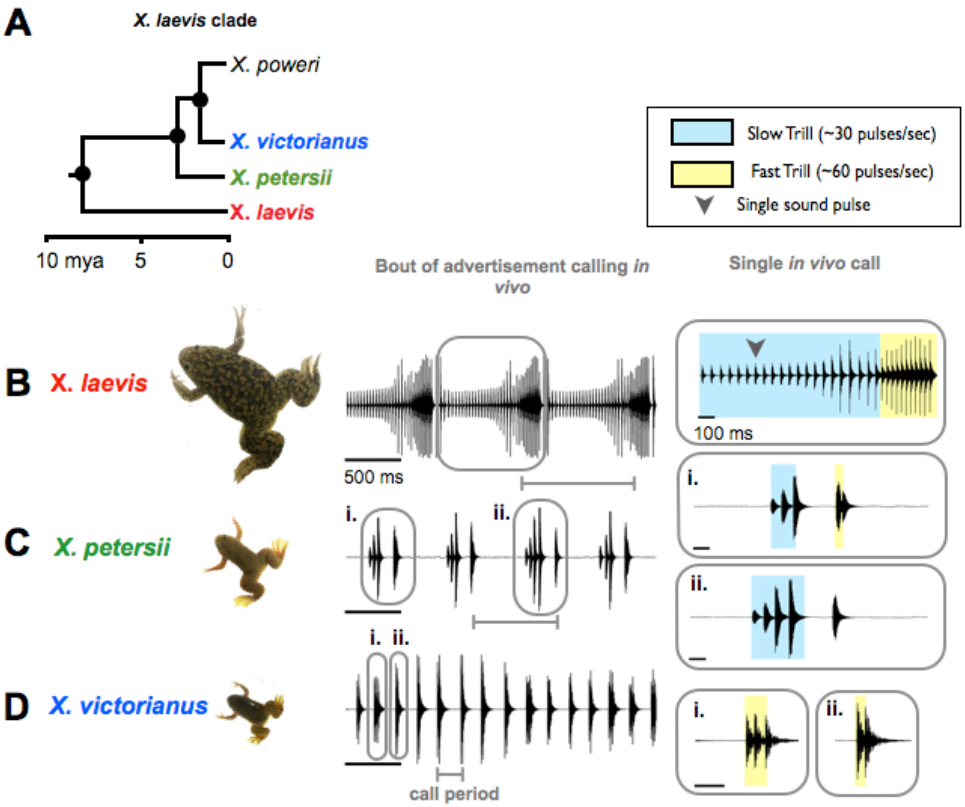

Figure 2. Species-specific advertisement call patterns in the *Xenopus laevis* clade

(**A**) The laevis clade includes four species: *X. laevis, petersii, victorianus* and *poweri*, estimated to have diverged from their most recent common ancestor 8.5 mya (Furman et al. 2015). (**B - D**) Representative male advertisement calls in *X. laevis, X. petersii* and *X. victorianus* consist of a series of sound pulses (trills) with characteristic temporal patterns and rates (Hz). (**B**) Oscillogram (intensity vs. time) of the *X. laevis* biphasic advertisement call. The slow trill (~30Hz, blue) alternates with the fast trill (~60Hz,

yellow). (**C**) Oscillogram of the biphasic *X. petersii* call. A short (i.e. 3-4 pulses) slow trill (blue) is followed by either (i) two fast pulses (yellow) or (ii.) a single sound pulse. (**D**) Oscillogram of the monophasic *X. victorianus* call. The call consists of short trills with either (i) three or (ii) two fast pulses (yellow).

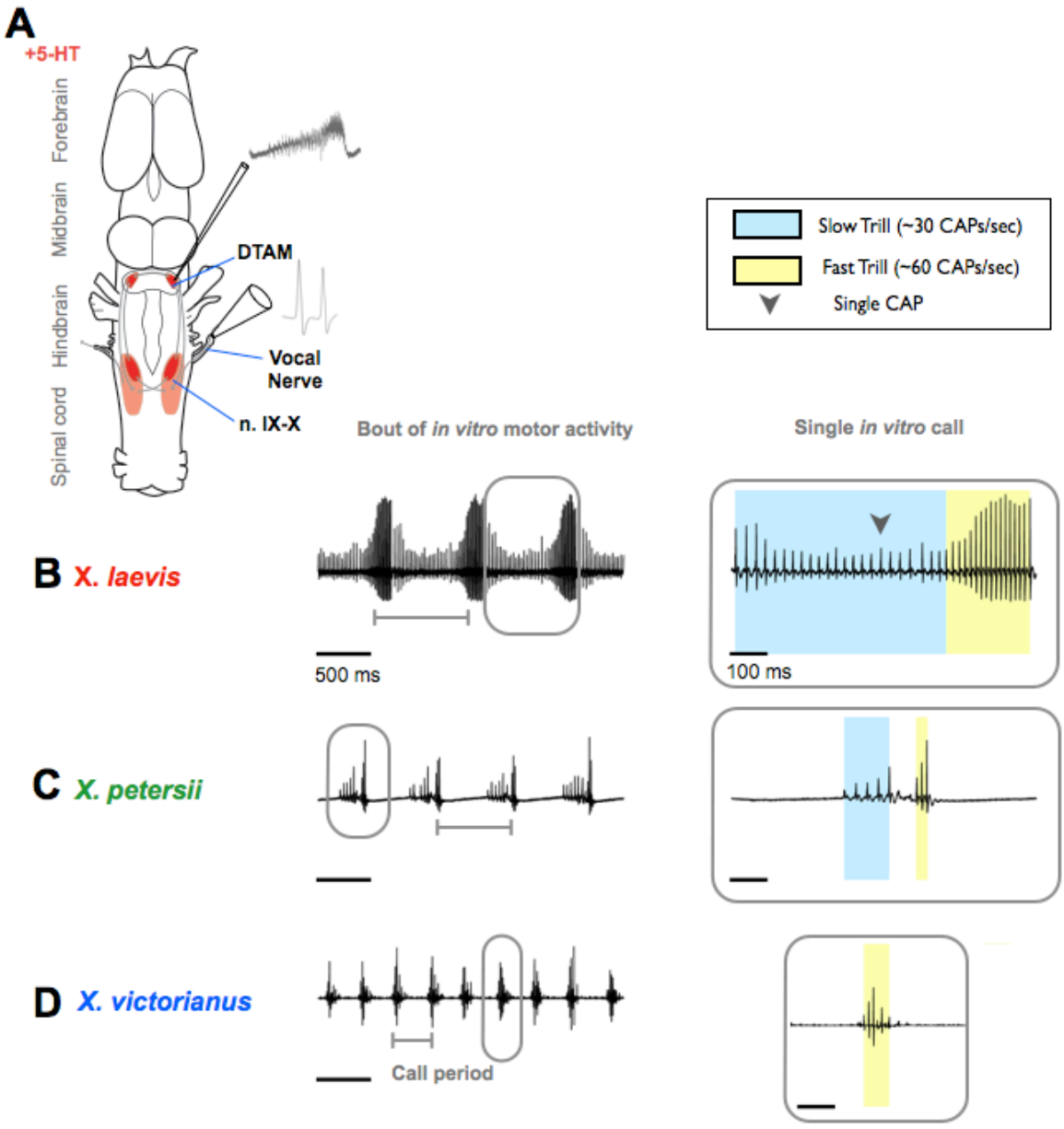
A
+5-HT
Forebrain
Midbrain
Hindbrain
Spinal cord
DTAM
Vocal Nerve
n. IX-X
Slow Trill (~30 CAPs/sec)
Fast Trill (~60 CAPs/sec)
Single CAP
Bout of in vitro motor activity
Single in vitro call
B X. laevis
500 ms
100 ms
C X. petersii
D X. victorianus
Call period

Figure 2. **5-HT application to the *in vitro* brain induces patterned vocal nerve activity across species**

(**A**) A schematic view of the isolated male hindbrain viewed from the dorsal surface; anterior is up. (**B-D**) In response to serotonin (5-HT) bath application, patterned bouts of activity – compound action potentials (CAPs) – produced by vocal motor neurons in nucleus (n.) IX-X, can be recorded from the vocal (laryngeal) nerve. *In vitro* patterns correspond to advertisement call patterns (Fig. 1) and are termed fictive calls. During the fast trill of a fictive call, a local field potential (LFP) can be recorded from nucleus DTAM of the rostral hindbrain. Laryngeal motor neurons are located in posterior n. IX-X (pink) and project to the larynx via the laryngeal nerve (4^{th} root of cranial nerve IX-X). Interneurons in anterior n. IX-X (red) project to n.IX-X and to DTAM. DTAM interneurons (red) provide monosynaptic, excitatory input to laryngeal motor neurons. Axons from DTAM cross the midline to innervate contralateral DTAM. (**B – D**) Left hand panel: Representative laryngeal nerve activity bouts in *X. laevis, X. petersii* and *X. victorianus* following bath application of 5-HT to the isolated brain. Right hand panel: single fictive calls with individually-labeled slow (blue) and fast (yellow) trills. (**B**) Bouts of activity recorded from the *X. laevis* laryngeal nerve include alternating slow and fast rate CAPs. (**C**) Bouts of activity recorded from the *X. petersii* laryngeal nerve also include alternating slow and fast CAPs; call duration and period are shorter than in *X. laevis.* D. (**D**) The *in vitro* nerve activity pattern produced by *X. victorianus* includes only fast rate CAPs.

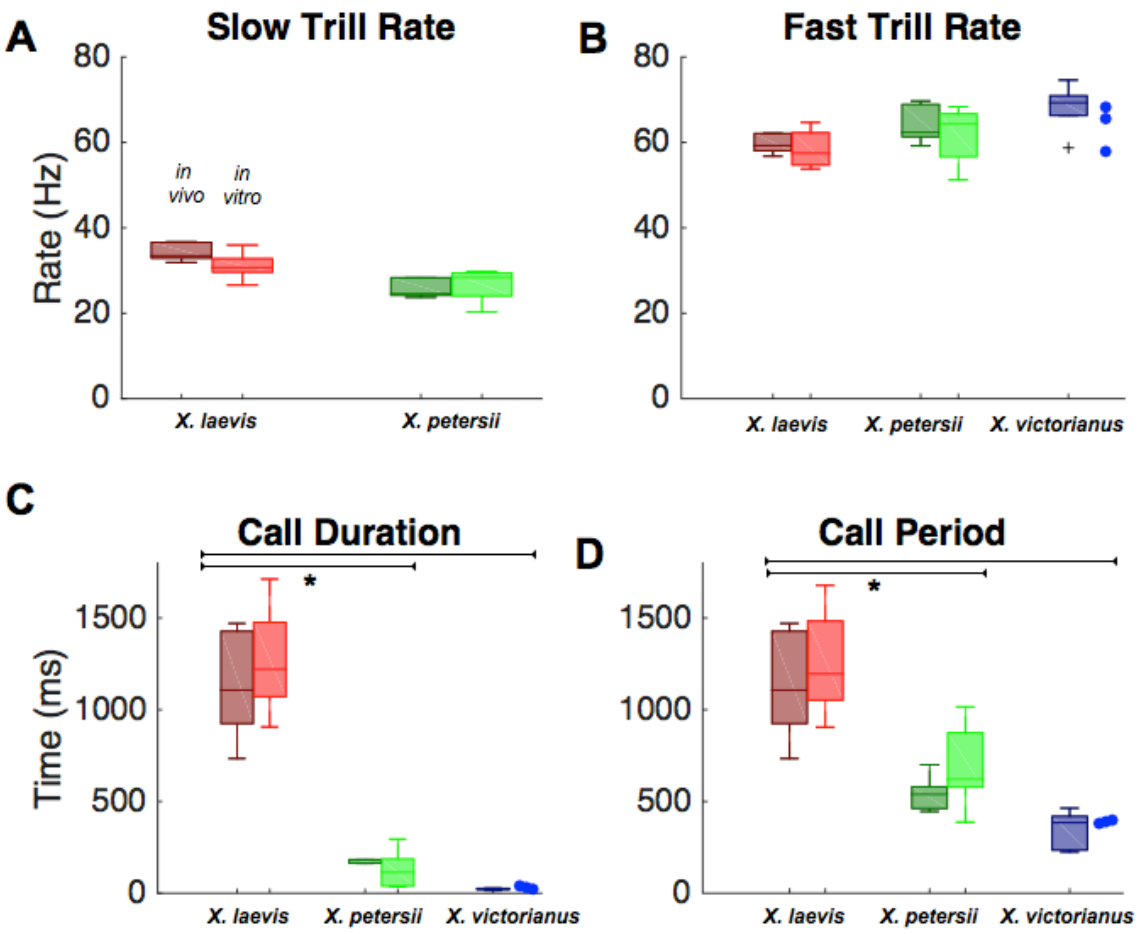

Figure 3. **Comparison of the temporal features of *in vivo* calling to *in vitro* nerve activity**

(**A- D**) Boxplots illustrate the 25th and 75th percentiles; the horizontal line is the median, whiskers were calculated using Tukey's method and depict the most extreme data value that is not an outlier, plus signs denote outliers. Red indicates *X. laevis* (*in vivo* n=5, *in vitro* n=5), green *X. petersii* (*in vivo* n=5, *in vitro* n=6), and blue *X. victorianus* (*in vivo* n=5, *in vitro* n=3), with the darker shade representing *in vivo* and the lighter shade *in vitro*. Asterisks denote significance ($p<0.05$, Tukey's multiple comparisons tests).

(**A**) In *X. laevis* and *X. petersii*, the slow CAP rate during *in vitro* nerve activity does not differ significantly from the advertisement call slow trill pulse rate *in vivo* (2-Way

ANOVA, $p > 0.05$)*; X. victorianus* advertisement calls do not include slow trills. Slow rates of actual calls (*in vivo*) and fictive calls (*in vitro*) also do not differ significantly between *X. laevis* and *X. petersii* ($p > 0.05$).

(**B**) Within each species, the fast *in vitro* CAP rate does not differ significantly from the fast advertisement call *in vivo* pulse rate (2-Way ANOVA, $p > 0.05$). Fast trill rate for actual and fictive calling differs significantly across species ($p = 0.03$, however $p > 0.05$ for all post hoc comparisons.

(**C**) Within each species, *in vitro* call duration does not differ significantly from *in vivo* advertisement call duration (Two-Way ANOVA, $p > 0.05$). However, across species, call duration does differ ($p < 0.0001$). *In vitro* and *in vivo* call duration is significantly longer in *X. laevis* than in *X. petersii* and *X. victorianus* (Tukey's multiple comparisons test, $p < 0.05$ for these comparisons).

(**D**) For each species, *in vitro* call period does not differ significantly from *in vivo* call period (Two-Way ANOVA, $p > 0.05$). However, across species, call period does differ significantly ($p < 0.0001$). *X. laevis in vitro* and *in vivo* call periods are significantly longer than *X. petersii* and *X. victorianus* call periods (Tukey's multiple comparisons tests, $p < 0.05$ for these comparisons).

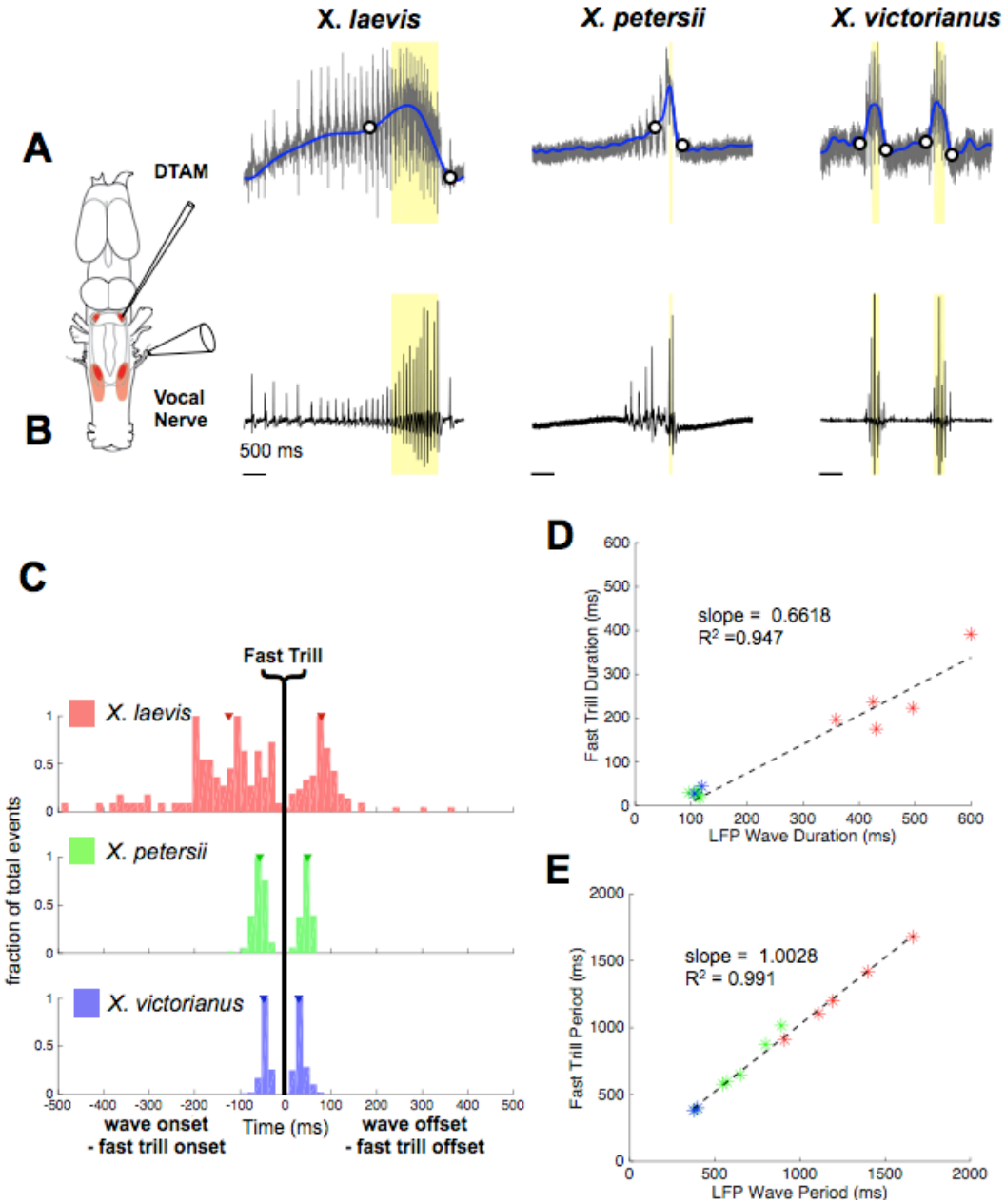

Figure 4. A local field potential wave in DTAM corresponds to fast trill in all species.

(**A**) Representative extracellular recording in DTAM (grey) and resulting LFP wave (blue, low pass filtered at 5Hz for *X. laevis* (n=5) and 20 Hz for *X. petersii* (n=6) and *X. victorianus* (n=2)) in response to 5-HT application coincides with the fast trill (yellow) of

the (**B**) fictive call simultaneously recorded from the laryngeal nerve (black). Wave onset and offset are depicted by open circles.

(**C**) The DTAM LFP begins before the start of each fast trill and ends after the trill stops. The fast trill onset is subtracted from the corresponding wave onset resulting in a negative number across species (median ± σ: *X. laevis*: -160.0 ± 115.8 ms, *X. petersii*: -59.2 ± 13.6, *X. victorianus*: -47.6 ± 10.0). The fast trill offset is subtracted from the wave offset, resulting in a positive value across species (*X. laevis*: 106.7 ± 73.4 ms after, *X. petersii*: 49.4 ± 8.3, *X. victorianus*: 28.3 ± 12.2. Y-axis bins are percent of total events and arrowheads indicate group medians.

(D) Linear regression analysis of mean fictive fast trill duration versus each animal's corresponding mean DTAM LFP wave duration. Asterisks depict individual animal's mean values ($R^2 = 0.947$, slope = 0.6618, $p < 0.0001$).

(E) Linear regression analysis of inter-call-period versus each animal's corresponding wave period. Asterisks depict individual animal's mean values ($R^2 = 0.991$, slope = 1.0028, $p < 0.0001$).

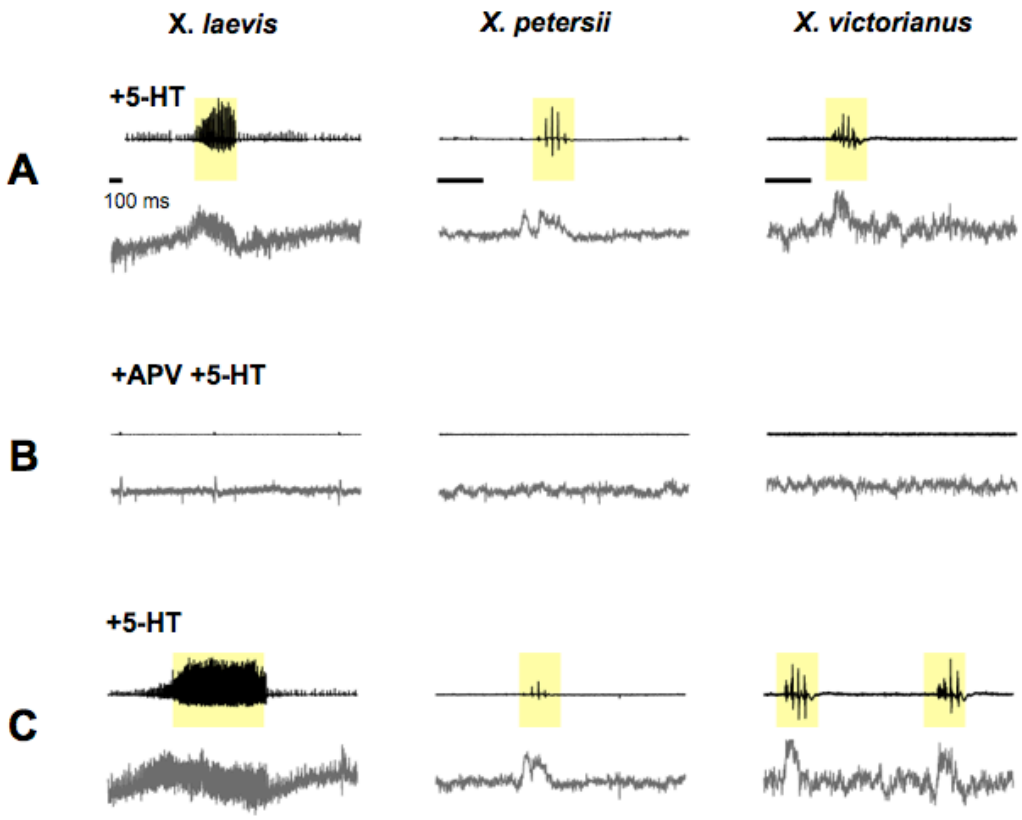

Figure 5. The DTAM LFP wave is NMDA-dependent

(A) Representative nerve (black, top) and DTAM recordings (bottom, grey) following 5-HT application *in vitro* in *X. laevis* (n=1), *X. petersii* (n=3), and *X. victorianus* (n=2). Fast trill is highlighted in yellow.

(B) Nerve (top) and DTAM (bottom) activity are abolished by 500 µM APV added 15 min prior to 5-HT application.

(C) Nerve (top) and DTAM (bottom) activity are restored following 1-hour washout and re-application of 5-HT.

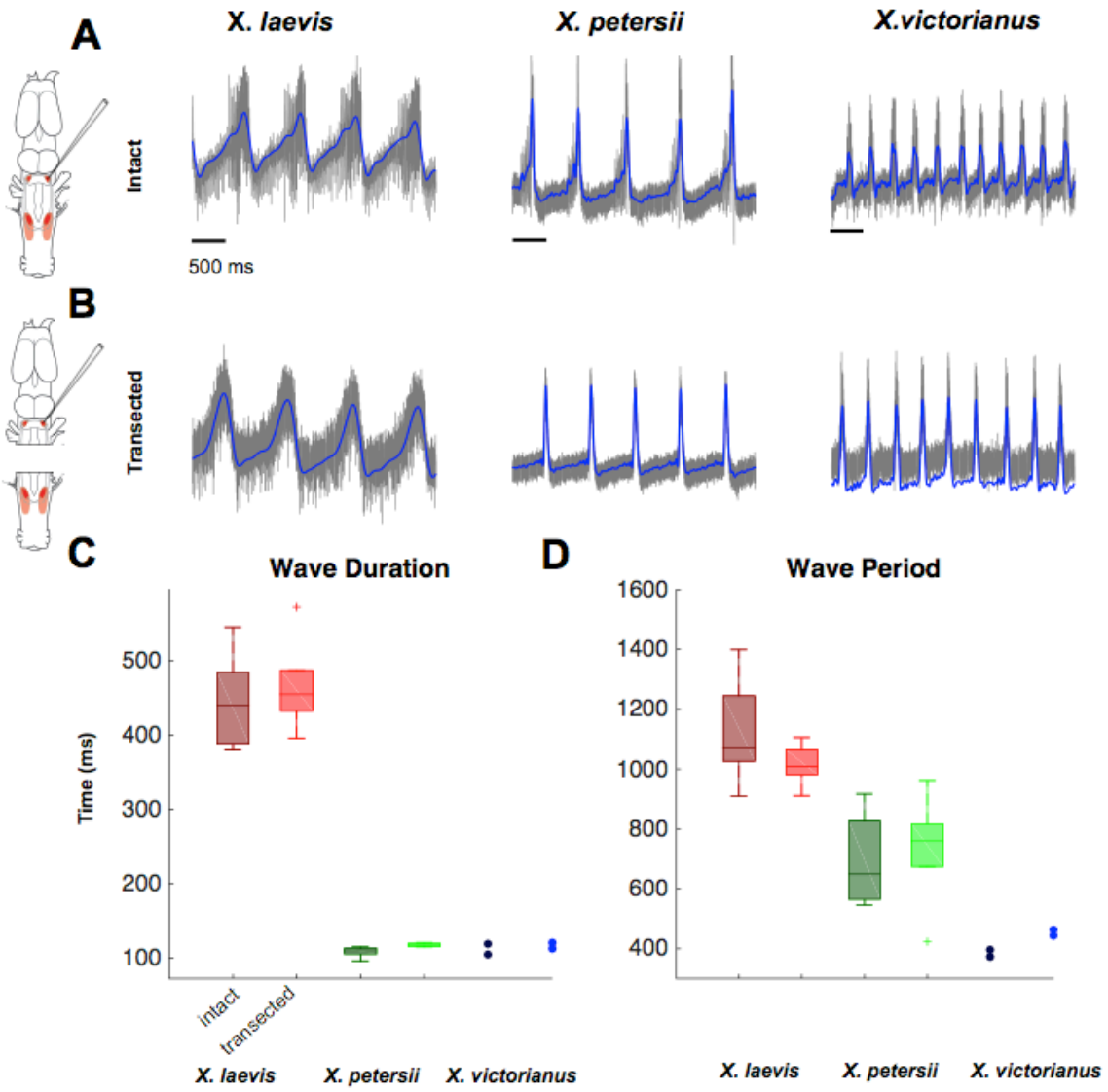

Figure 6. Species-specific LFP wave duration and period are independent of connection to caudal hindbrain

(A) Representative DTAM recording (grey) and LFP wave (blue) evoked by 5-HT application *in vitro*.

(B) Representative DTAM recording and LFP wave following transection caudal to DTAM that eliminates connections with motor nucleus N.IX-X.
(C) Boxplot (as described for **Fig. 3**) illustrating LFP wave duration prior to (*X. laevis* (n=5), *X. petersii* (n=6) and *X. victorianus* (n=2)) and following caudal hindbrain transection (*X. laevis* (n=5), *X. petersii* (n=5) and *X. victorianus* (n=2, plotted as individual means). Darker shade represents intact brains and the lighter shade, transected brains. Plus signs denote outliers. LFP wave durations are not significantly altered by transections ($p > 0.05$, 2-way ANOVA followed by Tukey's multiple comparisons tests with correction for multiple comparisons). *X. laevis* duration differs significantly from *X. petersii* ($p < 0.0001$, 2-way ANOVA, $p < 0.05$ for all comparisons). Mean ± σ: *X. laevis*: 444.2 ± 29.6 (intact), 465.3 ± 28.9 (transected), *X. petersii*: 108.7 ± 7.3 (intact), 118.0 ± 2.3 (transected), *X. victorianus:* 119.8, 105.4 (intact), 113.2, 121.1 (transected).
(D) Boxplot illustrating LFP wave period prior to and following hindbrain transection. LFP wave periods are not significantly changed by transections ($p < 0.05$, 2-way ANOVA followed by Tukey's multiple comparisons tests with correction for multiple comparisons). *X. laevis* period differs significantly from *X. petersii* ($p < 0.0002$, 2-way ANOVA, $p < 0.05$ for all comparisons)). Mean ± σ: *X. laevis*: 1,115.6 ± 188.8 (intact), 1,016.2 ± 71.4 (transected), *X. petersii*: 695.7 ± 157.5 (intact), 733.9 ± 194.4 (transected), *X. victorianus*: 372.9, 396.6 (intact), 442.5, 463.3 (transected).

Chapter III

Evolution of vocal circuits: tuning pre-motor neurons to generate divergent rhythms

Charlotte L. Barkan[1], Darcy B. Kelley[1,2], and Erik Zornik[3]

[1]Doctoral Program in Neurobiology and Behavior, Columbia University, New York, NY 10032 USA; [2]Department of Biological Sciences, Columbia University, New York, NY 10025 USA, [3]Biology Department, Reed College, Portland, OR 97202

ABSTRACT

To identify proximate mechanisms that serve the divergence of motor behaviors during evolution, we are investigating neural circuits that drive vocal behaviors in two closely related species that diverged ~8.5 million years ago, *X. laevis* and *X. petersii*. Both produce male advertisement calls that consist of alternating trains of sound pulses: a fast trill with an ~60 Hz pulse rate, and a slow trill with an ~30 Hz rate. While pulse rates are similar, calls of these species differ substantially in their duration and period; *X. laevis* trills are longer and slower than those of *X. petersii*. In a fictively calling *in vitro* brain preparation, in which compound action potential (CAP) patterns recorded from the vocal nerve correspond to sound pulse patterns of advertisement calls, we used whole cell blind-patch recordings to characterize premotor neurons in a key component of the vocal pattern generator, the hindbrain nucleus DTAM. These neurons' activity is tied to

temporal features of fast trills. We show that spikes in DTAM neurons typically precede vocal nerve CAPs by a few milliseconds, and thus spike at rates that correspond to CAP rates for the vocal nerve. In both species, many of these cells display a long-lasting depolarization (LLD) that coincides with each fictive fast trill. The LLD duration and period are strongly correlated with the duration and period of the fictive fast trill, respectively, and are significantly shorter in *X. petersii* than *X. laevis*. In the presence of tetrodotoxin, which eliminates synaptic inputs, cells oscillate in response to NMDA in a species-specific manner, with *X. laevis* brains responding to increasing doses by lengthening their oscillation duration and period, while *X. petersii* oscillations remain relatively short and rapid. Thus we have identified a population of premotor neurons that regulate species-typical vocal patterns, and whose cellular properties shape a subset of vocal patterns independent of network contributions.

INTRODUCTION

The motor circuits of closely related species are well suited for the study of the proximate mechanisms underlying divergent behaviors (Katz, 2016). Calls are stereotyped motor behaviors essential for successful courtship in many vocal species (Gerhardt and Huber, 2002). Male African clawed frogs, *Xenopus,* call underwater to attract female mates and suppress male rivals (Zornik and Kelley, 2016) using a unique advertisement call (Tobias et al., 2011).

Temporal features of behaviors are controlled centrally by finely tuned neural circuits. Recently diverged species often produce distinct behaviors, likely reflecting

evolutionary changes to the underlying circuits. These circuits can differ both in network properties such as connectivity, neuromodulation, synaptic strength and valence (e.g. Bumbarger et al., 2013; Newcomb and Katz, 2009; Chiang et al. 2006; Baltzley et al., 2010; Goaillard et al., 2009) and in intrinsic cellular properties such as bistability, ion channel expression, and current amplitude (e.g. Meyrand and Moulins, 1988a; 1988b, Goaillard et al., 2009). Divergence of any of these properties during speciation could lead to distinct behaviors in closely related species. Marked behavioral variation often reflects small differences in the tuning of neural circuits (Katz and Harris-Warrick 1999). These circuits provide a natural framework in which to examine how small changes to homologous neural networks might result in temporally distinct patterns. However, few studies of vertebrate motor circuits have identified discrete circuit properties that underlie behavioral divergence.

Courtship vocalizations are highly stereotyped motor behaviors shaped by sexual selection across species. Differences in courtship behaviors can contribute to pre-mating isolation and thus to speciation (Hoskin and Higgie, 2010). Male frogs typically produce a species-specific advertisement calls to attract appropriate female mates (e.g. Ryan and Rand, 1993; Gerhardt, 1994; Picker, 1983). Extant species of the genus of African clawed frogs each produce a unique advertisement call that serves as a species-identifier (Tobias et al., 2011). Because courtship calls diverge during speciation, these vocalizations are ideal for identifying motor circuit mechanisms that underlie behavioral differences in closely related species.

X. laevis and *X. petersii* are both part of the X. laevis clade – *X. laevis sensu lato* – and diverged approximately 8.5 million years ago (**Fig. 1A**) (Furman et al., 2015). Because they share a recent common ancestor, we expect that fine changes in their vocal motor circuits might underlie their different call patterns. *X. laevis* (**Fig. 1B**) and *X. petersii* (**Fig. 1C**) both produce a vocal pattern consisting of a train of slow rate sound pulses (slow trill) followed by a train of fast rate sound pulses (fast trill) (Tobias et al., 2011). While rates are similar across species for both slow and fast trill, the duration and period of their calls differ substantially, with *X. laevis* producing a call with a longer duration and period than *X. petersii* (Barkan et al., in review).

The *Xenopus* larynx generates pulses of sound resulting from synchronous activity of motor neurons in the vocal motor nucleus (n. IX-X; nucleus ambiguus; Albersheim-Carter et al., 2015) of the caudal hindbrain. In vivo recordings from the laryngeal nerve of advertisement calling *X. laevis* reveal that the pattern of nerve activity matches the sound pulse patterns (Yamaguchi and Kelley, 2000). Nerve patterns also closely resemble advertisement calls in isolated brain preparations. In *X. laevis* and *X. petersii*, isolated brains produce fictive behavior – compound action potential (CAP) patterns recorded from the vocal nerve that correspond to *in vivo* call patterns (Rhodes et al., 2007, Barkan et al., in review). Previous work has pinpointed a premotor rostral hindbrain nucleus DTAM (most probably homologous to the mammalian parabrachial nucleus; Wetzel et al., 1987), as responsible for differences in the temporal patterns of these species' advertisement (Barkan et al., in review). DTAM is part of the central pattern generator controlling temporal patterning of calls (Zornik et al., 2010). In both

species, a local field potential (LFP) wave intrinsic to DTAM represents species differences in call duration and period. In *X. laevis* the DTAM wave is generated by long-lasting depolarizations of a class of premotor cells, fast trill neurons (FTNs), whose phasic activity pattern corresponds to fictive fast trills (Zornik and Yamaguchi, 2012). In *X. laevis,* DTAM neurons monosynaptically excite motor neurons in the vocal motor nucleus (N. IX-X) (Zornik and Kelley, 2008) (**Fig. 1D**).

Here, we explore the hypothesis that retuning FTNs is responsible for species differences in temporal features of the advertisement call. Using whole-cell patch recordings, we identified a population of FTNs in *X. petersii* that appear to underlie species differences in call patterns and sought to determine the relative contributions of cellular properties and network activity of these homologous neurons to behavioral variation in call duration and period between X. *laevis* and *X. petersii*.

METHODS

Animal Care: All animal care and experimental procedures conformed to guidelines set forth by the National Institutes of Health and were approved by Reed College's Institutional Animal Care and Use guidelines (protocol no. 012013). Sexually mature *X. laevis* (n=10) and *X. petersii* (n=15) male frogs were used for all experiments. *X. laevis* were purchased from Nasco and *X. petersii* were from Xenopus Express (Brooksville,

FL). Animals were group housed with a recirculating water system in PETG aquaria (Aquaneering) on a 12L:12D schedule at 20°C and fed 2x weekly.

In vitro brain preparation: For these experiments (Fig. 1D), brains were isolated, bathed in 5-HT, CAPs recorded from the laryngeal nerve, and activity of neurons in DTAM monitored extracellularly (wave and spikes) and intracellularly (patch clamp). Frogs were deeply anesthetized by injection of 1.3% tricaine methanesulfonate (MS-222; Sigma; *X. laevis*: 500 - 700 µl, *X. petersii*: 200 µl) into the dorsal lymph sac. Brains were rapidly dissected from the skull and placed in ice-cold saline (in mM: 96 NaCl, 20 $NaHCO_3$, 2 $CaCl_2$, 2 KCl, 0.5 $MgCl_2$, 10 HEPES, and 11 glucose, pH 7.8, oxygenated with 99% O_2). Brains were allowed to recover for ~1 hour in saline following removal in a silicone elastomer-lined recording dish (Sylgard; Dow Corning, Midland, MI). Compound action potentials (CAPs) were recorded from the posterior rootlet of cranial nerve IX-X, which contains the axons of the laryngeal motor neurons (Simpson et al., 1986), using an extracellular suction electrode. The extracellular local field potential was recorded in DTAM using a carbon fiber electrode. The nerve and extracellular DTAM signal were amplified x1000 (Model 1700; A-M Systems, Carlsborg, WA) and band-pass filtered (10 Hz to 5 kHz), digitized at 10 kHz (Digi-data 1400A; Molecular Devices, Sunnyvale, CA), and recorded with Clampex software (Molecular Devices). The cerebellum and tectum were transected sagittally at the midline and reflected laterally to expose DTAM. Whole cell electrodes were constructed as previously described (Zornik and Yamaguchi, 2012) with thick-walled borosillicate capillary glass (1.5 mm outer

diameter; 0.86 mm inner diameter), and pulled with a Flaming/Brown style microelectrode puller (P1000; Sutter Instruments). Electrodes were placed into the fourth ventricle just below the surface of the tissue. Positive pressure was applied to the electrode that was then lowered into the tissue with a motorized micromanipulator (MC1000e, Siskiyou). Neurons were detected by advancing electrodes slowly (~1 um/sec) through the tissue between ~50 μm and ~200 μm below the ventricular surface until a rapid increase in resistance was detected. At this point, positive pressure was released, negative pressure was applied to achieve a gigaohm seal, and further brief negative pressure was applied to break into the cell and achieve a whole-cell patch recording. Serotonin (5-HT) was applied to the saline bath to achieve a final concentration of 60 μM to elicit fictive calling. Application occurred once every hour for a maximum of 5 minutes, at which time saline superfusion was resumed. Premotor vocal cells were identified by their simultaneous activity with fictive fast trill CAPs during 5-HT application. Square steps of positive and negative current were used to measure input resistance, action potential half width, spike threshold, sag index and burst index.

Pharmacology: To examine premotor vocal cells in the absence of synaptic connectivity, we applied tetrodotoxin (TTX) to a final concentration of 0.5 μM for 15 minutes after obtaining a stable recording and confirming the identity of the neuron. We then applied N-Methyl-D-aspartate (NMDA) to achieve an initial bath concentration of 25 μM. We continued to increase the NMDA concentration by 25 μM every 15 minutes until stable depolarizing oscillations occurred (6 *X. petersii* and 4 *X. laevis* cells). If recordings

remained stable, doses increased by 25 μM were applied every 15 minutes until a final concentration of 125 μM was achieved or the cell depolarized continuously. If the cell depolarized continuously, washout was reinstated to recover baseline resting potential.

Analyses:

Clampfit software was used to detect threshold search. If spikes occurred as doublets or triplets, the timing of the first spike was correlated with CAP times. A minimum of 15 calls, 100 CAPs, and 100 spikes were measured for each cell included in our analyses. Input resistance was determined from the steady-state membrane potential resulting from a series of 5 hyperpolarizing current steps beginning at -50 pA and increasing by steps of +10 pA or beginning at -100 pA and increasing by steps of +25 pA. The slope of the voltage-current curve was used to calculate resistance. Sag index was measured as: [(minimum voltage during the maximum hyperpolarizing current step) - (steady state voltage deflection in the final 500 ms of the current step)]/steady state voltage deflection as described in Farries et al. (2005). Burst index, defined as the mean of inter-spike-interval/minimum inter-spike-interval, was measured for each current step that evoked spiking and an overall mean was calculated for each neuron. Further analyses were carried out using custom-made MATLAB (Mathworks) scripts. If spikes occurred in doublets or triplets (the signal failed to return to baseline between subsequent spikes), only the first spike was measured. Instantaneous spike rate was measured as the reciprocal of each spike interval. For each spike, we found the nearest CAP and used this to measure spike to CAP delay. For each corresponding CAP, we measured the reciprocal

of the interval to the following CAP to calculate the instantaneous CAP rate. Spike to CAP delay histograms were created using the nearest CAP to each spike (bin width = 0.5 ms). Fast trill onset was determined as previously described (Barkan et al. in review). Briefly, when two or more sequential CAPs achieved an instantaneous rate of >50 Hz, the time of the first CAP was considered fast trill onset. Fast trill offset was measured as the time of the last CAP before the rate fell below 50 Hz. Some fast trill neurons displayed long lasting depolarizations (LLDs). To measure their properties, signals were low-pass filtered (*X. laevis*: 5 Hz, *X. petersii*: 20 Hz), and the 'findpeaks' function in the MATLAB Signal Processing Toolbox was used to measure their peak time by finding local maxima. LLD duration was defined as their width at half-height, and period was measured from the peak of one LLD to the peak of the subsequent LLD.

Statistics

Mann-Whitney U-tests in Prism 7 were used to compare spike rate during calling, CAP rate during calling spike to CAP delay, resistance, resting potential, action potential half-width, sag index, burst index, and spike threshold. Linear regression analyses comparing instantaneous spike rate to CAP rate and spike to CAP delayed, as well as those comparing call duration and period to LLD duration and period was performed using the 'LinearModel.fit' function in the Statistics and Machine Learning MATLAB Toolbox (Mathworks).

RESULTS

Neurons in DTAM are active during fictive calling in both species

A previous study (Barkan et al., in review) provided strong evidence to consistent with the hypothesis that DTAM controls species-specific call duration and period in both *X. laevis* and *X. petersii*. Furthermore, earlier work in *X. laevis* (Zornik and Yamaguchi, 2012) identified premotor vocal neurons, termed 'fast trill neurons' (FTNs), in DTAM that spiked phasically with nerve CAPs during fictive fast trills. To identify potential *X. petersii* FTN homologues that might underlie species differences in call pattern, we used obtained whole-cell recordings in DTAM in *X. laevis* and *X. petersii*.

Consistent with previous findings, FTNs in *X. laevis* (**Fig. 2A** top) depolarized and spiked only during fictive fast trills (**Fig. 2A** bottom). In *X. petersii,* we identified a similar population of DTAM neurons (**Fig. 2B** top) that also depolarized and spiked during fictive fast trills (**Fig. 2B** bottom). As in *X. laevis*, these *X. petersii* fast trill FTNs produced spikes that accompanied individual fictive fast trill CAPs recorded from the laryngeal nerve (**Fig. 2C-E**). In *X. laevis*, spikes occurred singly (**Fig. 2C**), doubly (**Fig. 2C** black arrowheads) or as triplets (not shown). In most cases, the first (or only) spike preceded each fast trill nerve CAP. In *X. petersii*, we also found cells with single spikes (**Fig. 2D**) and doublets (**Fig. 2E**, black arrowheads), in which the first spike typically preceded CAPs. For both species, the first spike in a doublet or triplet was used for further analysis. In total, we recorded 7 *X. laevis* FTNs from 6 animals and 7 *X. petersii* FTNs from 7 animals during sustained fictive calling.

FTN spikes correspond to CAPs

In most *X. laevis* FTNs, spikes preceded CAPs, with an average spike-to-CAP delay of 3.41 ± 1.45 ms (Mean ± SD), consistent with previous findings (Zornik and Yamaguchi, 2012). When we examined the spike to CAP delay in *X. petersii* FTNs, we found a similar relationship, with spikes preceding CAPs on average by 3.45 ± 1.77 ms. While there is no statistical difference between the spike-to-CAP delay between species (Mann Whitney U-test, $p > 0.05$), there was variation across cells in both species. To examine the variation in spike timing across cells and species, we plotted histograms for each cell showing the distribution frequencies of spike-to-CAP delays for all spikes (**Fig. 3A, B**). For most neurons in both species, the majority of spikes occurred before each CAP (indicated by a positive spike-to-CAP delay). In 6 out of 7 *X. laevis* cells and in 5 out of 7 *X. petersii* cells, the spike-to-CAP delay ranged from 1.5 to 7.5 ms. In some cells, however, CAPs often preceded spikes. We found that in 1 of 7 *X. laevis* FTNs and 2 of 7 *X. petersii* FTNs, most spikes followed CAPs (as indicated by a negative spike-to-CAP time) rather than preceding them. Thus, while FTN spikes are time-locked to CAPs and the range of variation is similar across species, the spike-to-CAP delay varies across FTNs.

FTN spike rates correlate with CAP rates

We compared instantaneous spike rate (**Fig. 4A**) and instantaneous CAP rate of each CAP following a spike (**Fig. 4B**) during fictive calling in each species. During fictive

calling bouts, mean spike rates were slower in *X. laevis* than *X. petersii* (Mean ± SD: *X. laevis*: 48.4 ± 9.90, *X. petersii*: 64.7± 5.93, Mann-Whitney, U=2, $p < 0.05$). The *X. laevis* spike rate is likely slower due to the presence of FTN spiking during the introductory phase of fast trill. This phase consists of slower rate CAPs of lower amplitude that both increase at fast trill onset. *X. petersii* calls lack the introductory phase and thus rarely have cells with slower rate spikes. CAP rate however, was not significantly different in *X. laevis* than *X. petersii* (Mean ± SD: *X. laevis*: 56.4 ± 4.86, *X. petersii*: 65.2 ± 7.76, Mann-Whitney, U=7, $p > 0.05$).

Next, we examined the relationship of spike rate to corresponding CAP rate and performed linear regressions. Across cells, the spike rate was highly correlated with the CAP rate in both *X. laevis* (**Fig. 4C**, $R^2 = 0.86$, slope = 0.806, $p<0.05$) and *X. petersii* (**Fig. 4D**, $R^2 = 0.892$, slope = 0.945, $p<0.05$). The correspondence between spike and CAP rates for each individual animal is consistent with the hypothesis that FTN activity controls the rate of fictive calls for both species.

Intrinsic cellular properties of DTAM FTNs are similar in both species

For 15 *X. laevis* FTNs and 11 *X. petersii* FTNs, we found no significant differences between species (Mann-Whitney tests, for all $p > 0.05$) in measures of resistance (MΩ), resting potential (mV), action potential half width (ms), sag index (a value > 0.1 indicates significant I_h current is present), burst index (a value > 1 indicates some burstiness is present and the cell does not spike uniformly) and spike threshold (pA) (**Fig 5A-F**). The

similarity in these intrinsic cellular properties between *X. laevis* and *X. petersii* is consistent with the hypothesis that these neurons are homologous cell types.

FTN activity matches call duration and period

Next, we examined FTN activity relative to duration and period of fictive calls. Many FTNs in both species exhibited long lasting depolarizations (LLDs) (**Fig 6A and B, Whole Cell**) that coincided with fictive fast trill **(Fig 6A and B, Nerve**), as well as an extracellular local field potential (LFP) wave **(Fig 6A and B, LFP)**. This LFP wave has previously been described in *X. laevis* and *X. petersii* and was found to strongly correlate with species-differences in call duration and period (Zornik et al., 2010; Barkan et al., in review). We examined duration and period of the FTN LLDs in relation to the fictive call duration and period. Just as *in vivo* fast trill and fictive fast trill duration and period are significantly longer in *X. laevis than X. petersii* (Barkan et al., in review), we also found that LLD duration and period in *X. laevis* are significantly longer than *X. petersii* (Mann Whitney tests, $p<0.05$, **Fig 6C, D**). We found that LLD duration and period are strongly correlated with fast trill duration and period, respectively (Duration regression: $R^2 = 0.969$, slope = 0.7665, $p<0.0001$, **Fig 6E,** Period regression: $R^2 = 0.993$, slope = 1.0293, $p<0.0001$, **Fig. 6F**). These temporal properties of FTNs are consistent with – and may contribute to – temporal properties of call differences between the two species.

Intrinsic FTN synaptic conductances may underlie species-specific vocal patterns

To examine whether species-specific characteristics of FTNs are intrinsic, we synaptically isolated FTNs with bath application of tetrodotoxin (TTX). After TTX treatment, NMDA was applied to induce membrane potential oscillations (*per* Zornik et al. 2012). Oscillations were evoked in 6 *X. petersii* and 3 *X. laevis* cells (**Fig 7A**). All FTNs that were held through this protocol produced oscillations. The concentration of NMDA required to achieve stable oscillations varied across cells: 25 to 75 μM in *X. laevis* and 25 to 100 μM in *X. petersii*. We next asked whether oscillation duration and period at each cell's threshold dose are consistent with each species' LLD duration and period. Values for each species do not differ significantly for either duration (**Fig. 7B**) or period (**Fig. 7C**) at the threshold dose (Mann Whitney U-test, $p > 0.05$ for each comparison).

We then determined how each cell responded to increasing concentrations of NMDA. *X. laevis* and *X. petersii* differed substantially in sensitivity of oscillations to increasing NMDA concentration. For a subset of the FTNs in which stable oscillations were achieved, we increased the bath-concentration of the drug by 12.5 or 25 μM every 15 minutes. In the 3 *X. petersii* cells that were exposed to multiple doses, there was no change in either oscillation duration or period as the NMDA concentration increased. In the 3 *X. laevis* cells, however, the duration (**Fig. 6D**) and period (**Fig. 6E**) of the oscillation increased substantially with increasing concentration. These limited observations suggest that FTNs in *X. petersii* are less sensitive to NMDA than FTNs in *X. laevis*.

DISCUSSION

Divergent vocal patterns are supported by homologous premotor neurons

We investigated the vocal motor circuits of two recently diverged species, *X. laevis* and *X. petersii*, to identify mechanisms underlying their distinct behaviors. *X. petersii* and *X. laevis* both produce an advertisement call that includes alternating slow and fast rate trills, but the period and duration of calls are much shorter in *X. petersii* than in *X. laevis,* and these call patterns are mirrored in the CAP patterns of each species' fictive advertisement call (Barkan et al., in review). We identified a group of premotor vocal cells in *X. laevis* and *X. petersii* that appear to underlie species differences in their vocal behavior. We found that these premotor neurons spike at fast rates that correlate tightly with fictive fast trill rates, and that in most cells, spikes are time-locked to CAPs. Across species, spike rates and CAP rates are similar. However, these cells differ in their long lasting depolarization (LLD) duration and period in a manner consistent with species differences in measures of call duration and period. While the basic cellular properties that we examined (e.g. resting membrane potential, membrane resistance, action potential half-width) were similar in *X. petersii* and *X. laevis*, we identified species differences in sensitivity to NMDA-evoked membrane oscillations in FTNs. These observations is consistent with the hypothesis that FTNs in the two species are homologous, and that differences in synaptic NMDA conductances are a candidate mechanism for driving divergent vocal patterns during speciation.

Advertisement calls of the Xenopodinae

The temporal features of the two most prominent call types – the male advertisement call and male and female release calls – have been surveyed across the genus *Xenopus* (Tobias et al., 2011; Tobias et al., 2014). Male advertisement calls temporal and spectral features serve as unique species identifiers. Male and female release calls are, in contrast, very similar across the phylogeny. This difference may reflect evolutionary selection for features of advertisement calls that distinguish diverging populations, avoiding the reproductive cost of hybridization (Mayr, 1963), versus general reproductive information (same sex or non-reproductive) conveyed by release calls.

Mechanisms underlying Xenopus advertisement call pattern evolution

In contrast to the divergent calls of closely related species studied here, two other *Xenopus* species – *X. boumbaensis* and *X. borealis* – produce similar calls that are genetically divergent (Tobias et al., 2011; Evans et al., 2016). A parsimony analysis suggested that the ancestral call for the *Xenopus* genus was a train of 2-14 pulses of sound (Tobias et al., 2011). Both *X. boumbaensis* and *X. borealis* however produce a call consisting of only a single pulse of sound, with each call separated by a long interval. The single sound pulse call could thus be a derived, convergent character (see Leininger and Kelley, 2015).

When fictive calling was recorded from the vocal nerve of isolated brains, *X. boumbaensis* produced a train of 2-3 rapid CAPs for each call, while *X. borealis*

produced only a single CAP (Leininger and Kelley, 2013). One scenario for producing this derived pattern in *X. boumbaensis*, suggested by the current results (and Barkan et al., in review), is shortening of the duration of FTN activity to ~20ms (as in *X. petersii*). FTN durations of ~20ms are associated with the multiple CAPs required for each sound pulse in all three species (Tobias et al., 1995; Leininger and Kelley, 2013; Barkan et al., in review). *X. borealis* does not require multiple CAPs to produce each sound pulse and its call pattern shortening likely reflects a different mechanism (see Leininger and Kelley, 2015).

Evolution of hindbrain circuits for respiration and vocalization

Sound production in vertebrates often requires respiration, and hindbrain neural circuits for breathing and calling are thus likely to be linked and to have co-evolved (*e.g.* Martin and Gans, 1972; reviewed in Leininger and Kelley, 2015). For instance, in many terrestrial frogs, vocalization requires DTAM activity and expiration (Schmidt, 1992; Schmidt, 1993). Vocalization became decoupled from respiration when Pipids became aquatic ~150 million years ago (Evans et al., 2004; Cannatella and De Sa, 1993; Irisarri et al., 2011). When DTAM is stimulated, and vocal motor neurons are activated, glottal motor neurons are inhibited (Zornik and Kelley, 2008) suggesting that respiration is suppressed during vocalization (the glottis gates the connection between the larynx and attached lungs and the buccal cavity), suggesting a rewiring of the ancestral circuit coupling respiration and vocalization.

Intrinsic FTN conductances may contribute to behavior variation

Different species produce distinctive vocal patterns. For courtship songs, these differences have been linked to the prezygotic isolating mechanisms that impede hybridization as populations diverge (*e.g.* Klump and Gerhardt , 2013). However they have not addressed the proximate mechanisms that drive vocal pattern divergence. *X. laevis* FTNs respond to increasing bath NMDA concentrations by lengthening their oscillation duration and period while *X. petersii* neurons do not. Intrinsic oscillations in central pattern generator neurons are frequently seen and are known in other systems to be induced by NMDA (e.g. Kiehn et al., 1996; MacLean et al., 1997; Prime et al., 1999). However, to our knowledge, no study has previously documented temporal differences in these oscillations that are directly correlated with species differences in temporal features.

We propose that for *Xenopus* FTNs encode call duration and period with their LLD during fictive calling. Call duration and period may be intrinsically encoded in FTNs, an idea supported by species-specific membrane oscillation periods when neurons are synaptically isolated. The species difference in sensitivity to NMDA concentrations suggests candidate molecular mechanisms, such as NMDA receptor expression level differences. If, for example, FTN neurons in *X. laevis* express more NMDA receptors, they could respond to increasing amounts of NMDA with greater NMDA currents that could induce longer oscillations. In contrast, *X. petersii* FTNs expressing NMDA receptors at lower levels might be saturated such that increasing doses of NMDA would

not increase the inward NMDA current. This scenario is consistent with models of TTX-NMDA induced oscillations in lamprey spinal neurons that revealed decreasing period with increasing bath concentration of NMDA (Tegner et al., 1998; but see Huss et al. 2008). NMDA receptor functionality – *e.g.* voltage sensing – could also differ between the species and the ongoing sequencing of the X. laevis clade genomes may reveal sequence differences between *X. laevis* and *X. petersii.*

LLDs during fictive calling, as well as NMDA-induced oscillations, are the result of a combination of inward and outward currents. It is thus also possible that a mutation or change in expression of one of the channels underlying these currents led to the species difference we observe in the oscillations and LLDs of *X. laevis* and *X. petersii*. Because of the slow temporal profile of these events, a likely candidate is calcium-activated potassium channels. El Manira et al. (1994) showed using TTX-NMDA-induced oscillations in spinal cord neurons that blocking one class of calcium-activated potassium channels (SK) led to oscillations with a lengthened duration and period. A naturally occurring and behaviorally relevant change in $I_{k(Ca)}$ has recently been identified. Using a genetic mapping approach, Ding et al. (2016) found that in two species of Drosophlia, a 9.7 Hz difference in sine song carrier frequency is due to insertion of a retroelement in a gene encoding a calcium-activated potassium channel. While ion channels are highly pleiotropic, alternative splicing and tissue specific expression make them ideal candidates for evolution of behavioral divergence. Changes to ion channels are good candidates for circuit variation that could result in behavioral divergence.

Evolution of behavior through circuit modification

While intrinsic features of FTNs and their synaptic conductances in *X. petersii* and *X. laevis* may partially account for differences in call duration and period, it is likely that changes to network properties, such as connectivity, neuromodulation and synaptic strength, also underlie species differences. Most of the work on this question has used invertebrates in which homologous neuron types can be identified and the circuits mapped in detail.

Evolution of a motor pattern through connectivity rewiring

Homologous neurons can be modified to serve different functions and thus allow distinct behaviors in different species. Bumbarger et al. (2013) showed that altered connectivity of homologous neurons resulted in distinct behaviors: *Caenorhabditis elegans* is a microbivore and feeds using pharyngeal pumping, but a related species, *Pristionchus pacificus*, is predatory and uses its jaws to feed. Extensive rewiring of their homologous neuronal network seems to be the cause of their behavioral differences. Furthermore, in a model of a reciprocally inhibitory two-cell circuit in the stomatogastric nervous system (STG), changing synaptic strengths results in changes to burst duration and period (Sharp et al., 1996).

Evolution of a motor response due to synaptic sign change

In leeches, two species display distinct behaviors in response to mechanical stimulation as a result of differences in synaptic connectivity of mechanoreceptors (Baltzley et al., 2010). One species responds to stimuli with a local, one-sided body contraction, while the other responds to the same stimulus with contraction of both sides of its body. This difference is at least partially explained by polysynaptic inhibitory connectivity of the locally-bending species, in contrast to polysynaptic excitatory connectivity of the full body bending species.

Evolution of behavior by co-opting another CPG's neuromodulatory function

In nudibranch sea slugs, some species swim with dorsal-ventral flexion while others swim with left-right flexions. Non-overlapping groups of homologous neurons make up separate CPGs that underlie these distinct behaviors. However, in left-right swimmers, a homologue from the dorsal-ventral CPG can neuromodulate the left-right CPG and thus influence the resulting behavior (Newcomb et al., 2012, Newcomb and Katz, 2009).

Fast trill duration and call period are intrinsic to FTNs, but fast trill rate is not.

Our work suggests that FTNs are able to encode fast trill duration and call period (this study, Barkan et al., in review). We find that when the connection between n. IX-X is removed, the DTAM LFP in both species remains the same in measures of duration and period. This strongly suggests that FTN LLDs remain unchanged in measures of duration and period when the connection to n. IX-X is severed. This supports the idea that fast trill

duration and period are intrinsic to FTNs. However, spike rate does not appear to be intrinsic to FTNs. Recent work in *X. laevis* found that disrupting the connection between n. IX-X results in highly variable FTN spike rates during 5-HT induced DTAM waves that are not consistent with the ~60 Hz rate during normal 5-HT induced fictive calling. Therefore, FTNs alone are not sufficient to encode the correct rates during fictive fast trill (Lawton et al., in review). No fictive calling occurs when DTAM is separated from N. IX-X (Rhodes et al, 2007, Lawton et al., in review). Together these observations suggest that across *Xenopus* species, connectivity between N. IX-X and DTAM is required to maintain the characteristic spike rate for fictive calling, but is not required for DTAM to encode fast trill duration or period.

Power of looking at closely related species with diverging behaviors

As discussed earlier, Ding et al. (2016) were able to use genetic approaches to identify differences in gene regulation of ion channels that resulted in distinct behavioral phenotypes in two different species. However, their approach did not enable identification of the neural circuit affected by this regulation change that results in species-specific courtship song. Our system is provides an ideal to complement their finding. We have identified premotor neurons that underlie the vocal patterns differences in two species. Given the extensive similarities of these cells, and the relatively recent divergence of these two species, it is likely that these are homologous neurons that underwent small but substantial changes during speciation that led to their divergent vocal patterns. A combination of genetic approaches and further functional studies, will

extend our understanding of the proximate mechanism underlying generation of distinct species call patterns.

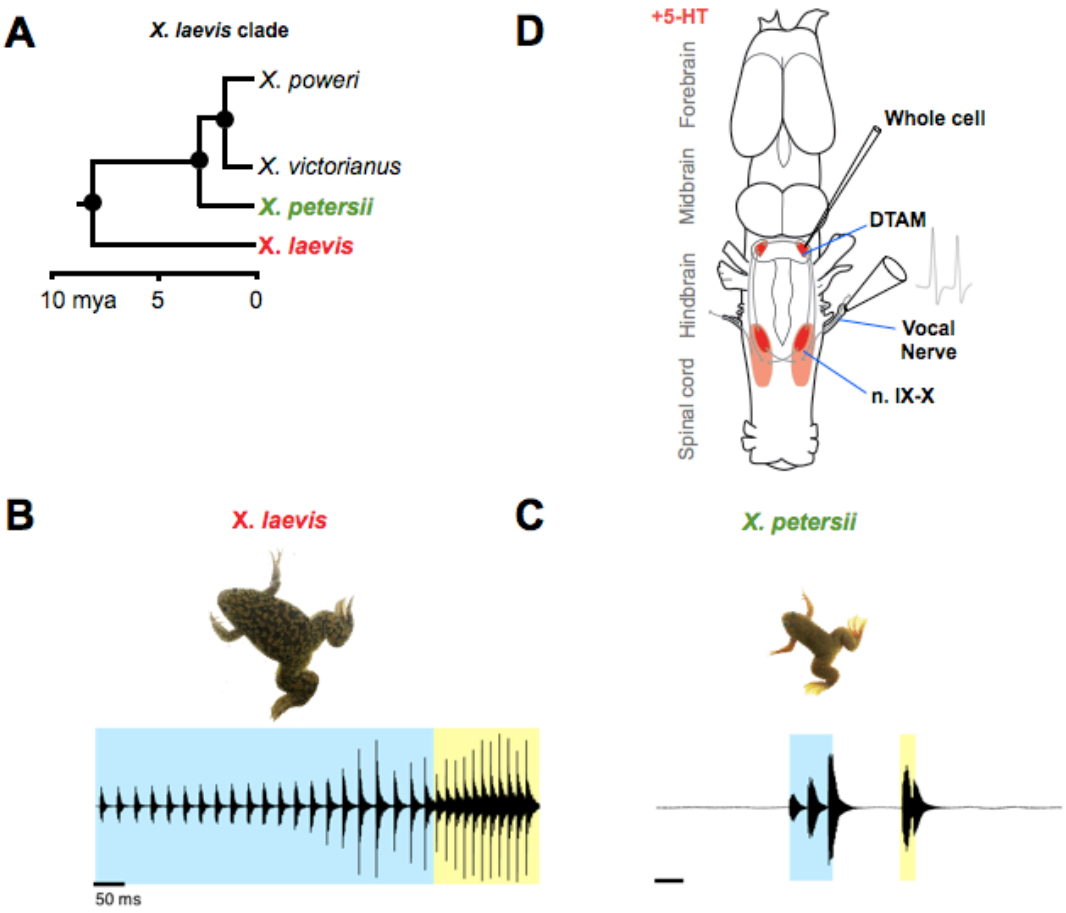

Figure 1: Evolution of the *Xenopus* vocal circuit

(A) The X. laevis clade or *X. laevis sensu lato* includes 4 species that diverged ~8.5 million years ago. Each species produces a unique advertisement call pattern.

(B) *X. laevis* produces a biphasic call consisting of a long, slow rate trill (~30 Hz sound pulses) followed by a long, fast rate trill (~60 Hz).

(C) *X. petersii* produces a biphasic call consisting of a brief, slow rate trill

(~30 Hz sound pulses) followed by a brief, fast rate trill (~60 Hz).
(D) A schematic representation of the known hindbrain vocal central pattern generator nuclei. Motor nucleus (n.) IX-X contains vocal motor neurons. These neurons send their axons via the vocal (laryngeal) nerve to the larynx, the vocal effector organ. Fictive calling can be recorded from the vocal nerve using a suction electrode. Premotor neurons in DTAM project monosynaptically to n. IX-X. In DTAM, whole cell and extracellular local field potential electrodes can record activity associated with fictive calling.

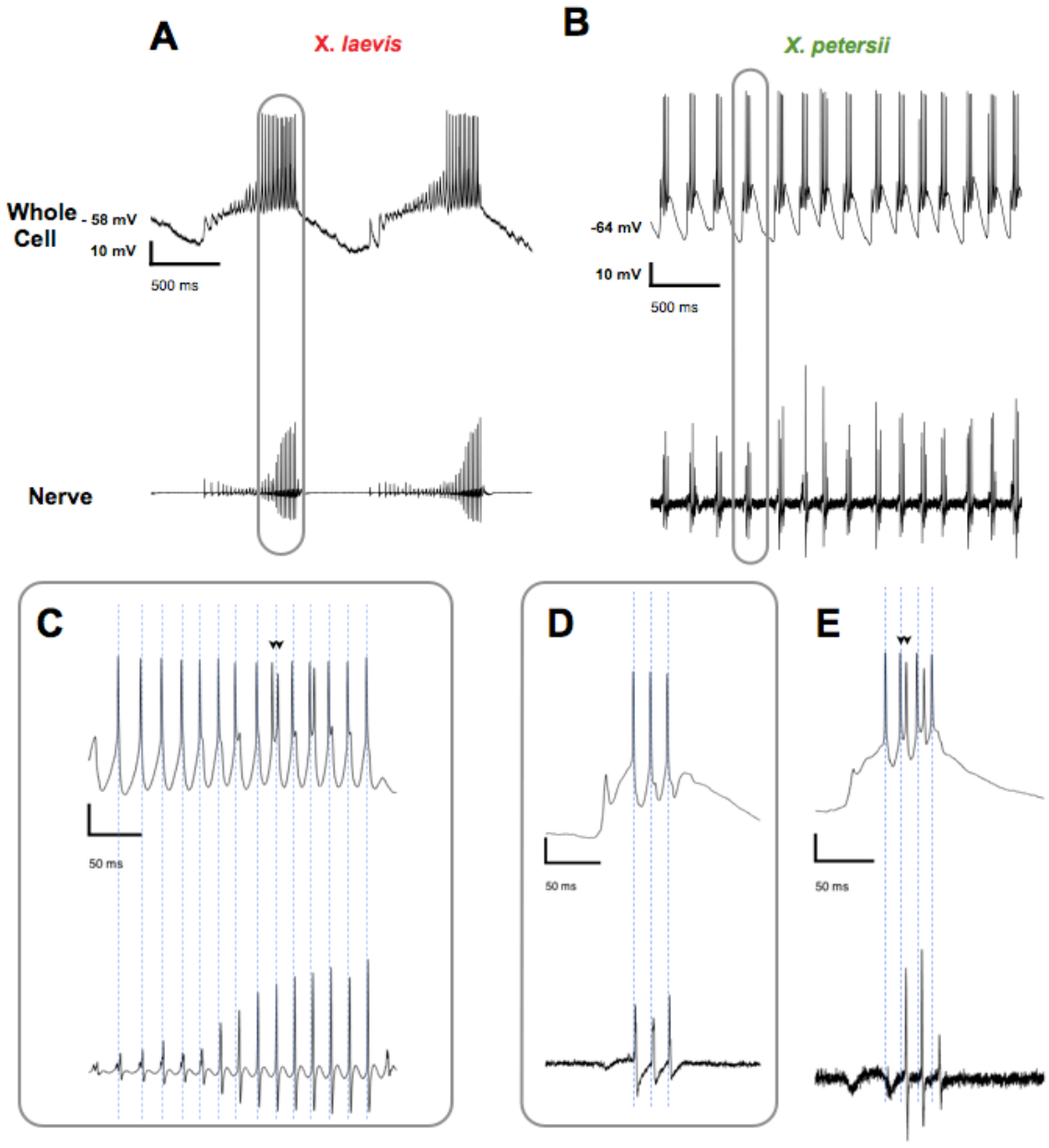

Figure 2: **FTN spikes coincide with fictive fast trill CAPs**

Representative traces of (A) *X. laevis* and (B) *X. petersii* fictive calling induced by 5-HT application. Consistent with actual calling (bottom trace), the *X. petersii* fictive call is significantly shorter than the *X. laevis* call in duration and period. Fast trill neurons

depolarize and spike in (A) *X. laevis* and (B) *X. petersii* during fictive fast trill. Spikes coincide with and usually precede CAPs by ~3.5 ms in (C) *X. laevis* and (D) *X. petersii*. Spikes often occur in pairs in (C) *X. laevis* (black arrowheads) and (E) *X. petersii* (black arrowheads).

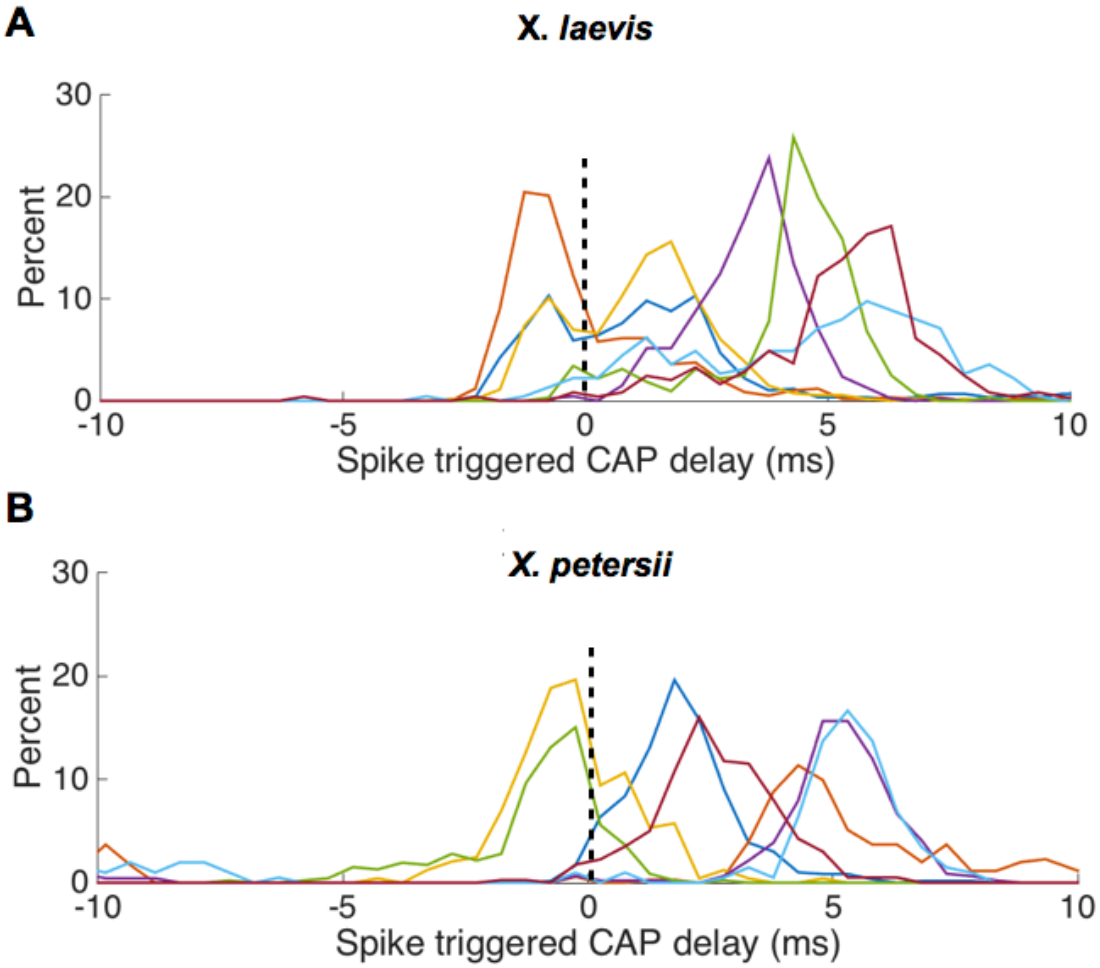

Figure 3: Consistent spike-triggered CAP delay between species

(A) For each *X. laevis* FTN spike, the delay to the closest CAP was measured. Histograms (bin width = 0.5 ms) depict the frequency of delays for each cell. In most cells, the majority of spikes preceded CAPs, leading to positive values for spike-to-CAP delay. However, for 1 cell the majority of CAPs preceded spikes (orange), as indicated by the negative spike-to-CAP delay value.

(B). For each *X. petersii* FTN spike, the delay to the closest CAP was measured. In most cells, the majority of spikes preceded CAPs, leading to a positive value for spike-to-CAP

delay. However, in 2 cells, the majority of CAPs preceded spikes (yellow, green).

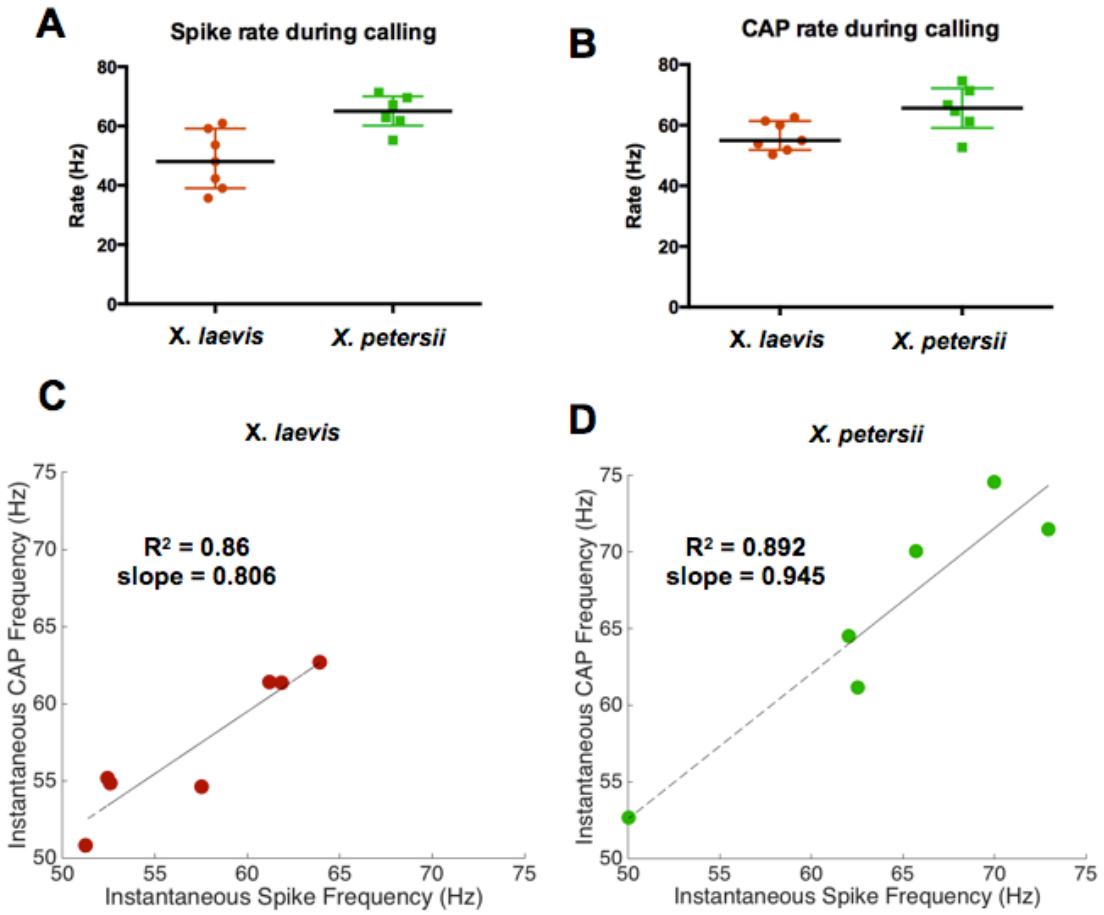

Figure 4: FTN spike rate is associated with CAP rate

(A) Spike rate in *X. laevis* is similar to, but slower, than spike rate in *X. petersii* ($p < 0.05$, Mann-Whitney U-test).

(B) CAP rate in *X. laevis* is not significantly different than CAP rate in X. *petersii* ($p > 0.05$, Mann-Whitney U-test).

(C) Linear regression revealed a strong correlation across *X. laevis* FTNs between their average spike rate and their average CAP rate ($p < 0.05$).

(D) Linear regression revealed a strong correlation across *X. petersii* FTNs between their average spike rate and their average CAP rate ($p < 0.05$).

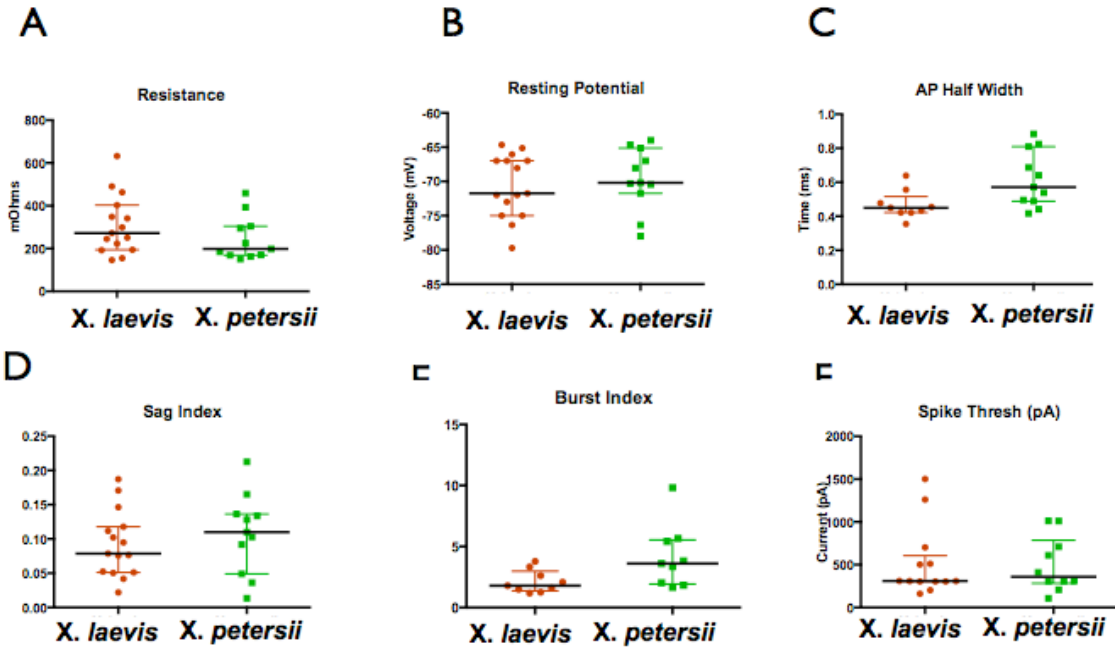

Figure 5: FTNs do not differ across species in intrinsic cellular measures

A comparison of *X. laevis* and *X. petersii* FTNs in measures of (A) resistance, (B) resting membrane potential, (C) action potential half-width, (D) sag index, (E), burst index, and (F) spike threshold revealed no significant differences between the species (Mann-Whitney U-tests, for all comparisons, $p > 0.05$).

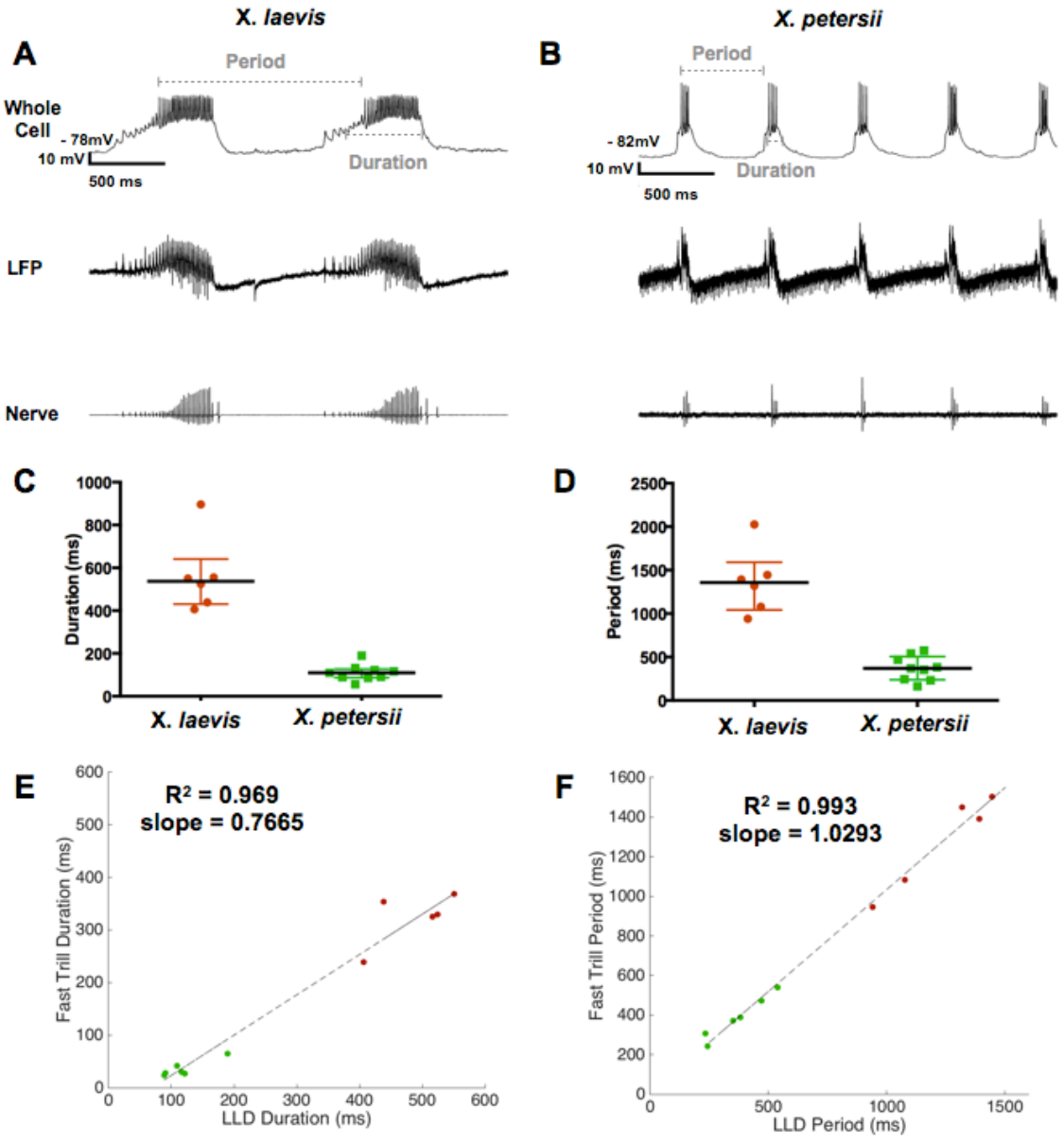
X. laevis
X. petersii
A
B
Period
Whole Cell
- 78mV
10 mV
500 ms
Duration
LFP
Nerve
- 82mV
C
D
Duration (ms)
Period (ms)
X. laevis
X. petersii
E
F
R² = 0.969
slope = 0.7665
Fast Trill Duration (ms)
LLD Duration (ms)
R² = 0.993
slope = 1.0293
Fast Trill Period (ms)
LLD Period (ms)

Figure 6: FTN LLD duration and period is strongly correlated with fast trill duration and period

Representative whole cell recordings from (A*) X. laevis* and (B) *X. petersii* FTN (top) during fictive calling (bottom). Both FTNs have an evident long-lasting depolarization (LLD) that coincides with their fictive fast trill. The duration of the LLD was measured from width at half-peak and the period was the distance from one LLD to the next. A LFP wave recorded in DTAM (middle) also corresponds to each LLD and is thought to be the extracellular correlate of the synchronous LLDs of many FTNs during fictive calling.

(C) The *X. laevis* LLD duration is significantly longer than the *X. petersii* LLD duration ($p < 0.05$, Mann-Whitney U-test).

(D) The *X. laevis* LLD period is significantly longer than the *X. petersii* LLD period ($p < 0.05$, Mann-Whitney U-test).

(E) Across FTNs, the *X. laevis* and *X. petersii* mean LLD duration strongly correlate with the mean fast trill duration ($p < 0.0001$).

(F) Across FTNs, The *X. laevis* and *X. petersii* mean LLD period strongly correlate with the mean fast trill period ($p < 0.0001$).

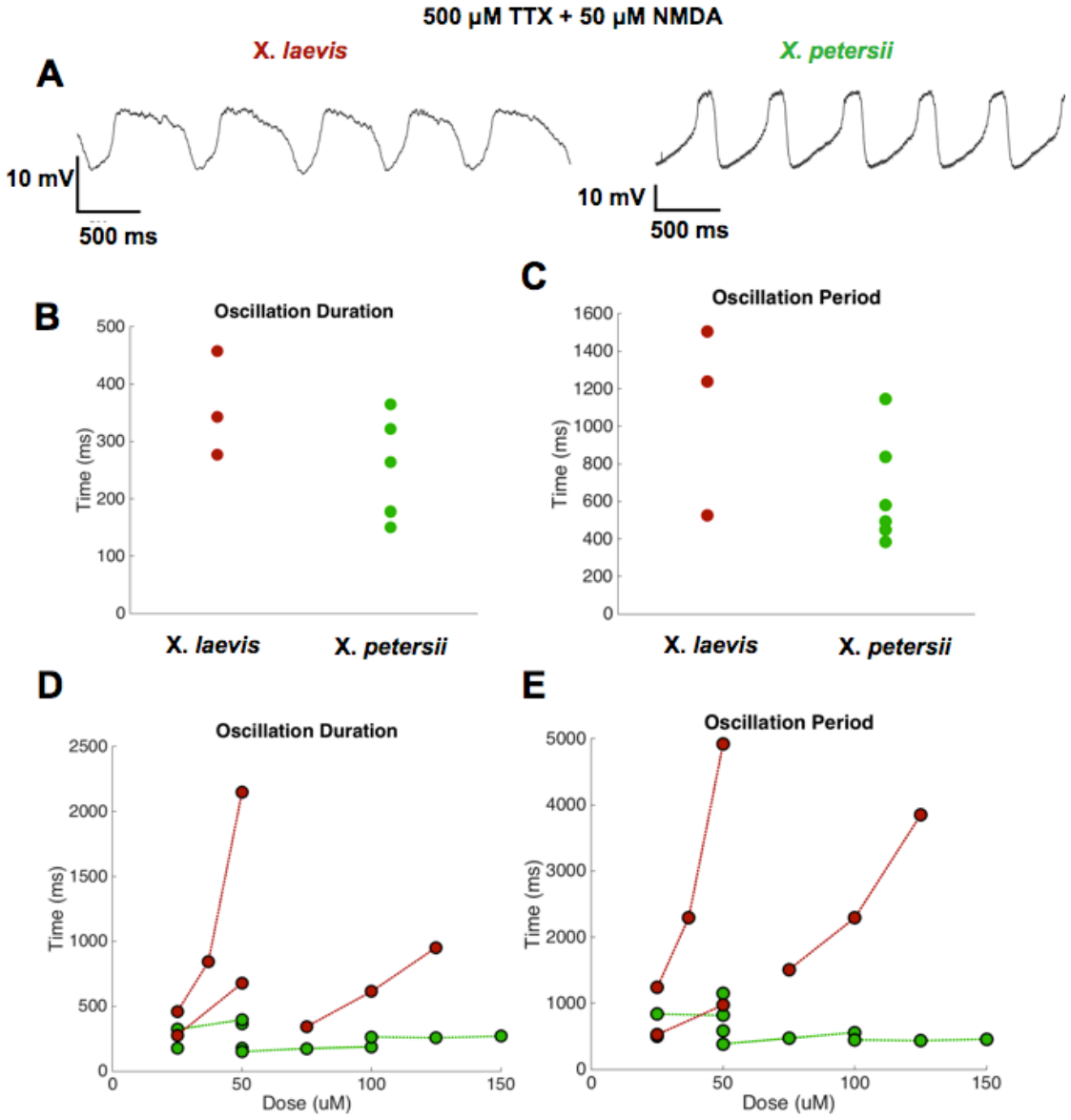

Figure 7: FTNs differ across species in their sensitivity to NMDA

(A) Representative traces of TTX+NMDA induced oscillations in *X. laevis* and *X. petersii* FTNs. There are no significant differences between NMDA-induced oscillation

(B) duration and (C) period across species (Mann-Whitney U tests, $p > 0.05$). However, there is a difference in (D) duration and (E) period in response to increasing NMDA dose in three *X. laevis* FTNs, but not in three *X. petersii* FTNs.

Chapter IV

Conclusion and future directions

ABSTRACT

In this chapter I summarize my findings from electrophysiological studies of the vocal central pattern generator of three species from the *Xenopus laevis sensu lato* clade. Results from my first study indicate that a premotor hindbrain nucleus, DTAM, is likely responsible for species-differences in call patterns across three species of this clade. The results of my next study, in which I employed whole-cell patch electrophysiology techniques, indicate that a single cell type in DTAM underlies these species differences. These experiments provide insight into proximate mechanisms underlying behavior variation in closely-related species. I finish by describing preliminary data investigating 1) mechanisms underlying intrinsic species differences in fast trill neurons encoding duration and period, 2) the role of the peripheral vocal effector as a behavior modifier in evolution, and 3) genetic approaches to behavior variation.

Ion channels could impart FTNs with intrinsic species-specific conductances

In *X. laevis*, *X. petersii*, and *X. victorianus*, a slow local field potential wave (LFP) underlies fictive fast trill. The duration and period of this LFP wave correlate strongly with fictive fast trill duration and period, respectively. Furthermore, when the

compartment of the hindbrain containing DTAM is separated rostrally from the midbrain and forebrain and caudally from the vocal motor nucleus, the duration and period of this wave remain unchanged. These results suggested that species-specific fast trill duration and period are encoded autonomously in DTAM (see Chapter 2). In the next chapter, I identify neurons that appear to underlie this LFP wave in *X. laevis* and *X. petersii*. These fast trill neurons (FTNs) exhibit long-lasting depolarizations (LLDs) during fictive fast trill. These LLDs correlate strongly with fast trill duration and period and the LFP wave (see Chapter 3). Thus, it is likely that FTNs drive fast trill duration and period, leading to the question; what FTN properties impart these species-specific durations and periods?

What FTN properties impart species-specific durations and periods?

We used TTX and NMDA to induce FTN oscillations that could be studied in the absence of synaptic input. TTX-resistant, NMDA-evoked membrane oscillations are thought to contribute to generating rhythmic movements (Hochman et al., 1994). What mechanisms underlie these oscillations? The NMDA receptor is a cation channel and glutamate receptor. Binding of magnesium (Mg^{2+}) or zinc to the receptor blocks the passage of cations through the channel. A possible scenario for NMDA-evoked oscillations is that initially some NMDA channels are not occupied by Mg^{2+} and these receptors are activated when NMDA binds the receptor, leading to depolarization of the cell's membrane via sodium, calcium, and potassium ion entry. This depolarization dislodges and repels blocker Mg^{2+} ions and more NMDA channels activate. At this point, voltage-dependent calcium channels also open and allow calcium entry into the cell.

Collectively, cation entry produces long lasting depolarizations (LLDs) of the cell. Eventually, cells repolarize due to opening of outward potassium channels, such as calcium-activated potassium channels and voltage-dependent potassium channels. At this point the cell repolarizes and the cycle begins again (Huss et al. 2008).

What outward currents terminate FTN oscillations?

As described in this scenario, one possible class of channels that may terminate the LLD is calcium-dependent potassium channels (K^+_{Ca}) (El Manira et al., 1994; Cazalets et al., 1999; Del Negro et al., 1999; Tahvildari et al., 2008). K^+_{Ca} channels comprise large conductance (BK), small conductance (SK), and intermediate conductance (IK) channels. SK channels are known to be involved in the termination of plateau potentials, persistent inward currents that involve NMDA receptors and potassium channels. In the lamprey locomotor circuit, selectively blocking SK channels with apamin leads to significant lengthening of NMDA-induced plateau potential oscillations in synaptically isolated motor neurons and interneurons (El Manira et al. 1994). Similarly in *X. laevis* and *X. petersii,* synaptically isolated fast trill neurons produce oscillations in the presence of NMDA similar to the LLDs produced during fictive calling. Thus differences in K^+_{Ca} channel expression and kinetics are likely explanations for the differences in LLD wave durations across species. For instance, if these channels were more abundant or opened more rapidly, the duration of the LLD (and thus the LFP reflecting the LLD) would decrease because the cell would repolarize more rapidly as intracellular Ca^{2+} levels rise.

I used a pharmacological approach to examine the involvement of calcium-activated potassium channels in the vocal CPG of *X. laevis*. I first obtained whole-cell recordings of cells in DTAM and then applied 5-HT to confirm their identity as fast trill neurons (FTNs). Using NMDA-induced oscillations, I applied a pharmacological blocker of SK channels (apamin) or a blocker of BK channels (iberiotoxin) and examined affects on call duration and period (**Fig. 1**). Neither blocker had a noticeable effect on NMDA-induced oscillations, so we turned our attention to other ion channels.

What inward currents initiate and sustain FTN oscillations?

Inward currents such as persistent inward sodium currents (I_{NaP}), calcium-activated non-selective cation currents (I_{CAN}), L-type calcium currents, and hyperpolarization-activated inward current (I_h) have also been identified as critical in generating motor rhythms such as locomotion, breathing, and eating (e.g. Del Negro et al. 2010, Del Negro et al. 2005, Sharp et al., 1996) and could play a role in *Xenopus* vocalization rhythms. I specifically investigated the role of L-type calcium channels, using the pharmacological blocker nifedipine (**Fig. 2A**). At low doses (FTN 9, 10), effects were not apparent, but at high doses, our findings suggest a role for L-type calcium channels. Specifically, a high dose of nifedipine (100 μM) noticeably lengthened NMDA-induced oscillation duration and period in one cell (FTN 11). I also investigated the role of I_{CAN} in NMDA-induced oscillations using pharmacological blocker flufanamic acid (**Fig. 2B**). At low doses, I noticed no large effects (FTN 9, 10). However, at a high dose (200 μM), flufanamic acid completely eliminated NMDA-oscillations (FTN 11). These oscillations were

successfully recovered after reinstating saline flow for 1 hour and then reapplying TTX and NMDA to the preparation. However, at high doses it is possible for there to be nonspecific interactions. For instance, flufanamic acid is known to affect gap junctions (Harks et al., 2001), which could certainly play a role in generation of NMDA-oscillations or LLDs. In addition, these experiments were performed in FTNs that had been exposed to a variety of pharmacological agents. However, these preliminary results support the possibility that both L-type calcium currents and calcium-activated non-selection cation currents may play a role in generating oscillations in FTNs.

Further work is required to delineate the role that various ion channels play in shaping the species-specific qualities of LLDs and NMDA-oscillations. It is very possible that species differences of FTN ion channel expression could result in divergence of the rhythmic oscillations they produce. These differences could be the result of genetic mutations to the channels themselves that affect their kinetics, or to the regulation of these genes to alter their expression levels or patterns.

The periphery can shape behavior differences across species

Shaping the final vocal behavior produced by the frog during courtship can also occur via the vocal organ. When motor neurons' axons exit the vocal motor nucleus, they project via the laryngeal nerve to the larynx. Here, they innervate a set of laryngeal dilator muscles. When a compound action potential arrives, the muscles contract. If the potential

is sufficiently large to activate many muscle fibers, the laryngeal disks pull apart and a pulse of sound is produced (Tobias and Kelley, 1987).

Synapses in the male *X. laevis* larynx are mostly weak, and repeated stimulation of the laryngeal nerve leads synapses to potentiate as more muscle fibers are recruited (Tobias et al., 1995; Ruet et al., 1998). Initial stimulation may not lead to sound, while repeated CAPs lead to sound pulses that increase progressively in intensity. In contrast, the female larynx has mostly strong synapses and reliably translates each nerve stimulus into pulses of sound (Tobias and Kelley 1988).

Recent studies comparing two other species in the *Xenopus* genus, *X. boumbaensis* and *X. borealis*, found that differences in synaptic strength contribute not only to sex differences in vocalizations, but also to species differences. *X. boumbaensis* and *X. borealis* both produce an advertisement call that consists of single pulses of sound separated by a long interval between calls. The fictive calling pattern recorded from the laryngeal nerve matches the *in vivo* call pattern in *X. borealis*; single CAPs are separated by long intervals. However, in *X. boumbaensis*, the nerve pattern consists of 2-3 fast rate CAPs separated by long intervals. These repeated CAPs produce the facilitation required for the vocal neuromuscular synapse to release neurotransmitter sufficient for a muscle action potential and contraction. In contrast, the synapses in *X. borealis* are strong and therefore translate CAPs to pulses faithfully. Thus, the larynx plays a role in transforming the brain's output into the actual behavior.

Does the larynx also play a role in shaping species specific vocal patterns in species of the *X. laevis* clade? I used the isolated larynx preparation previously developed

(Tobias et al. 1987) to examine the *X. laevis*, *X. victorianus* and *X. petersii* vocal organ. In this preparation, laryngeal nerves are stimulated bilaterally, while the EMG signal is recorded from the laryngeal dilator muscles and sound is recorded using a hydrophone submerged in the saline with the larynx. I found that in all species it is possible to elicit laryngeal sound patterns matching their *in vivo* calling pattern (**Fig. 3**). In all three species, we see potentiation in the form of increasing EMG potentials with repeated nerve stimuli. In *X. laevis* (not illustrated), *X. victorianus* (green arrow), and *X. petersii* (green arrow), the initial stimulus often fails to result in a sound pulse, thus, as is the case in *X. boumbaensis*, repeated stimuli are often required to potentiate the EMG response and produce the initial sound. This requirement acts as a form of filtering in which the laryngeal synapse transforms the brain's output to produce a sound pattern distinct from the CAP pattern. In *X. petersii*, I identified a second form of laryngeal filtering. At rates of ~50 Hz and higher, the initial stimulus is transformed into an EMG signal and a pulse of sound, but subsequent fast rate pulses fail to result in a sound. However, they do result in a potentiating EMG signal. High-speed video recordings of the isolated *X. laevis* larynx (collaboration with Coen Elemans at University of Southern Denmark) suggested that this filtering at fast rates is due to failure of the laryngeal discs to regain contact before the subsequent stimulus pulse. This form of filtering probably reflects the speed at which laryngeal muscles relax and this property differs across species. Whether central or peripheral factors are more malleable during speciation is subject to debate. Studies in *Xenopus* show that evolutionary forces can act at both levels to shape the final behavior produced by an animal.

Using genetic tools to focus functional studies

Measuring neuronal activity during a behavior is extremely useful in identifying which cells underlie a given motor pattern. In complex vertebrate systems or in small invertebrate brains in which neurons are difficult to visualize, genetic approaches have emerged in the past decade that can complement studies of brain activity.

One set of examples include genome wide association studies and quantitative trait loci (QTL) identification. These have begun to identify genetic differences that could result in species-specific behaviors. Two species of closely-related *Drosophila, D. simulans* and *D. mauritiana*, diverged ~240 thousand years ago and produce courtship songs that vary in their sine carrier frequency by 9.7 Hz. Ding et al. (2016) used QTL mapping to identify the insertion of a retroelement into a calcium-activated potassium channel gene, *slowpoke,* in *D. simulans*. These investigators used the reciprocal hemizygosity to determine that the retroelement insertion in *slowpoke* was responsible for the difference in courtship song patterns between two species. This test involves crossing two strains carrying the null allele with the reciprocal non-mutant strains. It allows examination of the wild-type allele in the alternative genetic background. As discussed previously, calcium-activated potassium channels are known to be involved in intrinsic properties of rhythm-generating cells. Specifically, they are believed to participate in termination of long depolarizations, such as plateau potentials (El Manira et al., 1994). Ideally, the authors would combine this finding with targeted study of the vocal cells

underlying the call patterns; however, the cells themselves have not been identified. A combination of our electrophysiological approach to characterize the song-patterning network with their genetic tools could provide a powerful understanding of how neural circuits can be tweaked to result in distinct behaviors across related species.

Work has begun in *Xenopus* to examine the genetic basis of vocal behavior. We crossed female *X. laevis* to male *X. petersii* in 2007 and 2008. When these two species are crossed, they produce viable offspring that can be easily raised to adulthood in the lab. Five males are now adults and we recording their advertisement calls (**Fig. 4**). F1 hybrid adult males produce an advertisement call (**Fig. 4C,** n = 3) that appears to be intermediate between the advertisement call of the parental species (**Fig. 4A, B,** n=5 for each species). Specifically, the calls have similar fast trill and slow trill rates (**Fig. 5A, B**, Krusal-Wallis U-test, $p > 0.05$ for both comparisons). However, there is a trend for call duration, call period, and fast trill duration for hybrids to be longer than *X. petersii*, but shorter than *X. laevis* (Figure 5, C-E, $p < 0.05$ for each Kruskal-Wallis U-test). While we did not find significant differences between F1 hybrids and their parent species ($p > 0.05$ for all comparisons using Dunn's Multiple comparisons tests) we did find significant differences between the parent species when compared to each other ($p < 0.05$ for all comparisons of *X. laevis* to *X. petersii*). With increased sample size, significant differences between F1 hybrids and their parents might emerge.

The effort to create *X. laevis* - *X. petersii* hybrids continues and new work will employ association mapping comparisons to genomic data from hybrids and their parents

to identify genetic regions associated with behavioral variants. Once genes are identified, other techniques, such as CRISPR can be used to create mutant and transgenic *Xenopus* (Xenopus Resource Center, Marine Biological Laboratory, Woods Hole, MA), in which we can examine the functional consequences of these genetic mutations.

Another approach to determine the genetic differences underlying call variation in *X. laevis* and *X. petersii* is to examine the transcriptome of FTNs in each species. One approach is to sequence the transcriptome of hindbrain tissue punches containing DTAM and compare both species to each other. However, this approach would include many cell types that are not FTNs and this could obfuscate the result. A more direct approach would be to sequence the transcriptome specifically of FTNs. A technique to do exactly this has recently been developed in rodents and it is now possible to use Patch-Seq to isolate single cells after measuring their electrophysiological properties and morphology and then sequence their RNA-transcripts (Cadwell et al., 2015). This new technique allows for association of genetic expression with variation in cellular properties that can lead to behavioral differences. For instance, using layer-1 mouse neocortex cells, a generalized linear model of single cell transcriptomes was able to classify cell type with 86% accuracy. Furthermore, it was possible to predict some electrophysiological properties of the cells, such as after-hyperpolarization amplitude and action potential amplitude. Thus, transcriptome analyses in *Xenopus* FTNs could provide insight into how genetic changes during evolution contribute to cellular properties that ultimately produce different motor patterns.

Concluding Remarks

We have shown that species differences in two closely related species are due to properties of cells in a premotor region of the hindbrain vocal circuit. Continued electrophyiological approaches combined with genetic techniques will allow future experiments to pinpoint the exact mechanistic differences between these two species' vocal circuits. The *Xenopus* genus provides a strong system in which to study the functional circuit differences underlying variation in call types between sexes, through development, and across species. Further experiments in closely related species are likely to provide unique insight into common ways evolutionary forces can act on circuits during speciation to result in distinct behaviors. With the advent of new techniques, I expect that such approaches will become even more feasible in the coming years.

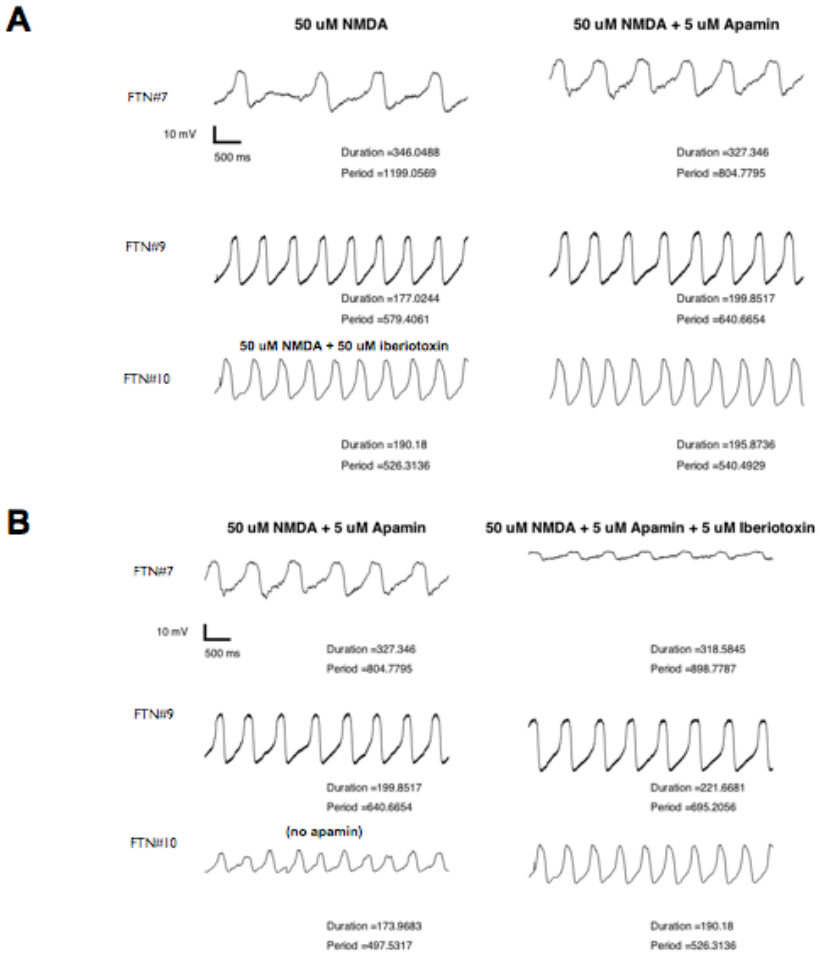

Figure 1. Blocking calcium-dependent potassium channels does not seem to lengthen FTN NMDA-oscillations

(A) Bath application of calcium-activated potassium channel small conductance SK blocker, 5 uM apamin, does not dramatically alter NMDA-oscillation duration or period.

(B) Bath application of calcium-activated potassium channel BK blocker, 5 uM iberiotoxin, does not dramatically alter NMDA-oscillation duration or period.

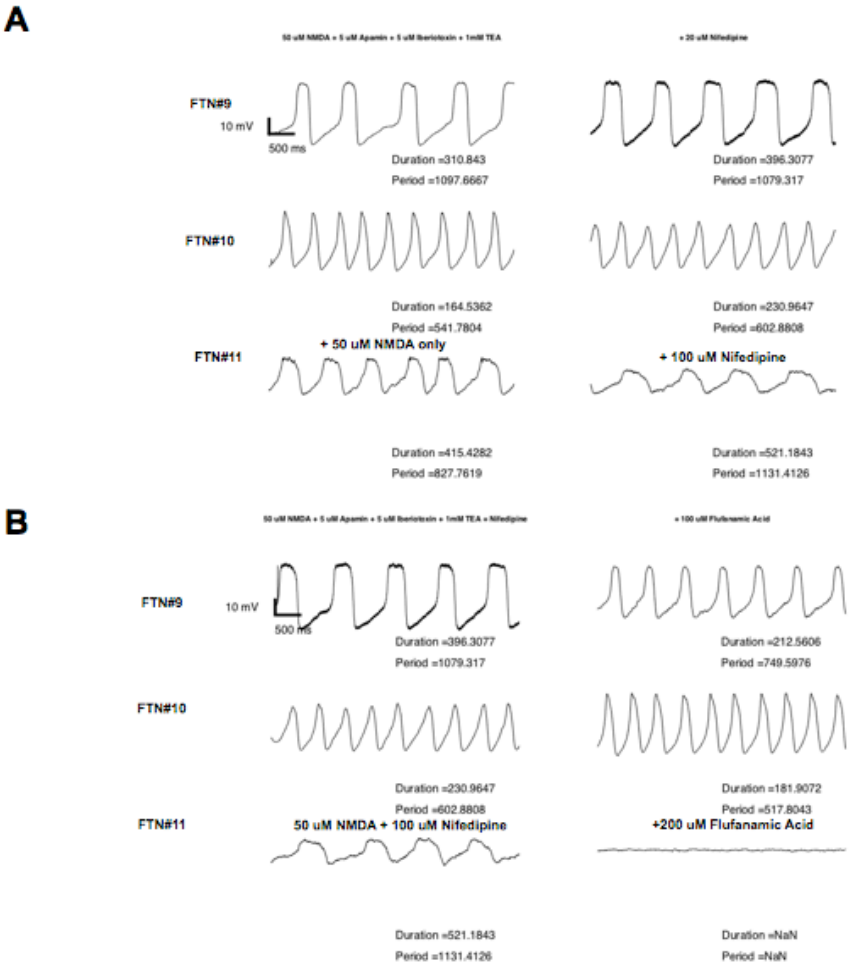

Figure 2. Blocking L-type calcium channels or calcium-activated non-specific cation channels with high doses may alter FTN NMDA-oscillations

(A) Bath application of L-type calcium channel blocker, nifedipine, does not dramatically alter NMDA-oscillation duration or period at low doses (20 uM). However, at a high dose (100 uM) oscillation and duration are substantially lengthened.

(B) Bath application of calcium-activated non-specific cation channel(I_{CAN}) blocker, flufanamic acid, does not dramatically alter NMDA-oscillation duration or period at low doses (100 uM). However, at a high dose (200 uM) oscillation and duration are

substantially lengthened.

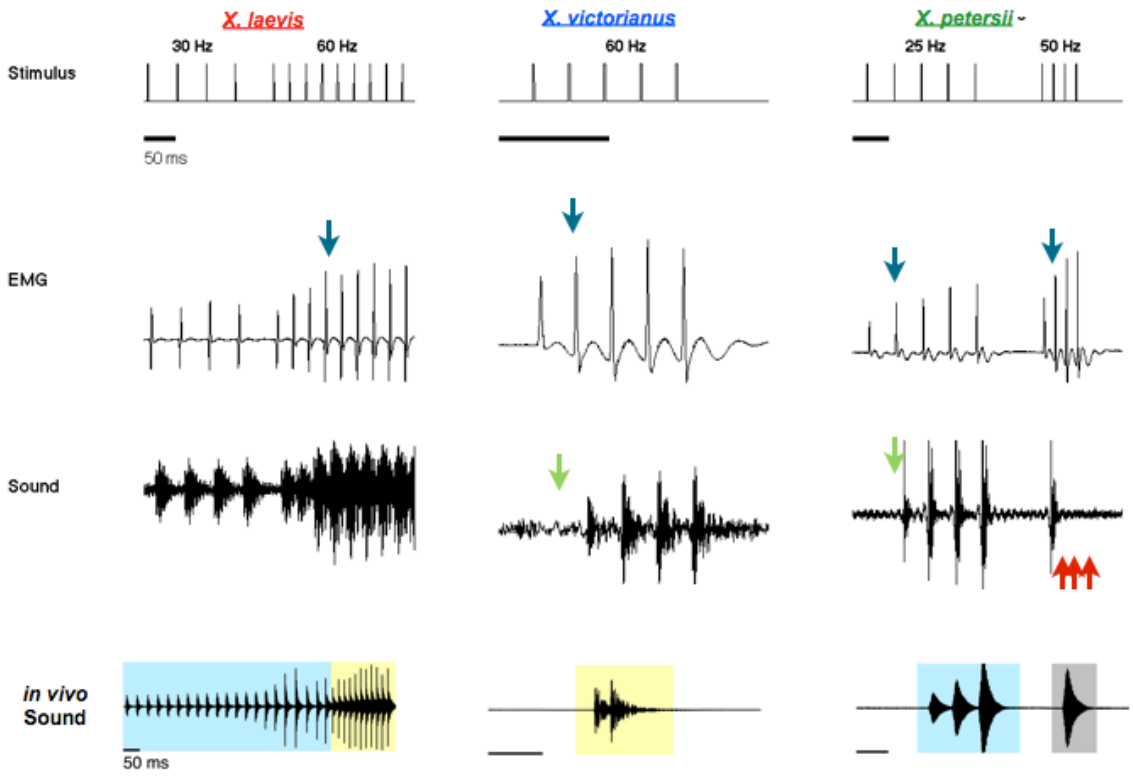

Figure 3. Evolution of the peripheral nervous system also influences behavior
Bilateral stimulation of laryngeal nerves with species-specific fictive CAP patterns (top) results in an EMG response, and sound production. These sounds closely resemble the pattern produced during *in vivo* calling (bottom). All species exhibit potentiation of the EMG (blue arrows) and initial sound pulse loss because of a requirement for EMG potentiation (green arrows, *X. laevis* not shown). A second form of laryngeal filtering is

present in *X. petersii*. Here, stimulus trains of ~50 Hz or greater fail to elicit sound after the initial stimulus (red arrows).

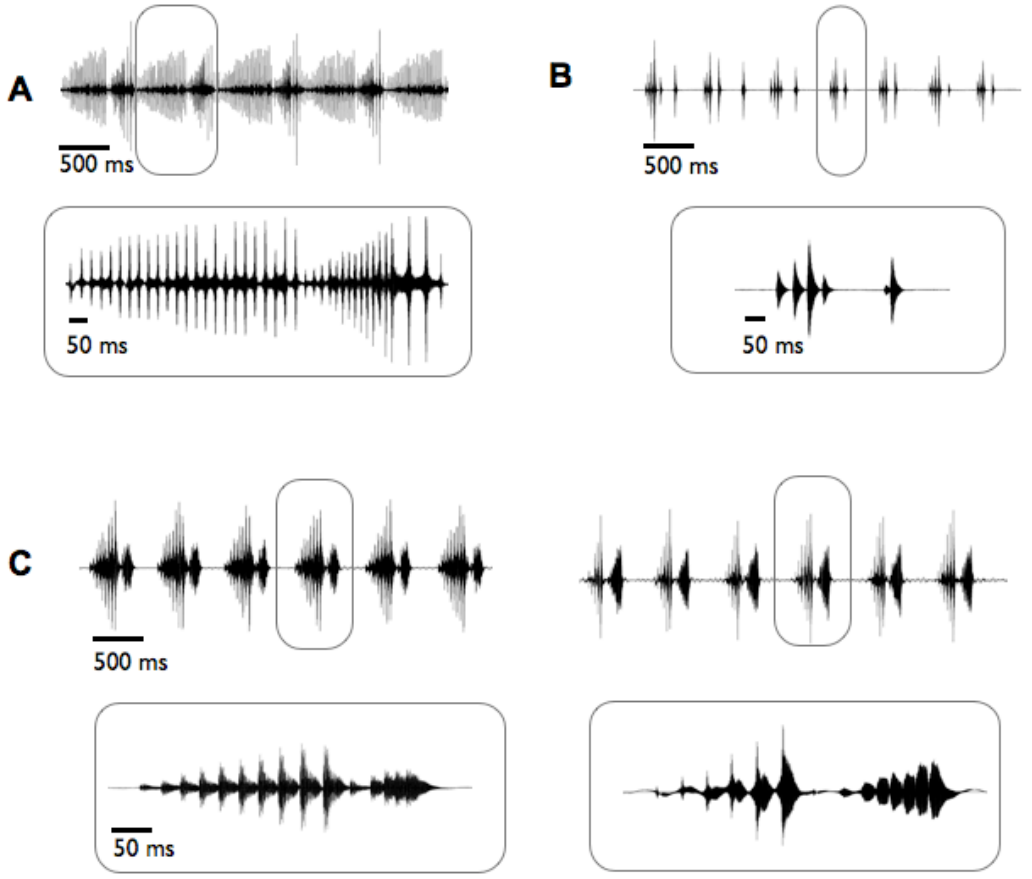

Figure 4. *X. laevis*-*X. petersii* hybrid advertisement calls

Female *X. laevis* frogs crossed with male *X. petersii* frogs can successfully mate in the lab. The calls of their offspring appear to be intermediate between measures of their parent's calls in terms of their call duration and period.

(A) Representative bout of advertisement calling of *X. laevis* male (top) and a single advertisement call (bottom).

(B) Representative bout of advertisement calling of *X. petersii* male (top) and a single advertisement call (bottom).

(C) Representative bouts of advertisement calling from 2 *X. laevis-X. petersii* hybrid males (top) and single advertisement calls (bottom).

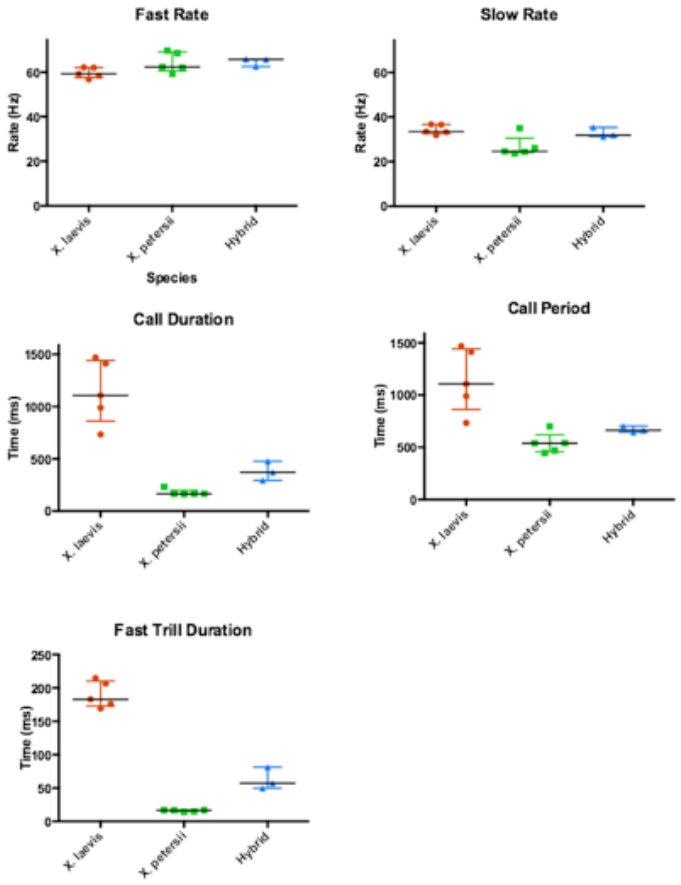

Figure 5. *X. laevis–X. petersii* hybrid advertisement calls are intermediate between parent species in measures of duration and period

Female *X. laevis* frogs crossed with male *X. petersii* frogs can successfully mate in the lab. The calls of their offspring appear to be intermediate between measures of their parent's calls in terms of their call duration, period, and fast trill duration, but remain similar in terms of slow and fast trill rate.

REFERENCES

Albersheim-Carter, J., Blubaum, A., Ballagh, I. H., Missaghi, K., Siuda, E. R., McMurray, G., Bass, A.H., Dubuc, R., Kelley, D.B., Schmidt, M.F., Wilson, M.F., Gray, P.A. (2015). Testing the evolutionary conservation of vocal motoneurons in vertebrates. *Respir. Physiol. Neurobiol*. **224**, 2-10.

Andersson, L. S., Larhammar, M., Memic, F., Wootz, H., Schwochow, D., Rubin, C.J., Patra, K., Arnason, T., Wellbring, L., Hjälm, G., et al. (2012). Mutations in DMRT3 affect locomotion in horses and spinal circuit function in mice. *Nature* **488**, 642–646.ss

Baltzley M.J., Lohmann K.J. (2008) Comparative study of TPep-like immunoreactive neurons in the central nervous system of nudibranch molluscs. *Brain Behav Evol*. **72,**192–206

Baltzley, M.J., Gaudry, Q., Kristan, W.B.J., Jr. (2010). Species-specific behavioral patterns correlate with differences in synaptic connections between homologous mechanosensory neurons. *J. Comp. Physiol. A Neuroethol. Sens. Neural Behav. Physiol*. **196,** 181–197.

Barkan, C.L., Zornik, E., Kelley, D.B., (in review). Evolution of vocal patterns: retuning hindbrain circuits during species divergence. *J. Exp. Bio.*

Bass, A. H., and Baker, R. (1997). Phenotypic specification of hindbrain rhombomeres and the origins of rhythmic circuits in vertebrates. *Brain. Behav. Evol.* **50**, 3–16.

Bongianni, F., Mutolo, D., Cinelli, E., and Pantaleo, T. (2014). Neural mechanisms underlying respiratory rhythm generation in the lamprey. . *Respir. Physiol. Neurobiol.* **224**, 1–10.

Brahic, C.J. and Kelley, D.B. (2003). Vocal circuitry in Xenopus laevis: telencephalon to laryngeal motor neurons. *J. Comp. Neurol*. **464**, 115–130.

Browaldh, N., Bautista, T.G., Dutschmann, M., and Berkowitz ,R.G. (2015). The Kölliker-Fuse nucleus: a review of animal studies and the implications for cranial nerve function in humans. *Eur. Arch. Otorhinolaryngol*. 1-6.

Bumbarger, D. J., Riebesell, M., Rödelsperger, C. and Sommer, R. J. (2013). System-wide rewiring underlies behavioral differences in predatory and bacterial-feeding nematodes. *Cell* **152**, 109–119.

Bumbarger, D. J., Riebesell, M., Rödelsperger, C., and Sommer, R. J. (2013). System-wide rewiring underlies behavioral differences in predatory and bacterial-feeding nematodes. *Cell*, **152**, 109–119.

Cadwell, C. R., Palasantza, A., Jiang, X., Berens, P., Deng, Q., Yilmaz, M., Reimer, J., Shen, S., Bethge, M., Tolias, K. F., et al. (2015). Electrophysiological, transcriptomic and morphologic profiling of single neurons using Patch-seq. *Nat. Biotechnol.*

Cannatella, D.C., and O. De Sa, R. (1993). Xenopus laevis as a model organism. *Syst. Biol.* **42**, 476-507.

Cazalets, J.-R., Sqalli-Houssaini, Y., and Magoul, R. (1999). Differential effects of potassium channel blockers on the activity of the locomotor network in neonatal rat. *Brain Res*. **827**, 185–197.

Chakraborty, M., and Jarvis, E.D. (2015) Brain evolution by brain pathway duplication. *Phil. Trans. R. Soc. B*. **370**, 20150056.

Chiang, J.T. A., Steciuk, M., Shtonda, B. and Avery, L. (2006). Evolution of pharyngeal behaviors and neuronal functions in free-living soil nematodes. *J. Exp. Biol.* **209**, 1859–1873.

Cinelli, E., Mutolo, D., Robertson, B., Grillner, S., Contini, M., Pantaleo, T., and Bongianni, F. (2014). GABAergic and glycinergic inputs modulate rhythmogenic mechanisms in the lamprey respiratory network. *J. Phys*. **592**, 1823–1838.

Cinelli, E., Robertson, B., Mutolo, D., Grillner, S., Pantaleo, T., and Bongianni, F. (2013). Neuronal mechanisms of respiratory pattern generation are evolutionary conserved. *J. Neurosci.* **33**, 9104–9112.

Del Negro C.A., Hsiao C.F., and Chandler S.H. (1999). Outward currents influencing bursting dynamics in guinea pig trigeminal motoneurons. *J. Neurophysiol*. **81**, 1478–1485.

Del Negro, C. A., Hayes, J. A., Pace, R. W., Brush, B. R., Teruyama, R., and Feldman, J. L. (2010). Synaptically activated burst-generating conductances may underlie a group-pacemaker mechanism for respiratory rhythm generation in mammals. *Prog. Brain Res*. **187**, 111–136.

Del Negro, C. A., Morgado-Valle, C., Hayes, J. A., Mackay, D. D., Pace, R. W., Crowder, E. A., and Feldman, J. L. (2005). Sodium and calcium current-mediated pacemaker neurons and respiratory rhythm generation. *J. Neurosci*, **25**, 446–453.

Dick, T.E., Bellingham, M.C., and Richter, D.W. (1994). Pontine respiratory neurons in anesthetized cats. *Brain Res.* **636**, 259-269.

Ding, Y, Berrocal, A, Morita, T, Longden, KD & Stern, DL (2016). Natural courtship song variation caused by an intronic retroelement in an ion channel gene. *Nature*. doi: 10.1038/nature19093

Elliott, T. M., Christensen-Dalsgaard, J., and Kelley, D. B. (2011). Temporally selective processing of communication signals by auditory midbrain neurons. *J. Neurophysiol*. **105**, 1620–1632.

Elliott, T. and Kelley, D. (2007). Male discrimination of receptive and unreceptive female calls by temporal features. *Journal of Experimental Biology* **210**, 2836.

Espinoza S.Y., Breen L., Varghese N., Faulkes Z. (2006). Loss of escape-related giant neurons in a spiny lobster, *Panulirus argus*. *Biol Bull*. **211**, 223–231

Evans, B. J. (2008). Genome evolution and speciation genetics of clawed frogs (Xenopus and Silurana). *Front. Biosci.* **13**, 4687–4706.

Evans, B. J., Carter, T. F., Greenbaum, E., Gvoždík, V., Kelley, D. B., McLaughlin, P. J., Pauwels, O. S. G., Portik, D. M., Stanley, E. L., Tinsley, R. C., et al. (2015). Genetics, Morphology, Advertisement Calls, and Historical Records Distinguish Six New Polyploid Species of African Clawed Frog (Xenopus, Pipidae) from West and Central Africa. *PLoS ONE* **10**, e0142823.

Evans, B. J., Kelley, D. B., Tinsley, R. C., Melnick, D. J., and Cannatella, D. C. (2004). A mitochondrial DNA phylogeny of African clawed frogs: phylogeography and implications for polyploid evolution. *Mol. Phylogenet. Evol.* **33**, 197–213.

Farley, G.R., Barlow, S.M., and Netsell, R. (1992). Factors influencing neural activity in parabrachial regions during cat vocalizations. *Exp. Brain Res.* **89**, 341-351.

Farries, MA, Meitzen, J, Perkel, DJ. (2005). Electrophysiological properties of neurons in the basal ganglia of the domestic chick: conservation and divergence in the evolution of the avian basal ganglia. *J. Neurophys*. **94**, 454-67.

Fénelon, V. S., Le Feuvre, Y. and Meyrand, P. (2004). Phylogenetic, ontogenetic and adult adaptive plasticity of rhythmic neural networks: a common neuromodulatory mechanism? *J Comp Physiol A Neuroethol Sens Neural Behav Physiol* **190**, 691–705.

Forster, H., Bonis, J., Krause, K., Wenninger, J., Neumueller, S., Hodges, M., and Pan, L. (2014). Contributions of the pre-Bötzinger complex and the Kölliker-fuse nuclei to respiratory rhythm and pattern generation in awake and sleeping goats. *Prog. Brain Res.* **209,** 73.

Furman, B. L. S., Bewick, A. J., Harrison, T. L., Greenbaum, E., Gvoždík, V., Kusamba, C., and Evans, B. J. (2015). Pan-African phylogeography of a model organism, the African clawed frog *'Xenopus laevis'*. *Mol. Ecol.* **24**, 909–925.

Gerhardt, H. C. (1994). The evolution of vocalization in frogs and toads. *Annu. Rev. Ecol. Syst.* **25**, 293–324.
Gerhardt, H. C., & Huber, F. (2002). *Acoustic communication in insects and anurans: common problems and diverse solutions*. University of Chicago Press.

Gerhardt, H. C., and Doherty, J. A. (1988). Acoustic communication in the gray treefrog, Hyla versicolor: evolutionary and neurobiological implications. *J. Comp. Physiol. A*. **162**, 261-278.

Goaillard, J.-M., Taylor, A. L., Schulz, D. J. and Marder, E. (2009). Functional consequences of animal-to-animal variation in circuit parameters. *Nat Neurosci* **12**, 1424–1430.

Hall, I.C., Ballagh, I.H., Kelley, D.B. (2013). The Xenopus amygdala mediates socially appropriate vocal communication signals. *J. Neurosci.* **33**, 14534-48.

Hanson, J. L., Rose, G. J., Leary, C. J., Graham, J. A., Alluri, R. K., and Vasquez-Opazo, G. A. (2016). Species specificity of temporal processing in the auditory midbrain of gray treefrogs: long-interval neurons. *J. Comp. Physiol. A Neuroethol. Sens. Neural Behav. Physiol.* **202**, 67–79.

Harks E.G., de Roos A.D., Peters P.H., de Haan L.H., Brouwer A., Ypey D.L., van Zoelen E.J., Theuvenet A.P. (2001). Fenamates: a novel class of reversible gap junction blockers. *J. Pharm. Exp. Therapeutics.* **298**, 1033-1041.

Harris-Warrick, R. M. (2010). General principles of rhythmogenesis in central pattern generator networks. *Prog. Brain Res.* **187**, 213–222.

Hess, D and Manira, A.E. (2001). Characterization of a high-voltage-activated IA current with a role in spike timing and locomotor pattern generation. *Proc. Natl. Acad. Sci. U.S.A*. **98**, 5276–5281.

Hochman, S. Jordan, L.M., Schmidt.B.J. (1994). TTX-resistant NMDA receptor-mediated voltage oscillations in mammalian lumbar motoneurons. *J. Neurophysiol.* **72**, 2559-2562.

Hoskin, C. J., and Higgie, M. (2010). Speciation via species interactions: the divergence of mating traits within species. *Ecol. Lett*. **13**, 409-20.

Huss, M., Wang, D., Trané, C., Wikström, M., Kotaleski, J.H. (2008) An experimentally constrained computational model of NMDA oscillations in lamprey CPG neurons *J. Comput. Neurosci*. **25**, 108–121.

Igawa, T., Kurabayashi, A., Usuki, C., Fujii, T., Sumida, M. (2008). Complete mitochondrial genomes of three neobatrachian anurans: a case study of divergence time estimation using different data and calibration settings. *Gene.* **407**, 116-129.

Irisarri, I., Vences, M., San Mauro, D., Glaw, F., Zardoya, R. (2011). Reversal to air-driven sound production revealed by a molecular phylogeny of tongueless frogs, family Pipidae. *BMC Evol Biol.* **11**, 114.

Jürgens, U. (2002). Neural pathways underlying vocal control. *Neurosci. and Biobehav. Rev.* **26**, 235-258.

Katz, P. S. (2011). Neural mechanisms underlying the evolvability of behaviour. *Philos Trans R Soc Lond, B, Biol Sci* **366**, 2086–2099.

Katz, P. S. (2016). Evolution of central pattern generators and rhythmic behaviours. *Proc. R. Soc. Lond. **B** Biol. Sci.* **371**, 20150057.

Katz, P. S., and Harris-Warrick, R. M. (1999). The evolution of neuronal circuits underlying species-specific behavior. *Current Opinion in Neurobiology*, **9(5)**, 628–633.

Kelley, D.B. (1980). Auditory and vocal nuclei in the frog brain concentrate sex hormones. *Science*. **207**, 553-5.

Kelley, D.B., Morrell, J.I., Pfaff, D.W. (1975). Autoradiographic localization of hormone-concentrating cells in the brain of an amphibian, *Xenopus laevis*. I. Testosterone. *J. Comp. Neurol*. **164**, 47-59.

Kiehn O., Johnson B.R., Raastad M. (1996). Plateau properties in mammalian spinal interneurons during transmitter induced locomotor activity. *Neuroscience* **75,** 263–273.

Kirkpatrick, M. and Michael J. Ryan, M.J. (1991). The evolution of mating preferences and the paradox of the lek. *Nature*. **350**, 33-38.

Klump, G.M., and Gerhardt, C.H. (2013). Mechanisms and functions of call timing. *Playback and Studies of Animal Communication.* 228, 153.

Koizumi, H., Mosher, B., Tariq, M.F., Zhang, R., Koshiya, N., and Smith, J.C. (2016). Voltage-Dependent Rhythmogenic Property of Respiratory Pre-Bötzinger Complex Glutamatergic, Dbx1-Derived, and Somatostatin-Expressing Neuron Populations Revealed by Graded Optogenetic Inhibition. *eNeuro.* **3**, ENEURO.0081-16.2016.

Lawton, K.J., Perry, W.M., Zornik, E., (in review). Motor neurons regulate premotor activity in a vertebrate central pattern generator. *J. Neurosci.*

Leininger, E. C., and Kelley, D. B. (2013). Distinct neural and neuromuscular strategies underlie independent evolution of simplified advertisement calls. *Proc. R. Soc. Lond. **B** Biol. Sci.* **280**, 20122639.

Leininger, E. C., and Kelley, D. B. (2015). Evolution of Courtship Songs in Xenopus : Vocal Pattern Generation and Sound Production. *Cytogen. and Genome Res*. **145**, 302–314.

Leininger, E. C., Kitayama, K., and Kelley, D. B. (2015). Species-specific loss of sexual dimorphism in vocal effectors accompanies vocal simplification in African clawed frogs (*Xenopus*). *J. Exp. Bio*. **218(6)**, 849–857.

Lillvis J.L., Katz P.S. (2013) Parallel evolution of serotonergic neuro- modulation underlies independent evolution of rhythmic motor behavior. *J. Neurosci*. **33**:2709–2717.

MacLean J.N., Schmidt B.J., Hochman S. (1997). NMDA receptor activation triggers voltage oscillations, plateau potentials and bursting in neonatal rat lumbar motoneurons in vitro. *Eur. J. Neurosci*. **9,** 2702–2711.

Manira, El, A., Tegnér, J., and Grillner, S. (1994). Calcium-dependent potassium channels play a critical role for burst termination in the locomotor network in lamprey. *J. Neurophysiol*. **72(4)**, 1852–1861.

Marder, E. and Bucher, D. (2001). Central pattern generators and the control of rhythmic movements. *Current Biology* **11**, R986–96.

Martin, W.F., and Gans, C. (1972). Muscular control of the vocal tract during release signaling in the toad Bufo valliceps. *J. Morph.* **137**, 1-27.

Mayr, E. (1963). Animal Species and Evolution. The Belknap Press of Harvard University Press, Cambridge, Massachusetts

Meyrand, P. and Moulins, M. (1988a). Phylogenetic Plasticity of Crustacean Stomatogastric Circuits: I. Pyloric Patterns and Pyloric Circuit of the Shrimp Palaemon Serratus. *Journal of Experimental Biology*.

Meyrand, P. and Moulins, M. (1988b). Phylogenetic plasticity of crustacean stomatogastric circuits: II. Extrinsic inputs to the pyloric circuit of the shrimp Palaemon Serratus. *Journal of Experimental Biology*.

Morona R., González A. (2009). Immunohistochemical localization of calbindin-D28k and calretinin in the brainstem of anuran and urodele amphibians. *J. Comp. Neurol.* **515**, 503-37.

Morquette, P., Verdier, D., Kadala, A., Féthière, J., Philippe, A. G., Robitaille, R., and Kolta, A. (2015). An astrocyte-dependent mechanism for neuronal rhythmogenesis. *Nat. Neuro*. **18**, 844-54.

Murakami Y., Pasqualetti ,M., Takio, Y., Hirano, S., Rijli, F.M., and Kuratani, S. (2004). Segmental development of reticulospinal and branchiomotor neurons in lamprey: insights into the evolution of the vertebrate hindbrain. *Development.* **131**, 983-995.

Newcomb J.M., Katz P.S. (2009) Different functions for homologous serotonergic interneurons and serotonin in species-specific rhythmic behaviours. *Proc R Soc B.* **276**: 99–108.

Newcomb, J. M., Sakurai, A., Lillvis, J. L., Gunaratne, C. A. and Katz, P. S. (2012). Homology and homoplasy of swimming behaviors and neural circuits in the Nudipleura (Mollusca, Gastropoda, Opisthobranchia). *Proc Natl Acad Sci USA* **109 Suppl 1**, 10669–10676.

Picker, M. D. (1983). Hormonal Induction of the Aquatic Phonotactic Response of Xenopus. *Behaviour*. **84**, 74–90.

Prime L, Pichon Y, Moore LE (1999). N-Methyl-D-aspartate-induced oscillations in whole cell clamped neurons from the isolated spinal cord of Xenopus laevis embryos. *J Neurophysiol.* 82:1069 –1073.

Prinz, A. A., Bucher, D. and Marder, E. (2004). Similar network activity from disparate circuit parameters. *Nat Neurosci* **7**, 1345–1352.

Rhodes, H. J., Yu, H. J., and Yamaguchi, A. (2007). Xenopus vocalizations are controlled by a sexually differentiated hindbrain central pattern generator. *J. Neurosci*. **27**, 1485–1497.

Roelants, K. and Bossuyt, F. (2005). Archaeobatrachian paraphyly and Pangaean diversification of crown-group frogs. *Systematic Biology.* **54**, 111-126.

Rubin, J.E., Hayes, J.A., Mendenhall, J.L., and Del Negro, C.A. (2009). Calcium-activated nonspecific cation current and synaptic depression promote network-dependent burst oscillations. *Proc. Natl. Acad. Sci. U.S.A*. **106(8)**, 2939–2944.

Russell,W. (1954). Experimental Studies of the Reproductive Behaviour of *Xenopus laevis*: I. The Control Mechanisms for Clasping and Unclasping, and the Specificity of Hormone Action. *Behaviour*. 113–188.

Ryan, M. J. (1998). Sexual selection, receiver biases, and the evolution of sex differences. *Science* **281**, 1999–2003.

Ryan, M. J., and Rand, A. S. (1993). Species recognition and sexual selection as a unitary problem in animal communication. *Evolution.* **47**, 647–657.

Saideman, S.R., Blitz, D.M., and Nusbaum, M.P. (2007). Convergent motor patterns from divergent circuits. *J. Neurosci.* **27**, 6664–6674.

Saideman, S.R., Blitz, D.M., and Nusbaum, M.P. (2007). Convergent motor patterns from divergent circuits. *J. Neurosci.* **27**, 6664–6674.

Sakurai, A., Gunaratne, C. A. and Katz, P. S. (2014). Two interconnected kernels of reciprocally inhibitory interneurons underlie alternating left-right swim motor pattern generation in the mollusk Melibe leonina. *J Neurophysiol* **112**, 1317–1328.

Sakurai, A., Newcomb, J. M., Lillvis, J. L. and Katz, P. S. (2011). Different roles for homologous interneurons in species exhibiting similar rhythmic behaviors. *Curr Biol* **21**, 1036–1043.

Schmidt, R.S. (1992). Neural correlates of frog calling: production by two semi-independent generators. *Behav. Brain Res.* **50**, 17-30.

Schmidt, R.S. (1993). Anuran calling circuits: inhibition of pretrigeminal nucleus by prostaglandin. *Horm. Behav*. **27**, 82-91.

Schul, J., and Bush, S. L. (2002). Non-parallel coevolution of sender and receiver in the acoustic communication system of treefrogs. *Proc. R. Soc. Lond. **B** Biol. Sci.*

Sharp, A. A., Skinner, F. K., and Marder, E. (1996). Mechanisms of oscillation in dynamic clamp constructed two-cell half-center circuits. *J. Neurophysiol*. **76(2)**, 867–883.

Simpson, H.B., Tobias, M.L., M.T., Kelley, D.B. (1986). Origin and identification of fibers in the cranial nerve IX-X complex of Xenopus laevis: Lucifer Yellow backfills in vitro. *J. Comp. Neurol.* **244**, 430-44.

Tahvildari B., Alonso A.A., Bourque C.W. (2008). Ionic basis of ON and OFF. *J. Neurophysiol*. **99**, 2006 –2011.

Tao, C., Zhang, G., Xiong, Y., and Zhou, Y. (2015). Functional dissection of synaptic circuits: in vivo patch-clamp recording in neuroscience. *Front. Neural Circuits*, **9**, 226.

Tegnér, J., Lansner, A., & Grillner, S. (1998). Modulation of burst frequency by calcium-dependent potassium channels in the lamprey locomotor system: Dependence of the activity level. *Journal of Computational Neuroscience*, **5,** 121–140.

Tegnér, J., Lansner, A., & Grillner, S. (1998). Modulation of burst frequency by calcium-dependent potassium channels in the lamprey locomotor system: Dependence of the activity level. *Journal of Computational Neuroscience*, **5,** 121–140.

Thoby-Brisson, M., Karlén, M., Wu, N., Charnay, P., Champagnat, J., and Fortin, G. (2009). Genetic identification of an embryonic parafacial oscillator coupling to the preBötzinger complex. *Nat. Neurosci.* **12**, 1028-1035.

Tinsley, R. & Kobel, H., eds. (1996). *The Biology of Xenopus* (Oxford Univ. Press, Oxford).

Tobias, M., Barnard, C., O'Hagan, R., Horng, S., Rand, M. and Kelley, D. (2004). Vocal communication between male Xenopus laevis. *Anim Behav* **67**, 353–365.

Tobias, M., Corke, A., Korsh, J., Yin, D. and Kelley, D. (2010). Vocal competition in male Xenopus laevis frogs. *Behavioral Ecology and Sociobiology* 1–13.

Tobias, M., Evans, B., Kelley, D. (2011). Evolution of advertisement calls in African clawed frogs. *Behaviour*, **148**, 519–549.

Tobias, M., Kelley, D. (1987). Vocalizations by a sexually dimorphic isolated larynx: peripheral constraints on behavioral expression. *J. Neurosci*, **7**, 3191-7.

Tobias M.L., Kelley D.B. (1988). Electrophysiology and dye-coupling are sexually dimorphic characteristics of individual laryngeal muscle fibers in Xenopus laevis. J. Neurosci. 8, 2422 – 2429.

Tobias M.L., Kelley D.B., Ellisman M. (1995) A sex difference in synaptic efficacy at the laryngeal neuromuscular junction of Xenopus laevis. J. Neurosci. 15, 1660 – 1668.

Tobias, M. L., Korsh, J. and Kelley, D. B. (2014). Evolution of male and female release calls in African clawed frogs. *Behaviour*.

Tobias, M. L., Viswanathan, S. S. and Kelley, D. B. (1998). Rapping, a female receptive call, initiates male-female duets in the South African clawed frog. *Proc Natl Acad Sci USA* **95**, 1870–1875.

Tomás-Roca, L., Corral-San-Miguel, R., Aroca P., Puelles, L., Marín, F. (2016). Crypto-rhombomeres of the mouse medulla oblongata, defined by molecular and morphological features. *Brain Struct. Func.* **221**, 815-838.

West-Eberhard, M.J. (1983). Sexual selection, social competition, and speciation. *Q. Rev. Bio.* **58**, 155-183.

Wetzel, D.M., Haerter, U.L., Kelley, D.B. (1985). A proposed neural pathway for vocalization in South African clawed frogs, *Xenopus laevis*. *J. Comp. Physiol. A*. **157**, 749–761.

Wetzel, D.M., Kelley, D.B. (1983). Androgen and gonadotropin effects on male mate calls in South African clawed frogs, Xenopus laevis. *Horm. Behav*. **17**, 388-404.
Xenopus laevis embryos. *J. Neurophysiol*. 82,1069 –1073.

Yager, D. D. (1992). A unique sound production mechanism in the pipid anuran *Xenopus borealis*. *Zool. J. Linn. Soc.* **104**, 351-375.

Yamaguchi, A., and Kelley, D. B. (2000). Generating sexually differentiated vocal patterns: laryngeal nerve and EMG recordings from vocalizing male and female African clawed frogs (*Xenopus laevis*). *J. Neurosci*. **20**, 1559–1567.

Yamaguchi, A., Gooler, D., Herrold, A., Patel, S., and Pong, W. W. (2008). Temperature-dependent regulation of vocal pattern generator. *J. Neurophysiol*. **100**, 3134–3143.

Yokota, S., Oka, T., Tsumori, T., Nakamura, S., and Yasui, Y. (2007). Glutamatergic neurons in the Kölliker-Fuse nucleus project to the rostral ventral respiratory group and phrenic nucleus: a combined retrograde tracing and in situ hybridization study in the rat. *Neuro. Res*. **59**, 341-346.

Young L.J., Nilsen R., Waymire K.G., Macgregor G.R., Insel T.R.(1999). Increased affiliative response to vasopressin in mice expressing the V_{1a} receptor from a monogamous vole. *Nature.* 400, 766-768.

Young L.J., Nilsen R., Waymire K.G., Macgregor G.R., Insel T.R. (1999). Increased affiliative response to vasopressin in mice expressing the V_{1a} receptor from a monogamous vole. *Nature.* **400**, 766-768.

Young L.J., Winslow J.T., Nilsen R., Insel T.R.(1997). Species differences in V1a receptor gene expression in monogamous and nonmonogamous voles: behavioral consequences. *Behav Neurosci*. **111**, 599-605.

Young L.J., Winslow J.T., Nilsen R., Insel T.R.(1997). Species differences in V1a receptor gene expression in monogamous and nonmonogamous voles: behavioral consequences. *Behav Neurosci*. **111**, 599-605.

Yu, H.J., and Yamaguchi, A. (2010). Endogenous serotonin acts on 5-HT2C-like receptors in key vocal areas of the brain stem to initiate vocalizations in *Xenopus laevis*. *J Neurophysiol.* **103**, 648-58.**269**, 847-852.

Zornik, E., and Kelley, D. B. (2007). Breathing and calling: neuronal networks in the Xenopus laevis hindbrain. *J. Comp. Neurology*. **501**, 303–315.

Zornik, E., and Kelley, D. B. (2008). Regulation of respiratory and vocal motor pools in the isolated brain of Xenopus laevis. *J. Neurosci*. **28**, 612–621.

Zornik, E., and Kelley, D. B. (2016). Hormones and vocal systems: insights from *Xenopus.* In *Hormones, Brain, and Behavior, Third Edition*. (Eds: Pfaff, D.W., Joels, M.). Amsterdam, Netherlands: Elsevier. (In Press).

Zornik, E., and Yamaguchi, A. (2012). Coding Rate and Duration of Vocalizations of the Frog, Xenopus laevis. *J. Neurosci*. **32**, 12102–12114.

Zornik, E., Katzen, A. W., Rhodes, H. J., and Yamaguchi, A. (2010). NMDAR-dependent control of call duration in Xenopus laevis. *J. Neurophysiol*. **103**, 3501–3515.